

Understanding the response of Greenland's marine terminating glaciers to oceanic and atmospheric forcing

Guest Editors:

Patrick Heimbach, Massachusetts Institute of Technology; Fiamma Straneo, Woods Hole Oceanographic Institution; Olga Sergienko, Princeton University

Mass loss from the Greenland ice sheet quadrupled from 1992-2001 to 2001-2011, resulting in a net contribution to sea-level rise of approximately 7.5 mm over the 1992-2011 period, roughly twice the Antarctic contribution. Roughly half of this loss is due to the speed up, thinning, and retreat of marine-terminating glaciers that began in the late 1990s and continues to this date. The underlying causes are not well understood, but evidence suggests that it was associated with changes at the marine termini. Thus, ice sheet-ocean interactions in Greenland have emerged as a new research frontier that is critical to understanding Greenland's contribution to global sea level rise.

Tackling this frontier, however, is far from trivial. Greenland's largest glaciers terminate in deep, long fjords. These fjords are remote, inaccessible, and choked with ice mélange composed of calved icebergs and sea ice, posing major challenges to scientists and instrumentation. The records of oceanic changes near the

Greenland outlet glacier ice-flow variability

Twila Moon

University of Washington

Ice mass loss from the Greenland Ice Sheet is a primary contributor to global sea level rise. The rate of ice loss has accelerated over the last couple of decades and Greenland currently contributes about 0.7-1.1 mm/yr to sea-level rise (260-380 Gt/ice per year; Enderlin et al. 2014; Shepherd et al. 2012). Predicting the potential rate and limits of future mass loss requires a clear understanding of ice sheet dynamics and how the ice sheet is coupled to the climate system. Roughly a third to a half of Greenland ice loss is due to discharge through iceberg calving at the ice-ocean interface, as opposed to *in situ* surface melt (Enderlin et al. 2014; Shepherd et al. 2012). Glacier velocity, as well as ice thickness, terminus advance and retreat, and the mechanisms controlling their variability, must be understood to calculate and predict ice sheet discharge. Characterization and understanding of ice sheet velocity contributes both to exploring the processes controlling ice dynamics and to constraining ice sheet models used to predict future mass loss and associated sea-level rise.

Modern satellite technology and analysis techniques now allow for a more comprehensive understanding of ice flow variability across the entire Greenland Ice Sheet, including year-to-year velocity changes. To take advantage of the lengthening satellite data record, an ice-sheet-wide survey of interannual velocity changes on Greenland outlet glaciers (glacier terminus width >1.5 km) was completed for 2000 through 2010 (Moon et al. 2012). The study examined winter velocities for 2000/01 and every year from 2005/06 through 2010/11 (subsequently referred to by the earlier year, so 2010/11 = 2010). Prior to this study, outlet glacier velocities had only been examined for smaller groups of glaciers or by comparing broad velocity snapshots with ~5-year sampling. The study revealed notable regional and local variability underlying mean speedup across much of the ice sheet.

IN THIS ISSUE

Greenland outlet glacier ice-flow variability	1
Understanding recent glacier and ocean changes in Greenland: Insights from the paleo-records	7
A new look at southeast Greenland barrier winds and katabatic flow	13
Atlantic water variability on the southeast Greenland shelf	20
Temperature variability in West Greenland's major glacial fjord: A driver of rising sea levels	25
Modeling of Greenland Ice Sheet and ocean interactions: Progress and challenges	31
Progress and challenges to understanding iceberg calving around the Greenland Ice Sheet	40

glaciers (or even on Greenland's continental shelves where fjords terminate) are almost non-existent, especially from the period preceding the 1990s. Furthermore, the processes through which the ocean may impact the glacier, including submarine melting or a weakening of the ice mélange, are complex, involving all components (ocean, atmosphere, sea-ice and glaciers) and a wide range of time and space scales. Thus progress on this complex topic requires a cross-disciplinary and multi-faceted approach, involving the international community working on various aspects of the problem.

A first successful effort in assembling such a community was a workshop held in June 2013, in Beverly, MA, entitled: 'Understanding the response of Greenland's Marine Terminating Glaciers to Oceanic and Atmospheric Forcing'. It brought together 90 oceanographers, glaciologists, atmospheric and climate scientists, including observationalists, modelers, and theoreticians. A whitepaper initiated by the U.S. CLIVAR Working Group on Greenland Ice Sheet-Ocean interactions (GRISO) served as background.

This edition of Variations is based on contributions spanning the range of topics covered at the workshop. It is representative of the challenges and advances across disciplines in understanding Greenland Ice Sheet Ocean interactions.

Regional velocity behavior is to some extent determined by geologic setting and climate. Broadly, the Greenland Ice Sheet can be divided into five regions with somewhat distinct regional outlet glacier characteristics (Fig. 1). Eastern and southwestern regions of the ice sheet both contribute relatively little to current ice discharge, with minimal likelihood that their ice discharge contribution will increase dramatically in the future (van den Broeke et al. 2009). Eastern Greenland is a low accumulation region with a high concentration of slow-moving, marine-terminating glaciers, with many at velocities <200 m/yr (~40% of the 38 glaciers). Fast-flowing, marine-terminating glaciers in the region have a mean velocity of 1040 m/yr. The southwestern region has only a few fast-flowing, marine-terminating glaciers (5 of 17 glaciers), with many (9) of the glaciers in this region terminating on land.

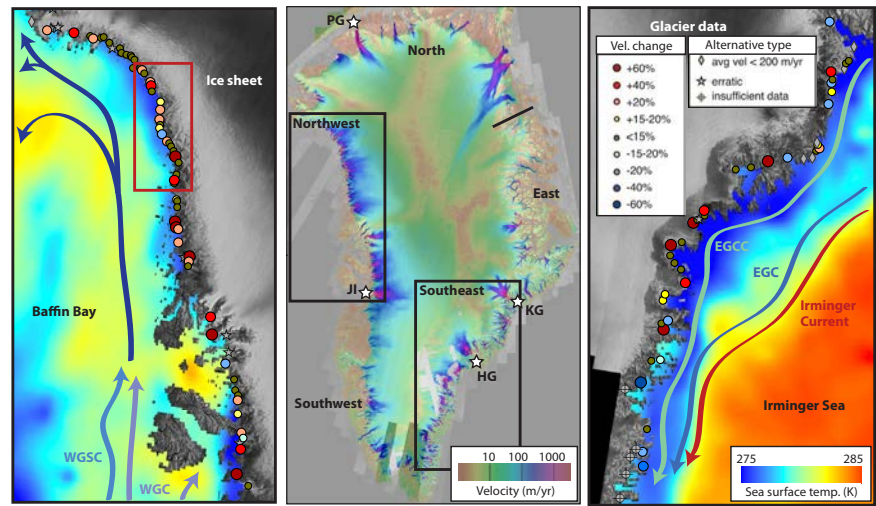


Fig. 1 Center panel: Velocity mosaic showing ice flow and focus regions for the northwest (left panel) and southeast (right panel). Side panels: Basic ocean circulation patterns are indicated on a representative sea surface temperature map and symbols indicate the location for each glacier and percent velocity change during 2005-2010 or other classification type (Moon et al., 2012). Large-scale ocean circulation: West Greenland Slope Current (WGSC), West Greenland Current (WGC), East Greenland Coastal Current (EGCC), East Greenland Current (EGC). Glaciers: Jakobshavn Isbræ (JI), Helheim Glacier (HG), Kangerdlugssuaq Glacier (KG), Petermann Glacier (PG). Red box in left-hand panel indicates the region of glaciers for data in Figure 3 (Moon et al., submitted 2014).

Northern Greenland is distinct from other regions because it is dominated by glaciers with long (>10 km) floating ice tongues, which can be sustained by the colder northern climate, including colder ocean temperatures (Straneo et al. 2012). These glaciers have low to modest mean velocities (300 to 1670 m/yr), with negligible change in velocities between 2000 and 2010. The floating ice tongues on these glaciers may act as buffers to prevent substantial interannual change due to modest terminus advance or retreat because the ice tongue may provide little lateral resistance at the ice edges. Thus, calving of icebergs from the end of an extended floating ice tongue results in only minor changes in resistance felt by the grounded ice (e.g., Nick et al. 2012). Future loss of the floating ice tongues on these northern glaciers, however, could lead to increased mass loss from the region, especially

US CLIVAR VARIATIONS

Editors: Mike Patterson and Kristan Uhlenbrock
 US CLIVAR Project Office
 1201 New York Ave. NW Suite 400
 Washington, DC 20005
 202-787-1682 www.usclivar.org
 © 2014 US CLIVAR

for glaciers with deep fjords extending towards the interior ice sheet, such as Petermann and 79 North (Nioghalvfjærdsfjorden glacier). Significant increases in velocity and associated mass loss after ice-tongue or ice-shelf disintegration were observed on Jakobshavn Isbræ in Greenland (Joughin et al. 2004) and on glaciers that previously connected to the Larsen B Ice Shelf in Antarctica (Rignot et al. 2004).

Ice discharge from the southeast and northwest regions currently accounts for most of the mass loss associated with glacier speedup and retreat (van den Broeke et al. 2009). The southeast has many fast-flowing (mean velocity of 2830 m/yr), marine-terminating glaciers, including Helheim and Kangerdlugssuaq Glaciers (Figs. 1 and 2). The region generally has high accumulation with steeper ice sheet surface slopes in some parts and glaciers flowing through long extended fjords in other parts. Greater surface slopes and the potential for extended glaciers to thin rapidly with speedup may both allow for faster and larger fluctuations in speed in the southeast as compared to other regions. The northwest also has a high concentration of fast-flowing (mean velocity of 1630 m/yr), marine-terminating glaciers, including Jakobshavn Isbræ (Figs. 1 and 2). Glaciers in the northwest are commonly embedded within the surrounding ice sheet, and convergent flow may limit rapid thinning associated with retreat for this region as compared to the southeast. Nonetheless, regional mean velocity increased significantly in both the northwest and southeast from 2000 to 2010 (Fig. 2). In 2010, average velocity increase in the northwest region was 28% of mean 2000 winter velocity, while the average southwest velocity increased 32%. Regional velocity patterns for the northwest and southeast were not, however, the same. The northwest mean velocity increased steadily from 2005-2010, on trend with the speedup observed between 2000 and 2005. In contrast, mean velocity in the southeast jumped sharply from 2000 to 2005 and then decreased during 2005-2006 before resuming a more modest annual increase. Data from 2010 to 2011 (not shown) indicate a continued increase in mean speed in the northwest and a slight decrease in southeast mean speed.

Along with notable regional differences in velocity behavior, the decade-long velocity record also reveals significant velocity variations on individual glaciers from year to year and from glacier to glacier within a region. Local spatial variability is evident, for example, in Figure 1. Combined with the high variability of individual interannual glacier behavior, the result is that predicting individual glacier behavior may not be possible without specific knowledge of local characteristics. Individual glacier variability is likely affected by a range of local factors, including local climate; glacier, fjord, and ice-sheet bed geometry; near-terminus sea ice

or ice mélange characteristics; and small-scale variability in the ocean and subglacial hydrologic environments.

The importance of the local environment for determining ice-flow speeds is in part due to the potentially high sensitivity of outlet glaciers to changes at the glacier terminus. Changes in ice thickness and surface slope also play a role in controlling ice velocity, but here we will focus on terminus advance and retreat. Observations, modeling, and theory support the hypothesis that

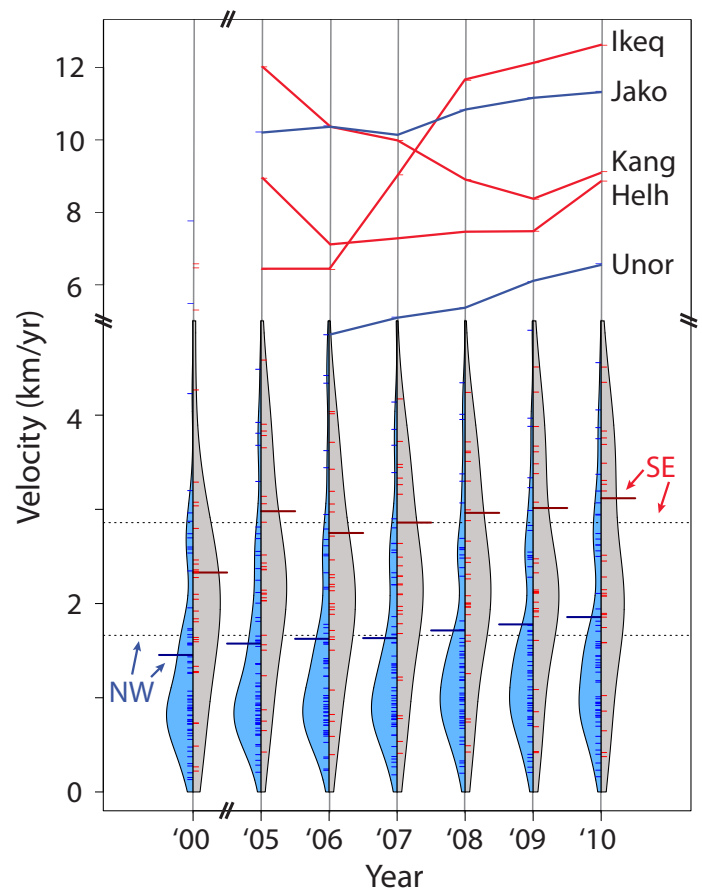


Fig. 2 Bottom: Distribution of glacier speeds (short ticks), smoothed speed density (colored bars), and mean speeds (long ticks) for 7 years' data. The northwest region is shown in blue with blue tick marks (left side) and the southeast region in gray with red tick marks (right side). Dashed black lines indicate regional mean speed over the entire decade (top for southeast, bottom for northwest). Only glaciers with sufficient data for both 2000 to 2005 and 2005 to 2010 are included. Top: Velocity plots for Jakobshavn (Jako), Upernavik North (Unor), Kangerdlugssuaq (Kang), Helheim (Helh), and Ikeq Fjord (Ikeq) (figure from Moon et al. 2012).

changes in ice-front position can have notable effects on glacier velocity (e.g., Podrasky et al. 2012; Nick et al. 2009; Joughin et al. 2008). Glacier velocity is expected to increase in response to terminus retreat through a combined reduction in resistive stress and increase in ice thickness as the calving front retreats into deeper water. To maintain force balance, basal traction must increase, which occurs through ice-flow speedup.

Modulations in terminus position are not the result of a single, simple process. Instead, terminus change may be affected by a variety of mechanisms, many of which depend on ocean conditions. Formation and breakup of ice mélange (a combination of icebergs, bergy bits, and sometimes sea ice) and sea ice at the glacier terminus may in part control the timing and length of the calving season by suppressing or allowing calving, respectively. Observations of Jakobshavn Isbræ, for example, show that velocity for this high-discharge glacier may be significantly modified by terminus advance and retreat, which may in turn be largely controlled by changes in the ice mélange within the Jakobshavn Fjord (Amundson et al. 2010). New measurements from northwest Greenland (Moon et al., submitted 2014) also suggest that sea ice and ice mélange conditions can influence the timing of seasonal calving activity and ultimately may affect interannual terminus position and associated velocity changes. Another mechanism by which ocean conditions can influence terminus position is through subsurface melt of the terminus face that may undercut or thin the terminus, allowing for increased calving. Summer melt rates of up to several meters per day have been observed on some Greenland glaciers (e.g., Enderlin and Howat 2013) and broad patterns of retreat, for example in the southeast, as well as the timing of rapid retreat on Jakobshavn have been connected to warming subsurface ocean waters (e.g., Holland et al. 2008;

Rignot et al. 2012). Thus, understanding the connected ice-ocean system is critical to moving forward with predictions of future dynamical changes for the Greenland Ice Sheet.

While mostly focusing here on interannual ice-flow variability, seasonal velocity patterns deserve a brief mention. Seasonal velocity records are limited, but do suggest that many glaciers may experience a regular seasonal pattern of speedup and slowing. For example, Jakobshavn commonly speeds up in summer, with subsequent seasonal slowing, which appears connected to terminus position and ice mélange conditions (Joughin et al. 2008). Observations for several glaciers north of Jakobshavn also indicate regular season patterns of spring to summer speedup followed by slowing (Howat et al. 2010), as do new observations of marine-terminating glaciers in northwest Greenland (Moon et al., submitted 2014; Fig. 3). Data beginning in 2004 show average annual variations in velocity of ~500 m/yr for these northwest glaciers (Carr et al. 2013; Moon et

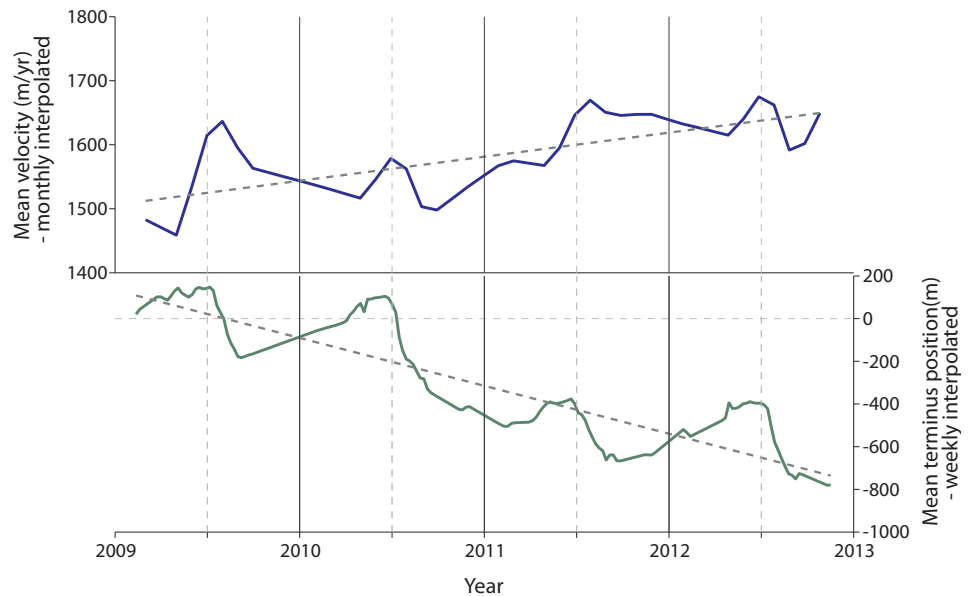


Fig. 3 Top: Mean velocity for 16 northwest Greenland glaciers from 2009 through 2012, determined using monthly-interpolated data (on average from 5 velocity measurements per year) and including linear trend (grey dotted line). Magnitude of annual variability in plot is substantially lower than measured (~500 m/yr) due to interpolation and averaging. Bottom: Mean terminus position relative to first measured position for 16 northwest Greenland glaciers. Mean determined using weekly-interpolated data (on average from 88 terminus position measurements per year), with linear trend indicated (grey dotted line). General pattern of seasonal velocity and terminus behavior is evident along with an interannual pattern of terminus retreat and speedup.

al., submitted 2014). Understanding the seasonal variability of ice flow across the ice sheet, however, remains severely limited by sparse temporal sampling. Seasonal velocity for many of the northwest glaciers measured appears closely linked to changes in subglacial hydrology due to ice sheet surface melt, rather than just responsive to terminus advance or retreat. Research on seasonal velocity behavior on land-terminating glaciers in Greenland suggests, however, that velocity fluctuations due to hydrologic changes may play little role in year-to-year speedup (Sole et al. 2008; 2013). Thus, ocean-related mechanisms for ice speedup (e.g., increased subsurface temperature and reduced sea ice and ice mélange causing enhanced terminus retreat) still stand as the most likely causes for sustained multi-year retreat and associated interannual speedup (Howat et al. 2010; Carr et al. 2013; Moon et al., submitted 2014).

Understanding variability of Greenland outlet glacier speeds remains a complex challenge, likely involving the interplay of all elements of the glacier-ocean system. As a result, broad regional patterns may be well aligned with large-scale climate behavior, while individual glaciers may show widely varying behavior due to localized conditions. Focused data collection in several categories is critical to advancing knowledge of ice sheet behavior and how it links to climatic and environmental changes. Needed observations include high-temporal-resolution velocity observations on an ice-sheet-wide scale, high-resolution bed elevation and bathymetric data, data on subglacial discharge, and subsurface oceanographic measurements.

Sparse sampling of velocity data in regards to seasonal behavior remains a challenge for understanding the mechanisms responsible for seasonal velocity changes on marine-terminating glaciers and how these are linked to sustained interannual speedup or slowing. Sub-daily velocity measurements on southwestern land-terminating Greenland glaciers and >35 km inland from a marine-terminating glacier indicate that meltwater input to the ice sheet bed and subglacial hydrology may control most of the seasonal velocity changes for regions relatively far from a calving terminus (e.g., Bartholomew et al. 2011; Sole et al. 2013). While this research can inform understanding of marine-terminating glaciers, as mentioned earlier, its applicability is limited when considering the complex ocean-glacier system of larger and faster-moving marine-terminating glaciers. For these glaciers, subglacial hydrology and terminus position likely both influence velocity, but their importance may shift from glacier to glacier and depending on the timescale of interest. High-temporal-resolution velocity measurements from many or all Greenland

outlet glaciers are needed to better understand the dominant mechanisms controlling velocity and how they vary both spatially and temporally. Spaceborne interferometric synthetic aperture (InSAR) capabilities have played a key role in creating our current knowledge regarding ice flow and future missions carrying InSAR instruments are imperative for increasing temporal resolution and extending the current time series.

Fjord topography, such as the absence or presence of a sill, likely plays an important role in regulating the circulation and characteristics of water within a fjord (e.g., Stigebrandt 2012). Circulation of fjord waters is also regulated by discharge of surface-glacial melt water at the base of the glacier terminus, which provides an important buoyancy source (Straneo et al. 2011; Jenkins 2011). Since submarine melt depends on the transport of heat to the ice-ocean boundary, understanding mechanisms that control circulation and heat transport (e.g., bathymetry and subglacial discharge) is critical for determining potential submarine melting and associated glacier terminus advance or retreat. Beneath the ice sheet, topography also has a strong influence on retreat. For example, many outlet glaciers around the ice sheet are on reverse-slope beds (i.e., the bed depth increases inland from the ice-ocean boundary), which can allow for instability and rapid glacier retreat (e.g., Pfeffer 2007). Small-scale topographic features such as over-deepening or sills can dramatically affect the terminus position and associated velocity changes. Both bathymetry and bed topography, therefore, must be measured at the scale of individual glaciers. A concerted effort to continue to acquire appropriate data and improve our high-resolution knowledge of subglacial topography and discharge and bathymetry will be critical for predicting future ice sheet behavior.

Finally, subsurface oceanographic measurements can be more difficult and costly to acquire than sea surface temperatures, which can be attained via remote sensing at km-scale resolution (e.g., Fig. 1). Yet, maximum ocean temperatures generally occur below the surface within Greenland fjords and can be notably different than surface temperatures (e.g., Straneo et al. 2012). Circulation of these warmer waters likely has the largest impact on terminus melt and may also affect the presence and condition of ice mélange. Increasing the number and coverage of subsurface ocean measurements (including but not limited to water temperatures) is necessary for understanding ice-ocean interactions for the wide range of outlet glaciers around the Greenland Ice Sheet.

While understanding and predicting variability in Greenland Ice Sheet motion remains a challenge, substantial progress has been made. We now recognize that large, rapid changes

in ice-flow do occur, and investigations continue to improve our knowledge of both long-term interannual change and short-term seasonal variability. Studies have also revealed that velocity changes are likely linked to ocean conditions via several potential mechanisms. Understanding both the individual processes at work and the range of behaviors across

the entire ice sheet, however, requires continued research on all elements of the ocean-glacier system (see also Straneo and Heimbach 2013; Joughin et al. 2012). Progress on all fronts will be crucial in the continued effort to understand ice sheet dynamics and the current and future impacts of climate change, including sea-level rise.

References

- Amundson, J.M., M. Fahnestock, M. Truffer, J. Brown, M.P. Luethi, and R.J. Motyka, 2010: Ice mélange dynamics and implications for terminus stability, Jakobshavn Isbræ, Greenland. *J. Geophys. Res.-Earth*, **115**, F01005, doi:10.1029/2009JF001405.
- Bartholomew, I.D., P. Nienow, A. Sole, D. Mair, T. Cowton, M.A. King, and S. Palmer, 2011: Seasonal variations in Greenland Ice Sheet motion: Inland extent and behaviour at higher elevations. *Earth Planet. Sci. Lett.*, **307**, 271–278, doi:10.1016/j.epsl.2011.04.014.
- Carr, J.R., A. Vieli, and C. Stokes, 2013: Influence of sea ice decline, atmospheric warming, and glacier width on marine-terminating outlet glacier behavior in northwest Greenland at seasonal to interannual timescales. *J. Geophys. Res.-Earth*, **118**, 1210–1226, doi:10.1002/jgrf.20088.
- Enderlin, E.M., and I.M. Howat, 2013: Submarine melt rate estimates for floating termini of Greenland outlet glaciers (2000–2010). *J. Glaciol.*, **59**, 67–75, doi:10.3189/2013JoG12J049.
- Enderlin, E.M., I.M. Howat, S. Jeong, M.J. Noh, J.H. Angelen, and M.R. Broeke, 2014: An improved mass budget for the Greenland Ice Sheet. *Geophys. Res. Lett.*, doi:10.1002/(ISSN)1944-8007.
- Holland, D.M., R.H. Thomas, B. De Young, M.H. Ribergaard, and B. Lyberth, 2008: Acceleration of Jakobshavn Isbrae triggered by warm subsurface ocean waters. *Nat. Geosci.*, **1**, 659–664, doi:10.1038/ngeo316.
- Howat, I.M., J.E. Box, Y. Ahn, A. Herrington, and E.M. McFadden, 2010: Seasonal variability in the dynamics of marine-terminating outlet glaciers in Greenland. *J. Glaciol.*, **56**, 601–613.
- Jenkins, A., 2011: Convection-driven melting near the grounding lines of ice shelves and tidewater glaciers. *J. Phys. Oceanogr.*, **41**, 2279–2294, doi:10.1175/JPO-D-11-03.1.
- Joughin, I., W. Abdalati, and M. Fahnestock, 2004: Large fluctuations in speed on Greenland's Jakobshavn Isbrae glacier. *Nature*, **432**, 608–610, doi:10.1038/nature03130.
- Joughin, I., I.M. Howat, M. Fahnestock, B. Smith, W. Krabill, R.B. Alley, H. Stern, and M. Truffer, 2008: Continued evolution of Jakobshavn Isbrae following its rapid speedup. *J. Geophys. Res.-Earth*, **113**, F04006, doi:10.1029/2008JF001023.
- Joughin, I., R.B. Alley, and D.M. Holland, 2012: Ice-sheet response to oceanic forcing. *Science*, **338**, 1172–1176, doi:10.1126/science.1226481.
- Moon, T., I. Joughin, B. Smith, and I. Howat, 2012: 21st-Century evolution of Greenland outlet glacier velocities. *Science*, **336**, 576–578, doi:10.1126/science.1219985.
- Nick, F.M., A. Vieli, I. M. Howat, and I. Joughin, 2009: Large-scale changes in Greenland outlet glacier dynamics triggered at the terminus. *Nat. Geosci.*, **2**, 110–114, doi:10.1038/NGEO394.
- Nick, F.M., A. Luckman, A. Vieli, C.J. Van der Veen, D. van As, R.S.W. van de Wal, F. Pattyn, A.L. Hubbard, and D. Floricioiu, 2012: The response of Petermann Glacier, Greenland, to large calving events, and its future stability in the context of atmospheric and oceanic warming. *J. Glaciol.*, **58**, 229–239.
- Pfeffer, W.T., 2007: A simple mechanism for irreversible tidewater glacier retreat. *J. Geophys. Res.*, **112**, F03S25, doi:10.1029/2006JF000590.
- Podrasky, D., M. Truffer, M. Fahnestock, J. M. Amundson, R. Cassotto, and I. Joughin, 2012: Outlet glacier response to forcing over hourly to interannual timescales, Jakobshavn Isbræ, Greenland. *J. Glaciol.*, **58**, 1212–1226, doi:10.3189/2012JoG12J065. <http://openurl.ingenta.com/content/xref?genre=article&issn=0022-1430&volume=58&issue=212&page=1212>.
- Rignot, E., G. Casassa, P. Gogineni, W. Krabill, A. Rivera, and R. Thomas, 2004: Accelerated ice discharge from the Antarctic Peninsula following the collapse of Larsen B ice shelf. *Geophys. Res. Lett.*, **31**, L18401, doi:10.1029/2004GL020697.
- Rignot, E., I. Fenty, D. Menemenlis, and Y. Xu, 2012: Spreading of warm ocean waters around Greenland as a possible cause for glacier acceleration. *Ann. Glaciol.*, **53**, 257–266, doi:10.3189/2012AoG60A136.
- Shepherd, A. and Coauthors, 2012: A reconciled estimate of ice-sheet mass balance. *Science*, **338**, 1183–1189, doi:10.1126/science.1228102.
- Sole, A., A.J. Payne, J. Bamber, P. Nienow, and W. Krabill, 2008: Testing hypotheses of the cause of peripheral thinning of the Greenland Ice Sheet: is land-terminating ice thinning at anomalously high rates? *The Cryosphere*, **2**, 1–14.
- Sole, A., P. Nienow, I. Bartholomew, D. Mair, T. Cowton, A. Tedstone, and M.A. King, 2013: Winter motion mediates dynamic response of the Greenland Ice Sheet to warmer summers. *Geophys. Res. Lett.*, **40**, 3940–3944, doi:10.1002/grl.50764.
- Stigebrandt, A., 2012: Hydrodynamics and circulation of fjords. *Encyclopedia of Lakes and Reservoirs*, L. Bengtsson, R.W. Herschy, and R.W. Fairbridge, Eds., *Encyclopedia of Earth Sciences Series*, Springer Science+Business Media B.V., 327–344 <http://www.springerlink.com/index/10.1007/978-1-4020-4410-6>.
- Straneo, F., D.A. Sutherland, D. Holland, C. Gladish, G. Hamilton, H. Johnson, E. Rignot, Y. Xu, and M. Koppes, 2012: Characteristics of ocean waters reaching Greenland's glaciers. *Ann. Glaciol.*, **53**, 202–210, doi:10.3189/2012AoG60A059.
- Straneo, F., and P. Heimbach, 2013: North Atlantic warming and the retreat of Greenland's outlet glaciers. *Nature*, **504**, 36–43, doi:10.1038/nature12854.
- Straneo, F., R. G. Curry, D. A. Sutherland, G. S. Hamilton, C. Cenedese, K. Vage, and L. A. Stearns, 2011: Impact of fjord dynamics and glacial runoff on the circulation near Helheim Glacier. *Nat. Geosci.*, **4**, 322–327, doi:10.1038/NGEO1109.
- van den Broeke, M., J. Bamber, J. Ettema, E. Rignot, E. Schrama, W.J. van de Berg, E. Meijgaard, I. Velicogna, and B. Wouters, 2009: Partitioning recent Greenland mass loss. *Science*, **326**, 984–986, doi:10.1126/science.1178176.

Understanding recent glacier and ocean changes in Greenland: Insights from the paleo-records

Camilla S. Andresen¹, Anne E. Jennings², David H. Roberts³, Colm O’Cofaigh³,
Antoon Kuijpers¹, and Jerry M. Lloyd²

¹Geological Survey of Denmark and Greenland

²University of Colorado

³Durham University

In the last decade increased mass loss from the Greenland Ice Sheet (GrIS) and ocean warming have received wide attention – both amongst scientists and the wider public. Within the epoch of satellite-based glacier observations outlet glacier retreat has accelerated significantly, leading to concern as to the extent of future mass balance change and contribution to increased sea level change.

Use of satellite data has enabled GrIS mass changes to be estimated since the early 1990’s, but we lack an understanding of the longer-term context of these changes. Without longer records it is difficult to assess whether the mass loss of the recent decade is unprecedented or is part of a recurring pattern acting on inter-annual, inter-decadal, or centennial timescales. The same problem applies to oceanographic measurements. Only in a few places does the instrumental record extend back more than several decades; for most fjords there is no data or, at best, a record for the past five years or so.

An understanding of longer-term ocean and glacier changes is important for understanding future ice-sheet changes in relation to climate change. What are the longer term modes of variability for the oceanographic changes around Greenland, and what is the sensitivity of the ice sheet and its outlet glaciers to these? One option to improve our understanding is to use geological records peripheral to the GrIS as they provide an exceptional opportunity to unravel past changes in glacier and ocean variability.

Examples of proxies used to reconstruct ocean and glacier changes

Through repeated glacial cycles the GrIS has advanced over the shallow continental shelf, in many places all the way to the shelf edge. This has occurred at least 5 times during the past 4.5 million years (Nielsen and Kuijpers 2013). During repeated glacial cycles the ice sheet has both eroded and deposited sediment across the shelf and has focused deposition in deep troughs, trough mouth

fans, and small basins, leaving a sedimentary archive of ice sheet-ocean interaction. Analysis of the composition and deposition rate of this sediment archive can unravel changes in ice sheet behavior, while the content of microorganisms can reveal past changes in oceanic water properties and sea ice cover. Typically, sedimentation rates are highest near the glacier terminus. Thus sediment archives from fjords with marine terminating glaciers can be used to reconstruct outlet glacier fluctuation and explore near shore variability of ocean waters on inter-annual timescales. In contrast, down-fjord and on the continental shelf, ice sheet and glacial meltwater influences are diminished as marine processes become more dominant. At times when the ice margin has advanced to the shelf edge, usually via the cross-shelf troughs, the archive of ice sheet fluctuations and ice sheet-ocean interactions is stored in the trough mouth fans. Thus, sediment archives can elucidate ocean and sea ice variability in great detail.

A widely applied sediment-based proxy for glacier changes is ice rafted debris (IRD). It refers to all sediment incorporated into glacier ice. This sediment load is subsequently released from calved icebergs drifting away through fjords and out on the shelf. By carefully assessing a specific site in terms of iceberg production rates, iceberg residence times, bathymetry, and oceanographic variability, the IRD variability in a sediment core can be used to reconstruct past changes in ice front calving and position.

Land-based field investigations combining geomorphology with dating techniques, such as radiocarbon dating or surface exposure dating of rocks, are an important method to assess rates and patterns of deglaciation and serve to complement marine based investigations. In the last decade cosmogenic surface exposure dating, in particular, has helped us understand GrIS behavior over the last 15,000 years. As ice retreats and the bedrock underneath it, or boulders released from it, are exposed to the atmosphere, cosmic rays interact with target atoms in the bedrock, such as Si, O, Ca, K, Cl, to produce isotopes such as

^{26}Al , ^{21}Ne , ^{10}Be , ^{36}Cl . The number of these isotopes accumulating in a rock surface will be proportional to the length of time the rocks are exposed and the respective rates of radioactive decay for each isotope. This relationship can be used to derive the time when the glacier disappeared from a specific geographic location.

The following case studies reveal different aspects of past ocean and glacier variability (see Fig. 1 for site location): 1) marine sediment archives from Sermilik Fjord in southeast Greenland revealing rapid response of a major outlet glacier to inter-annual climate variability during the past 100 years; 2) marine and terrestrial records revealing long-term ice stream behavior and ocean changes near Ummannaq and Disko Bugt in west Greenland showing that the glacier responded to a variety of forcing factors.

Case study 1: A 100 year long record of glacier and ocean changes by Sermilik Fjord, Southeast Greenland

A large number of sediment cores have been collected in Sermilik Fjord near Helheim Glacier in southeast Greenland. Sermilik Fjord is a 600-900 meter deep, ca. 100 km long and 8 km narrow fjord filled with thick sequences of sediment (Andresen et al. 2010). The third-most active outlet glacier on Greenland, Helheim Glacier terminates into a deep fjord, which allows waters from the Irminger Sea to come into contact with the glacier terminus and its mélange. The oceanographic conditions on the southeast Greenland shelf are characterized by the cold and fresh East Greenland Current system. Off southeast Greenland, this cold upper (<250 m) layer is underlain by warmer and saltier waters from the Irminger Current, a branch of the North Atlantic Current. Due to vigorous fjord/shelf exchanges, the water conditions near the glacier terminus largely reflect those on the shelf where ca. 4°C warm subsurface waters are found beneath a 200-300 meter thick layer of -1°C to +1°C cold Polar water (Straneo et al. 2010).

Based on analysis of five cores from the upper half of the fjord, the past 100 years of variability in glacier calving, shelf temperature, and water renewal rate inside the fjord have been reconstructed (Figs. 1 and 2). Glacier calving has been reconstructed from three sediment cores by estimating the flux of sand deposited from icebergs exiting the fjord. The underlying hypothesis is that the more calving, the more icebergs exit the fjord, and the more coarse debris is deposited (Andresen et al. 2012). This record has documented (with a time resolution of 1-3 years) a series of episodes of increased calving, of which the most recent period, 2000-2005, is only matched in magnitude by an episode of increased calving around the late 1930s. Increased inflow of warm subsurface waters into deeper fjords may increase the calving rates

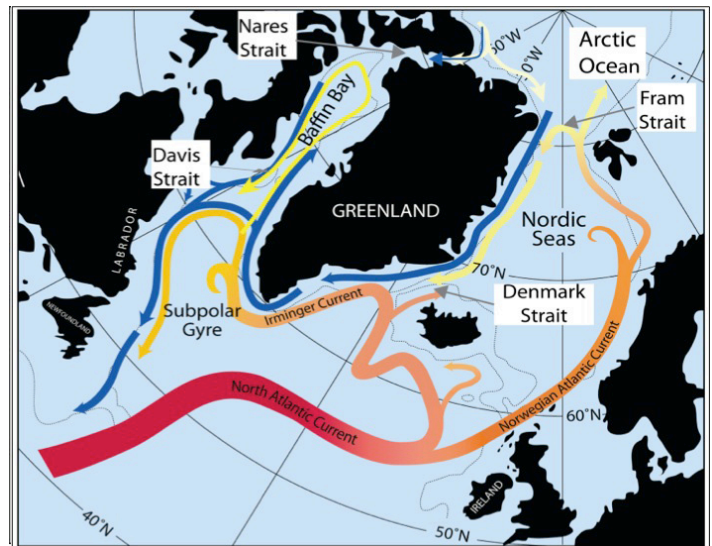


Fig. 1 Map of Greenland with locations of case study sites.

of outlet glaciers. It is hereby shown that regional climatic modes, the North Atlantic Oscillation (NAO) and the Atlantic Multi-decadal Oscillation (AMO) influence glacier calving through modulation of the occurrence of warm subsurface water in the shelf-fjord system, and that episodes of inflow of cold polar waters may potentially stabilize the glacier termini. Specifically, it is found that *high* calving activity coincides with a negative phase of the NAO, which is not surprising as a negative NAO phase is associated with a warm subpolar gyre and increased penetration of Atlantic water on the shelf. This also applies to the observed co-variability between the NAO and regional winds, air temperatures, and variability in both the polar-water and Atlantic-water source regions (Dickson et al. 2000).

A recent study of a fjord sediment core from the mid-Sermilik Fjord confirms that oceanographic changes on the adjacent shelf are indeed linked to regional changes of the Irminger Current, such as the AMO, and to changes in the East Greenland Current (Andresen et al. 2013). This study shows for the first time that alkenone-derived water temperature reconstructions are also applicable to waters around Greenland. In the open ocean, alkenone biomarkers are mainly produced by the prymnesiophytae, *Emiliania huxleyi*, growing in the photic zone, and the unsaturation index of the C_{37} alkenones (U_{37}^K) in marine waters has been shown to be highly correlated to water temperature on a global scale (Prah et al., 1988). The 100 year long record of alkenone SST values from the mid-fjord core is found

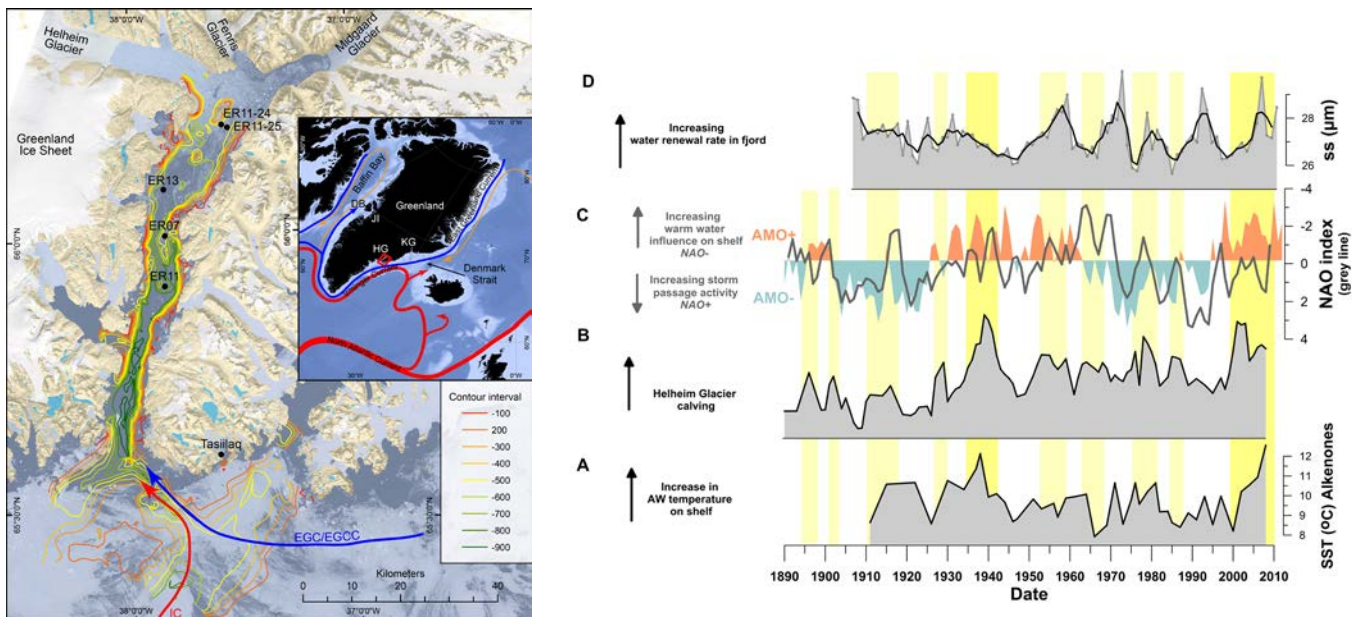


Fig. 2 Case study 1: Left: Sermilik Fjord with locations of investigated core sites. Right: Sediment core data from Sermilik Fjord near Helheim Glacier. (A) ER07 alkenone-derived SST reconstruction (Andresen et al. 2013). (B) Calving variability of Helheim Glacier (cores ER13, ER07 and ER11, Fig. 1; Andresen et al. 2012). Yellow bands highlight episodes of increased calving with the two most pronounced episodes in dark yellow. (C) NAO winter time Index (Hurrell 1995) and AMO Index (from Enfield et al. 2001). (D) Mean sortable silt () in core ER11-24. Three-point running mean shown in black (Andresen et al. 2014).

to range from 8°C to 12°C (Fig. 2). This, however, contrasts with colder values (0-4°C) obtained from recent hydrographic surveys inside the fjord. Advection of allochthonous alkenones produced in the warm Irminger Current waters circulating on the shelf likely accounts for this difference. Indeed, the temperature range of the alkenone-derived record is similar to in situ observations of 8-11°C observed in Irminger Sea water on the shelf just outside Sermilik Fjord. Support for the proxy temperature data is given by the observation that the reconstructed temperature variability in the fjord over the past 100 years resembles the reconstructed variability over the shelf, using remote instrumental time series. The coincidence between marked peaks in both calving and alkenone SST offshore in the late 1930s supports earlier suggestions that the heat content of the subsurface waters is an important control on Greenland outlet glacier stability.

Apart from heat content of the inflowing waters, it is also suggested that the *renewal rate* of this water may influence submarine melting at the glacier terminus (Straneo et al. 2011). A 100-year long proxy record for the renewal rate of the subsurface ocean waters in Sermilik Fjord has recently been reconstructed, based on

investigations of two sediment cores obtained from the head of the fjord (Andresen et al. 2014; Fig. 2). These cores consist mainly of current-sorted very fine-grained sediments, deposited from the melt water plume and with only relatively minor content of IRD (due to diluting from the high rates of melt water plume sediment deposition near the glacier margin). By calculating the *mean sortable silt* (denoted and estimated as the mean grain size of the 10-63 μm fraction), which is a proxy for current speed at the seabed (McCave et al. 1995), the relative variability in the water renewal rate has been reconstructed. It is found that episodes of increased water renewal rates lasting 3-5 years coincide with a positive NAO index. This is not surprising as low pressure systems and northeasterly storms are observed more frequently along the east coast of Greenland during positive NAO years as a result of the northward shift in the North Atlantic storm track (Cappelen et al. 2001). However, the previous studies of sediment cores obtained from the mid-region of the fjord showed that Helheim Glacier destabilization coincides with a negative NAO index (Andresen et al. 2012). Therefore this study concludes that inter-annual variability in storm-induced flushing of the fjord, and thus water renewal rate, in itself, is not the controlling factor for inter-annual

variability in glacier destabilization. Instead it is plausible that more frequent storms along the SE Greenland coast may depress the halocline at the coast and, therefore, thicken (on average) the Polar Water layer in the fjord at the expense of the subsurface Atlantic Water layer, thus resulting in reduced submarine melting.

These three reconstructions clearly show the great potential of using sediment cores to gain insight into inter-annual ocean and glacier variability. Such cores provide an excellent opportunity to link paleo records with instrumental records and hereby validate proxies.

Case study 2: Long-term ice stream behavior by Ummannaq and Disko Bugt

The Ummannaq Ice Stream (UIS) and the Jakobshavn Isbræ (JI) are large ice streams that drained the GrIS during the last glacial cycle (Fig. 1). They flowed westwards and moved on to the continental shelf and the shelf break edge. Together, they exerted significant control on ice and water flux into Baffin Bay and the North Atlantic.

The formation of the UIS was triggered through a convergent network of regional fjords, which guided multiple small ice streams to the coast where flow converged into the Ummannaq trough and triggered ice stream onset. Geomorphological evidence of glacially scoured and streamlined terrain, common in fjord-head areas from the Ummannaq region, shows warm-based ice above 1000 m above sea level (masl). It has been hypothesized that as ice thickened above 1000 masl, ice flow ignored topography and the UIS onset zone migrated westward towards the Ummannaq trough. Model output for the UIS predicts even thicker warm-based ice than field based observations suggest (up to and above 1266 masl), but as ice flowed westwards, the elevation of warm-based erosion dropped to ~700 masl through the Ummannaq trough (Roberts et al. 2013). The floor of the Ummannaq trough became heavily streamlined as ice flowed to the shelf edge break and delivered glaciogenic sediment to the Ummannaq trough mouth fan (Ó Cofaigh et al. 2013; Fig. 3).

Geophysical and marine geological research has also shown that an ancestral JI extended as a fast flowing ice stream to the shelf edge (Roberts and Long 2005; Ó Cofaigh et al. 2013) via Egedesminde Dyb to the Disko Trough Mouth Fan. Ice also flowed north through Vaigat Strait and merged with the UIS.

Deglaciation

The UIS and JI ice streams experienced dramatic and rapid ice sheet mass loss between the Last Glacial Maximum (20 Ka BP) to the middle Holocene (5 Ka BP). To document the drivers of ice retreat, such as ocean warming, and to reconstruct the position

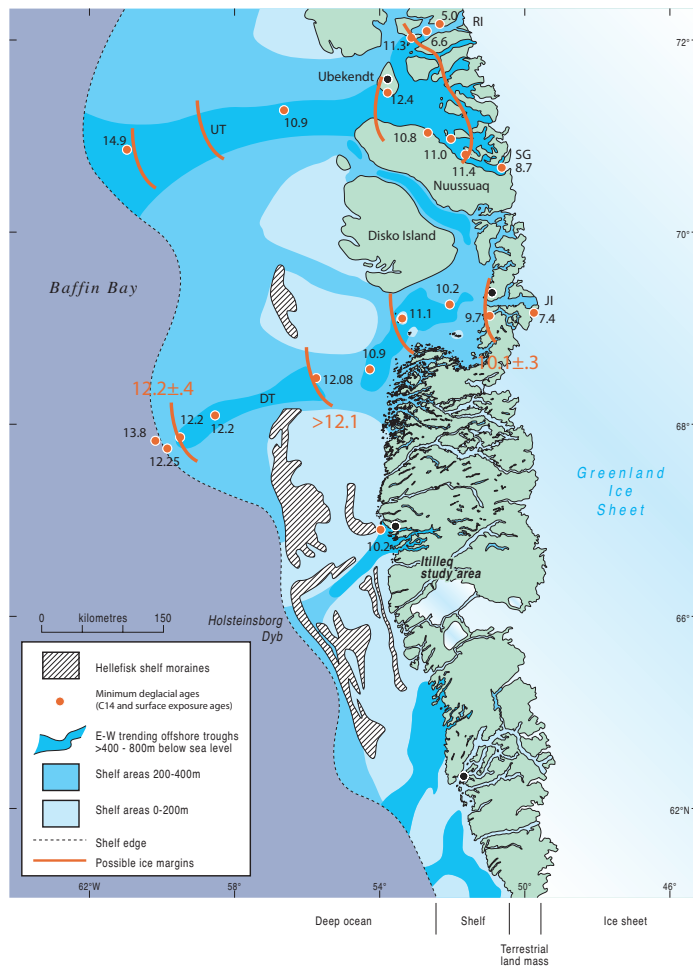


Fig. 3 Case study 2: Overview of the Ummannaq trough and Disko Bugt region showing bathymetry and deglacial dates along the troughs. UT: Ummannaq Trough. JI: Jakobshavn Isbræ. RI: Rink Isbræ. SG: Store Gletscher. The Hellefisk moraines are not dated but may be of Late Glacial Maximum age.

of the ice margin through time requires the study of sites that lie beyond the ice margin (e.g., Fig. 3). Work in progress on sediment cores from the trough-mouth fans formed on the continental slope in front of the ice streams shows that ocean warming (flow of West Greenland Current Atlantic Water into Baffin Bay along the west Greenland margin) preceded ice sheet retreat from the shelf edge, and likely played an important role in initiating and sustaining ice sheet retreat across the shelf (Sheldon et al. 2012; Jennings et al. 2012; Jennings et al. 2014). Indeed, recent work from the shelf edge and upper slope suggests ingression of warm Atlantic Water at 17.1 ka BP along the slope and onto the outer shelf at 14.4 – 13.8 ka BP (Sheldon et al. 2012; Jennings 2013).

Radiocarbon dating of glacial marine sediments overlying subglacial till on the outer shelf show that deglaciation of the Uummannaq system began shortly before 14.9 Ka BP (Ó Cofaigh et al. 2013; Sheldon et al. 2012) and by 12.4 ka BP the outer/ middle shelf and Ubekendt Ejland likely became ice free (Roberts et al. 2013; Ó Cofaigh et al. 2013; Fig. 3).

The Younger Dryas was a marked and abrupt climatic cooling in the high latitude northern hemisphere lasting from 12.8 to 11.5 Ka BP. The summit of the GrIS suddenly cooled by around 15°C, and it is believed that the cooling was caused by a shut-down of the North Atlantic meridional overturning circulation, due to sudden release of melt water from a collapse of the North American ice sheets. The ancestral JI re-advanced during the Younger Dryas, overriding the evidence on the shelf of the Late Glacial Maximum ice advance and producing gravity flow deposits on the Disko Trough Mouth Fan (Ó Cofaigh et al. 2013). Radiocarbon dates and sediment core data indicate that JI retreat from the Younger Dryas re-advance to the mid shelf was achieved rapidly by calving, a process that produced a thin, coarse grained sediment sequence (Jennings et al. 2014; Fig. 3). It is yet unknown if the UIS re-advanced during this cooling and grounded on the mid-shelf. But following initial deglacial retreat, the UIS underwent a rapid collapse with over 100 km of eastward retreat to Uummannaq, Ikerasak, and Karrat by ~11.4 - 10.8 ka BP (Roberts et al. 2013; Lane et al. 2013). Retreat may have accelerated east of Ubekendt Ejland because of fjord widening and bathymetric overdeepening, but rising sea-level, increasing insolation, and air temperatures were all contributing factors.

Holocene

¹⁰Be studies in Disko Bugt show that the ice margin was retreating from outer Disko Bugt by 10.8 ± 0.5 ka (Kelley et al. 2013) and by ca. 10.2 ka BP, the ice margin had already retreated to the head of Disko Bugt (Fig. 3; Lloyd et al. 2005; Young et al. 2011; Kelley et al. 2013). In contrast to the outer shelf, geophysical profiles and cores show thick rapidly deposited sediments in Disko Bugt associated with iceberg rafting, glacial melt water plumes, and sediment gravity flows generated during early Holocene retreat of the JI (Hogan et al. 2011). This retreat was linked to the establishment of a 'palaeo-West Greenland Current' in the inner part of Disko Bugt in the early Holocene characterized by warmer subsurface water masses (Lloyd et al. 2005). Large-scale surface water sediment plumes reached far west onto the Disko Bugt open shelf, a situation that persisted until about 6000 years ago (Perner et al. 2013). These conditions were accompanied by relatively high (summer) temperatures which prevailed over the Arctic in the early to middle Holocene, the so-called Holocene Thermal Optimum (HTM). The HTM was generated by orbital changes

and resulted in a several degree Celsius warming in the northern hemisphere in the first half of the Holocene. Thus by the middle Holocene most of the Disko Bugt glaciers had retreated far inland, although a marked short-lived re-advance was observed around 8.2 Ka BP (Young et al. 2011). In contrast, the retreat of the UIS margin was much more variable with topographic pinning playing an important part in modulating ice margin response to climate forcing. While Store Gletscher, retreated between 9.3 and 8.7 ka in response to both increasing air and ocean temperatures, Rinks Isbrae became topographically pinned for several thousand years (until 6.5 ka BP) and ignored climate forcing through the HTM.

Records of ocean and glacier changes for the past 5000 years (mid-Holocene) are as yet sparse from Uummannaq, but a large number of sediment cores from Disko Bugt have provided details on the history here. The cores show that since mid-Holocene times repeated multi-centennial periods of enhanced advection of warmer subsurface water with the West Greenland Current occurred. These periods were characterized by increased iceberg rafting linked to increased iceberg calving in relation to destabilization of the JI (Andresen et al. 2011). Similarly, surface water masses experienced alternating warming and cooling phases (Moros et al. 2006), presumably linked to a change in melt water production and atmospheric conditions as, for instance, documented for the (warm) Medieval Climate Anomaly and colder Little Ice Age. Within this context regional climate complexity related to large-scale atmospheric circulation patterns (e.g., NAO) may have resulted in diverging patterns of warming and cooling when compared with distant areas elsewhere in the Northern Hemisphere as, for instance, Europe.

The long-term trend in the various records documents the final onset of the late Holocene cooling, i.e., Neoglaciation, in the Disko Bugt area at 3500 yr BP (Perner et al. 2012). Again, orbital changes overall are responsible for the renewed glacier growth. A renewed westward advance of the JI margin is also reflected in the increased responses of the iceberg rafting to centennial-scale warm water incursions after this time, including its development of a floating ice front particularly after 2000 yr BP (Andresen et al. 2011).

The factors controlling the retreat behavior of the ice streams since the Last Glacial Maximum are thus complex and varied. Determining and understanding the processes that control the dynamic behavior of marine terminating ice streams during periods of pronounced climatic variability remains vital if we are to improve our modeling capability and reliably predict future ice sheet stability and sea level change.

References

- Andresen, C.S., D. McCarthy, C. Dylmer, M.-S. Seidenkrantz, A. Kuijpers, and J. Lloyd, 2011: Interaction between subsurface ocean waters and calving of the Jakobshavn Isbræ during the late Holocene. *The Holocene*, **21**, 211–224.
- Andresen, C.S., F. Straneo, M.H. Ribergaard, A.A. Bjørk, T.J. Andersen, A. Kuijpers, N. Nørgaard-Pedersen, K.H. Kjær, F. Schjøth, K. Weckström, and A.P. Ahlstrøm, 2012: Rapid response of Helheim Glacier in Greenland to climate variability over the past century. *Nat. Geosci.*, **5**, 37–41.
- Andresen, C.S., M.A. Sicre, F. Straneo, D. Sutherland, T. Schmith, M.H. Ribergaard, A. Kuijpers, and J.M. Lloyd, 2013: A 100 yr record of alkenone based SST changes offshore Southeast Greenland. *Cont. Shelf Res.*, **71**, 45–51.
- Andresen, C.S., S. Schmidt, M.-S. Seidenkrantz, F. Straneo, A. Grycel, K.H. Kjær, N. Nørgaard-Pedersen, C. Hass, L.M Dyke, J.M. Olsen, and A. Kuijpers, 2014: A 100-year record of changes in water renewal rate in Sermilik Fjord and its influence on calving of Helheim Glacier, Southeast Greenland. *Cont. Shelf Res.*, in revision.
- Cappelen, J., P.V. Jørgensen, E.V. Laursen, L.S. Stanius, and R.S. Thomsen, 2001: *The observed climate of Greenland, 1958–99 – with climatological standard normal, 1961–1990*. Technical Report 00-18, Danish Meteorological Institute, 154 p.
- Dickson, R.R., T.J. Osborn, J.W. Hurrell, J. Meincke, J. Blindheim, B. Adlandsvik, T. Vinje, G. Alekseev, and W. Maslowski, 2000: The Arctic Ocean response to the North Atlantic Oscillation. *J. Climate*, **13**, 2671–2696.
- Enfield, D.B., A.M. Mestas-Nunez, and P.J. Trimble, 2001: The Atlantic Multidecadal Oscillation and its relationship to rainfall and river flows in the continental U.S.. *Geophys. Res. Lett.*, **28**, 2077–2080.
- Hogan, K.A., J.K. Dix, J.M. Lloyd, A.J. Long, and C.J. Cotterill, 2011: Seismic stratigraphy records the deglacial history of Jakobshavn Isbræ, West Greenland. *J. Quat. Sci.*, **26**, 757–766.
- Hurrell, J.W., 1995: Decadal trends in the North Atlantic Oscillation: Regional temperatures and precipitation, *Science*, **269**, 676–679.
- Jennings, A.E., 2013: The role of ocean warming in Central West Greenland ice stream retreat: LGM through Deglaciation. US CLIVAR International Workshop: Understanding the response of Greenland's marine terminating glaciers to oceanic and atmospheric forcing, June 4–7, 2013. <http://www.usclivar.org/meetings/griso-workshop-agenda>
- Jennings, A.E., J.T. Andrews, C. Sheldon, C. Ó Cofaigh, A. Kilfeather, and J.D. Dowdeswell, 2012: Ice sheet-ocean interactions on the Central West Greenland Margin during the Last Deglaciation and the early Holocene. AGU Fall Meeting, Dec. 3–7, 2012.
- Jennings, A.E., M.E. Walton, C. Ó Cofaigh, A. Kilfeather, J.T. Andrews, J.D. Ortiz, A. De Vernal, and J.D. Dowdeswell, 2014: Paleoenvironments during Younger Dryas–Early Holocene retreat of the Greenland Ice Sheet from outer Disko Trough, central west Greenland. *J. Quat. Sci.*, **29**, 27–40.
- Kelley, S.E., J.P. Briner, and N.E. Young, 2013: Rapid ice retreat in Disko Bugt supported by 10Be dating of the last recession of the Greenland Ice Sheet. *Quat. Sci. Rev.*, **82**, 13–22.
- Lane, T.P., D.H. Roberts, B.R. Rea, C. Ó. Cofaigh, A. Vieli, and A. Rodés, 2013: Controls upon the Last Glacial Maximum deglaciation of the northern Uummannaq Ice Stream System, West Greenland. *Quat. Sci. Rev.*, in press, doi:10.1016/j.quascirev.2013.09.013.
- Lloyd, J.M., L.A. Park, A. Kuijpers, and M. Moros, 2005: Early Holocene palaeoceanography and deglacial chronology of Disko Bugt, West Greenland. *Quat. Sci. Rev.*, **24**, 1741–1755.
- McCave, I.N., B. Manighetti, and S.G. Robinson, 1995: Sortable silt and fine sediment size/composition slicing: Parameters for paleocurrent speed and paleoceanography. *Paleoceanogr.*, **10**, 593–610.
- Moros, M., K.G. Jensen, and A. Kuijpers, 2006: Mid to late-Holocene variability in Disko Bugt, central West Greenland. *Holocene*, **16**, 357–367.
- Nielsen, T. and A. Kuijpers, 2013: Only 5 southern Greenland shelf edge glaciations since the early Pliocene. *Nat. Sci. Rep.*, **3**, doi:10.1038/srep01875.
- Ó Cofaigh, C., J.A. Dowdeswell, A.E. Jennings, K.A. Hogan, A. Kilfeather, J.F. Hiemstra, R. Noormets, J. Evans, D.J. McCarthy, J.T. Andrews, J.M. Lloyd, and M. Moros, 2013: An extensive and dynamic ice sheet on the West Greenland shelf during the last glacial cycle. *Geology*, **41**, 219–222.
- Perner, K., M. Moros, A.E. Jennings, J.M. Lloyd, and K.L. Knudsen, 2012: Holocene palaeoceanographic evolution off West Greenland. *Holocene*, **23**, 374–387.
- Prahl, F.G., L.A. Muehlhausen, and D.L. Zahnle, D, 1988: Further evaluation of long-chain alkenones as indicators of Paleooceanographic conditions. *Geochemica Cosmochimica Acta*, **52**, 2303–2310.
- Roberts, D.H. and A.J. Long, 2005: Bedrock signatures of the Jakobshavn Isbrae ice stream, West Greenland: implications for ice stream and ice sheet dynamics. *Boreas*, **34**, 25–42.
- Roberts, D.H., B. Rea, T. Lane, C. Schnabel, and A. Rodés, 2013: New constraints on Greenland ice sheet dynamics during the last glacial cycle: Evidence from the Uummannaq ice stream system. *J. Geophys. Res.: Earth Surf.*, **118**, 519–541.
- Sheldon, C.M., A.E. Jennings, J.T. Andrews, C. Ó Cofaigh, J.A. Dowdeswell, and A. Kilfeather, 2012: Deglacial history and paleoceanography of the Umanak System, West Greenland. European Geophysical Union General Assembly, Vienna, Austria, April 23–27, 2012.
- Straneo, F., G.S. Hamilton, D.A. Sutherland, L.A. Stearns, F. Davidson, M.O. Hammil, G.B. Stenson, and A. Rosing-Asvids, 2010: Rapid circulation of warm subtropical waters in a major glacial fjord in East Greenland. *Nat. Geosci.*, **3**, 182–186.
- Straneo, F., R. Curry, D.A. Sutherland, G. Hamilton, C. Cenedese, K. Väge, and L.A. Stearns, 2011: Impact of fjord dynamics and subglacial discharge on the circulation near Helheim Glacier in Greenland. *Nat. Geosci.*, **4**, 322–327.
- Young, N.E., J.P. Briner, Y. Axford, B. Csatho, G.S. Babonis, D.H. Rood, and R.C. Finkel, 2011: Response of a marine-terminating Greenland outlet glacier to abrupt cooling 8200 and 9300 years ago. *Geophys. Res. Lett.*, **38**, L24701, doi:10.1029/2011GL049639.

A new look at southeast Greenland barrier winds and katabatic flow

Kent Moore¹ and Ian Renfrew²

¹University of Toronto, Canada

²University of East Anglia, UK

Although the seas around southeast Greenland have been known to be a hazard to maritime traffic as a result of the high winds that occur in the region, including the sinking of the MS Hans Hedtoft with the loss of 95 lives in a northeasterly gale near Cape Farewell during January 1959 (Hocking 1969; Rasmussen 1989), Doyle and Shapiro (1999) were the first to provide a quantitative description of a high-speed surface wind system in the region. Using an idealized model of flow past an obstacle similar to Greenland and case studies of the two observed events, they identified a shallow orographic jet, that they referred to as a tip jet, characterized by westerly surface winds in excess of 30 m/s that formed to the east of Cape Farewell. Moore (2003) used the NCEP Reanalysis to show that the surface wind field in the vicinity of Cape Farewell was bimodal in nature with the possibility of both high-speed westerly or easterly winds that were subsequently referred to by Renfrew et al. (2009) as either westerly tip jets, the sort identified by Doyle and Shapiro (1999), or easterly tip jets. In addition, Moore (2003) showed that both classes of tip jets were associated with the interaction of extra-tropical cyclones with the high topography of southern Greenland.

Moore and Renfrew (2005) used scatterometer winds from the QuikSCAT satellite to confirm the earlier results, to provide first-order dynamical explanations, and to further show that the southeast coast of Greenland was a region where high-speed northeasterly surface flow occurred, i.e., barrier flow. Subsequently a global climatology of QuikSCAT winds indicated that the southeast coast of Greenland was in fact the windiest location on the ocean's surface (Sampe and Xie 2007). Local maxima in the occurrence frequency of barrier winds were identified in the QuikSCAT data (Moore and Renfrew 2005) in regions referred to as Denmark Strait North (DSN) and Denmark Strait South (DSS); and diagnosed more clearly in Moore (2012). Harden and Renfrew (2012) noted that these maxima were collocated with steep coastal topography and demonstrated, through idealized simulations, that the enhanced wind speeds in these regions were the result of cross-isobar acceleration arising from the deceleration of the

flow impinging on these topographic barriers. Thus these local maxima are examples of so-called corner jets that in the Northern Hemisphere result in an acceleration of the wind to the left of the barrier (Barstad and Gronas 2005).

Southeast Greenland also experiences strong outflow wind events that are triggered by radiative cooling over the central Greenland Ice Sheet (Rasmussen 1989; Heinemann 1999). These katabatic wind events can become channeled down the steep topography of the large fjord systems in the region, most notably the Sermilik and Kangerdlugssuaq Fjords, resulting in high-speed wind events along the coast, known locally as piteraqs (Rasmussen 1989). In February 1970, a pitearaq with wind speeds estimated to be in excess of 90 m/s (the last recordings on the town's anemometer before it was destroyed indicated mean winds of 54 m/s with gusts to 70 m/s) devastated the small town of Tasiilaq situated near the mouth of the Sermilik Fjord (Cappelen et al. 2001).

This exceptional event was associated with a deep low-pressure system over the Denmark Strait and it has been proposed that its severity was the result of the compounding effects of the drainage flow off the ice sheet and the northwesterly flow that occurred after the low's passage (Cappelen et al. 2001). The important role that cyclones play in severe piteraqs was subsequently confirmed in a number of case studies (Klein and Heinemann 2002; Mills and Anderson 2003) as well as in a climatology of these events in the vicinity of the Sermilik Fjord (Oltmanns et al. 2014).

Cape Farewell tip jets, southeast Greenland barrier winds, and katabatic flow all play an important role in the regional weather and climate (Renfrew et al. 2008; Harden et al. 2011; Oltmanns et al. 2014). In addition, the elevated air-sea fluxes of heat, moisture, and momentum associated with these wind events impact the regional surface oceanography (Haine et al. 2009; Daniault et al. 2011) as well as contributing to the lower limb of the Atlantic Meridional Overturning Circulation (AMOC). In particular, the elevated air-sea heat fluxes associated with

westerly Cape Farewell tip jets and northwesterly katabatic flow have been proposed to be the atmospheric forcing that drives the formation of Labrador Sea Water in the Irminger Sea, an important component of the AMOC (Pickart et al. 2003a; Pickart et al. 2003b; Våge et al. 2009; Oltmanns et al. 2014).

Straneo et al. (2010) argued that barrier flow is important in the exchange of water between fjords and the open ocean along the southeast coast of Greenland. Through this process, it is hypothesized that barrier flow has contributed to the recent presence of warm subtropical waters in these fjords that has been argued to play a role in the recent rapid retreat of the outlet glaciers in the region (Howat et al. 2011). Katabatic flow can also act to advect sea ice away from the coast resulting in the formation of polynyas (Bromwich and Kurtz, 1984) that can have an impact on the ecology of the region (Arrigo 2007). These strong outflow winds can also result in the removal of a fjord's ice mélange, a mixture of sea ice and icebergs that inhibits glacier calving, thereby contributing to the destabilization of glaciers in the region (Amundson et al. 2010, Howat et al. 2011; Walter et al. 2012; Oltmanns et al. 2014).

Southeast Greenland is a data sparse and remote region with limited surface and upper-air observations, making it a challenge to investigate the structure and dynamics of these weather systems and their impact on the coupled climate system. In addition, coastal settlements, where observations are typically made, are usually situated in locations where the topography results in relatively benign microclimates that may not be representative of surrounding regions (Cappelen et al. 2001; Oltmanns et al. 2014). For example the DMI weather station at Tasiilaq, the settlement closest to the Sermilik Fjord, has a mean winter wind speed of 2.6 m/s with a directional constancy of 0.23; while the automatic weather station situated approximately 16 km away, inside the fjord, has a winter mean wind speed of 5.2 m/s with a directional constancy of 0.74 (Oltmanns et al. 2014). Scatterometer winds can provide information on the surface expression of these weather systems over the open ocean (Moore and Renfrew 2005) but provide no information over sea ice or over land. As a result, atmospheric reanalyses – the assimilation of meteorological observations into a consistent numerical weather prediction model – provide a representation of the atmosphere that is suitable for the analysis of climate variability in such an area (Moore, 2003; Våge et al. 2009; Harden and Renfrew 2012; Moore 2012; Oltmanns et al. 2014).

However all these weather systems are mesoscale phenomena that have horizontal length scales on the order of 200-400 km (Moore and Renfrew 2005; Renfrew et al. 2008; Oltmanns et al. 2014). As a consequence, they may be poorly-resolved in most global reanalysis products that typically have effective horizontal resolutions on the

order of 400 km or greater (Condrón and Renfrew 2013; Laffineur et al. 2014). This is consistent with the results of Duvivier and Cassano (2013), who argued that Weather Research and Forecasting (WRF) model simulations with horizontal resolutions of 50 km or greater under-represented the evolution of Greenland tip jets and barrier flow as well as their air-sea fluxes.

As a consequence, there is a clear need to develop climatologies of these weather systems with sufficient horizontal resolution to capture their fine scale structure. The recent completion of the Arctic System Reanalysis (ASR; Bromwich et al., 2014) that uses the Polar WRF regional forecast model to generate a regional reanalysis of the Arctic and that has a horizontal resolution of either 15 km or 30 km offers the possibility of achieving this goal.

In this article, we compare and contrast the representation of barrier winds and katabatic flow along the southeast coast of Greenland in the Interim Reanalysis from the ECMWF (ERA-I), a typical latest generation global atmospheric reanalysis (Dee et al. 2011), with that from the ASR. These two reanalyses are the result of very different data assimilation systems and underlying numerical models with differing numerical cores, parameterizations, and resolutions. For example, the ERA-I is based on a global spectral model and a highly-advanced 4D variational data assimilation scheme; while the ASR is based on a regional gridpoint model and a 3D variational data assimilation scheme that is optimized for use at high latitudes (Dee et al. 2011; Bromwich et al. 2014). Among these optimizations are the use of a land-surface scheme that includes the implementation of fractional sea ice cover with variable thickness and snow cover as well as an improved representation of the albedo of snow and ice (Bromwich et al. 2014). One point of commonality between the two is that the ERA-I is used to provide initial and lateral boundary conditions for the ASR (Bromwich et al. 2014). The interim version of the ASR that will be used in the article covers the period from 1 January 2000 to 31 December 2010 at a horizontal grid resolution of 30 km resulting in an effective horizontal resolution of ~200 km, i.e., 5-7 times the nominal grid resolution (Skamarock 2004). The ERA-I has a horizontal grid resolution of 0.75° implying an effective horizontal resolution of ~400 km.

A comparison with surface and upper-air data for the one year period from December 2006 to November 2007 indicated that the annual mean biases in surface meteorological fields in the ERA-I and ASR are comparable but that the ASR typically has smaller root mean square errors and higher correlations (Bromwich et al. 2014). A comparison of radiosonde and dropsonde data collected during a mesoscale cyclogenesis event over the Iceland Sea that was investigated during the Greenland Flow Distortion Experiment (Renfrew et al. 2008) indicated

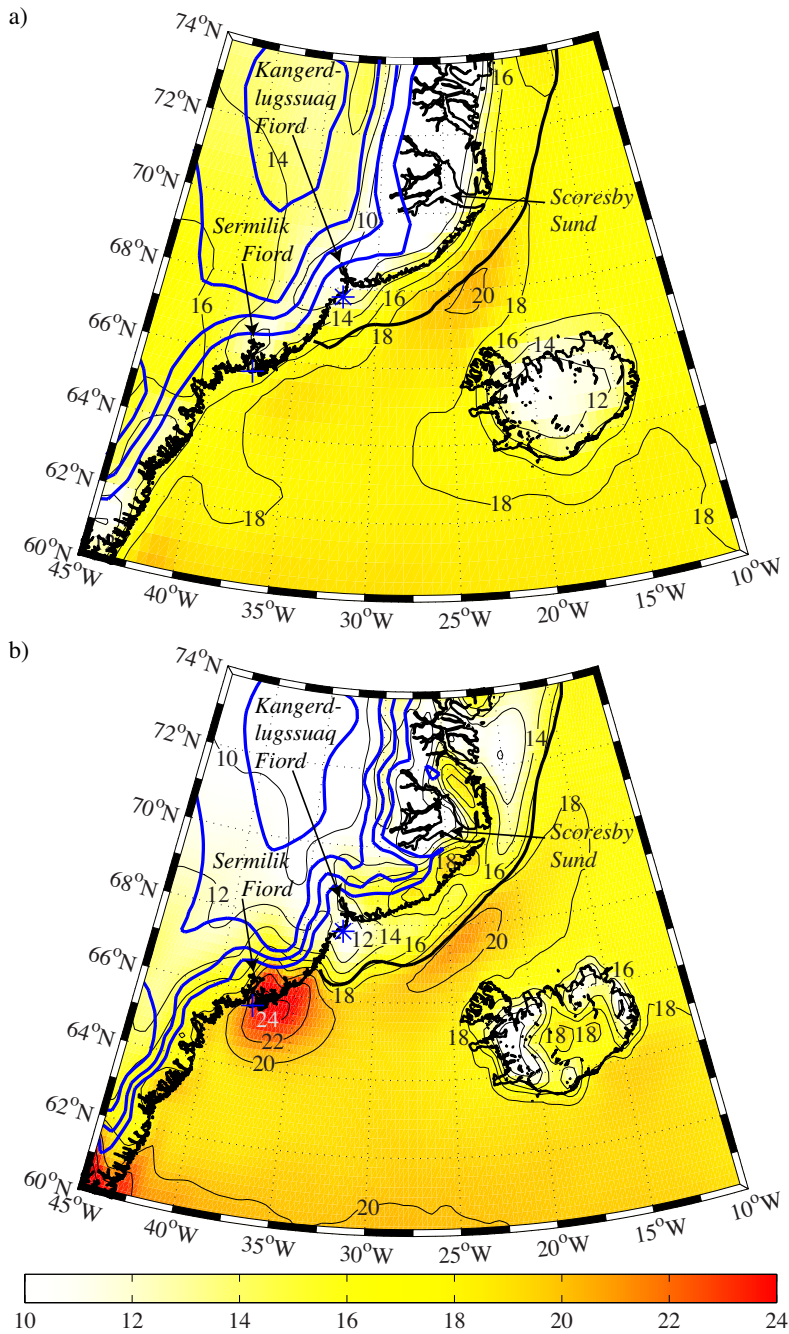


Fig. 1 The 95th percentile 10 m wind speed (m/s) during winter (DJF) 2000-2010 as represented in the: (a) ERA-I and (b) ASR-I. The thick black line represents the winter mean 50% sea ice concentration contour in the respective reanalyses. The thick blue lines represent the 1500, 2500, 3000, and 3500 m height contours in the respective analyses. The major fjords along the southeast coast of Greenland are indicated. The ‘*’ and ‘+’ represent the locations of the DMI weather stations at Aputiteeq and Tasiilaq respectively.

that the ASR typically had a reduced extremal bias in wind speed throughout the troposphere as compared to the ERA-I (Bromwich et al. 2014).

Figure 1 shows the 95th percentile 10 m wind speed from both the ERA-I and ASR-I during the winter months (DJF) for the period of overlap, i.e., 2000-2010. In general, the ASR-I field has more spatial structure as compared to that from the ERA-I. Over the Greenland Ice Sheet and the sea ice along its southeast coast, the 95th percentile wind speeds are generally higher in the ERA-I as compared to the ASR-I. In addition, the gradient across the marginal ice zone is generally more pronounced in the ASR-I. This is most evident in the vicinity of the Denmark Strait where there is a local maximum in the 95th percentile wind speeds present in both reanalyses. In the ERA-I, this maximum is quite diffuse and extends over the sea ice; while in the ASR-I it is focused over the open water. The gradient in the wind speed across the ice edge is most likely the result of the rougher surface of the sea ice as compared to the open ocean (Liu et al., 2006; Petersen and Renfrew 2009). It is likely that the ASR-I with its higher effective spatial resolution is able to better resolve this gradient. The 95th percentile wind speeds in the ASR-I are also significantly higher than those in the ERA-I in the vicinity of the Sermilik Fjord. The same is also true over east Greenland in the vicinity of Scoresby Sund, where there are a number of local maxima present in the ASR-I that are absent in the ERA-I. Finally the ASR-I captures more detail regarding the topographic flow distortion due to Iceland than does the ERA-I.

The diagnostic presented in Figure 1 clearly demonstrates the wealth of additional detail regarding the impact that the high topography of Greenland has on the surface flow in the region that is contained in the ASR-I as compared to the ERA-I. However it does not allow for a partition of the associated high-speed wind events into barrier and katabatic flow. This is possible if one takes into account the distinct directionality of barrier flow, i.e., along the barrier, in this case northeasterly (Moore and Renfrew 2005), and that of katabatic flow, i.e., down-slope, in this case northwesterly

(Oltmanns et al. 2014). Figure 2 shows the occurrence frequency of high-speed northeasterly and northwesterly surface flow during the winter months as represented in the ERA-I and ASR-I. The threshold criterion for high-speed northeasterly flow was set at 15 m/s, while that for northwesterly flow was set at 10 m/s. These thresholds were chosen partly based on wind climatologies. The former captures details of the barrier flow while the latter threshold was also used by Oltmanns et al. (2014) in their definition of katabatic flow events at Sermilik Fjord as represented in the ERA-I.

With regard to barrier flow (i.e., northeasterly high-speed winds), both the ERA-I (Fig. 2a) and ASR-I (Fig. 2b) capture the DSN and DSS locations along the southeast coast of Greenland where high-speed barrier winds are common (Moore and Renfrew 2005). As discussed by previous authors (Harden and Renfrew 2012; Moore 2012), the DSN location is in the vicinity of the steep coastal topography to the north, i.e., upwind, of the Kangerdlugssuaq Fjord with the DSS location is in the vicinity of a similar topographic barrier to the north of the Sermilik Fjord. The DSN maximum in the ASR-I is located over the open water with an enhanced gradient along the ice edge along with an extension inland over the steep topography just to the south of Scoresby Sund, while this maximum is more diffuse in the ERA-I. The occurrence frequencies in the DSS location are considerably higher in the ASR-I and have a pronounced inland extension over the steep coastal topography to the north of Sermilik Fjord. Both of these landward extensions of high-speed barrier flow are consistent with notion that these maxima are the result of ‘left-handed’ corner jets forced by these topographic barrier (Barstad and Gronas 2005). There is also a similar corner jet present along the southeast coast of Iceland that is better resolved in the ASR-I.

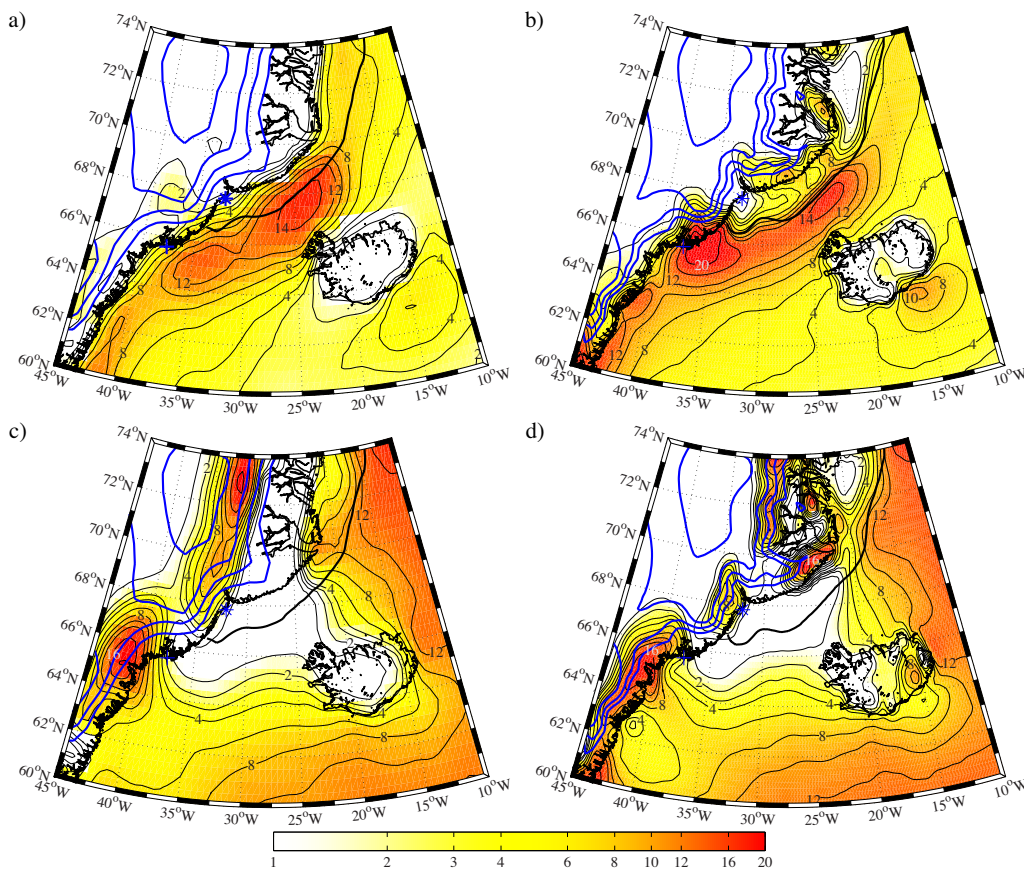


Fig. 2 The frequency of occurrence (%) of northeasterly 10m winds in excess of 15 m/s during the winter (DJF) 2000-2000 as represented in the: (a) ERA-I and (b) ASR-I. The frequency of occurrence (%) of northwesterly 10m winds in excess of 10 m/s during the winter (DJF) 2000-2000 as represented in the: (c) ERA-I and (d) ASR-I. The thick black line represents the winter mean 50% sea ice concentration contour in the respective reanalyses. The thick blue lines represent the 1500, 2500, 3000, and 3500 m height contours in the respective analyses. The ‘*’ and ‘+’ represent the locations of the DMI weather stations at Aputiteeq and Tasiilaq respectively.

Turning our attention to the katabatic winds (i.e., northwesterly flow), one again sees that there is more detail in the ASR-I (Fig. 2d) as compared to that from the ERA-I (Fig. 2c). Along the steep topographic gradient to the east of the Greenland’s North Dome, the ERA-I has an extended quasi-linear region where there is an elevated

occurrence frequency for high-speed northwesterly flow. The feature extends southwards to the Kangerdlugssuaq Fjord and represents the tendency for the katabatic flow to flow down the topographic gradient (Rasmussen 1989). In the ASR-I this feature is broken into two distinct segments by the topographic ridge to the south of Scoresby Sund, a feature that is not well represented in the ERA-I. The coastal terminus of this ridge, in agreement with Rasmussen (1989), is also a region where the ASR-I indicates that katabatic flow occurs. Both reanalyses indicate that the highest occurrence frequency for katabatic flow occurs to the south of Sermilik Fjord near 65°N 40°W. As was the case farther north, the ASR-I is better able to capture the minimum in the occurrence frequency that occurs along the topographic ridge separating the Kangerdlugssuaq and Sermilik Fjords. This southern maximum for katabatic flow, which is in the vicinity of the large Ikertivaq and Koge Bugt Fjords (Murray et al. 2010), has a pronounced offshore extension as was found to be the case for composite katabatic flow at Sermilik Fjord (Oltmanns et al. 2014). Such an extension is not evident in the vicinity of the Kangerdlugssuaq Fjord, most likely as a result of the increase in roughness over the sea ice.

In the vicinity of the major fjord systems along Greenland's southeast coast, both reanalyses have comparable occurrence frequencies of northwesterly flow with wind speeds in excess of 10 m/s. As discussed by Oltmanns et al. (2014), the ERA-I (and by extension the ASR-I) underestimates the wind speeds during these outflow events. The similarity in behavior between the two reanalyses in this regard suggests that both are resolving the density-driven component of the flow but even the 30 km resolution of the ASR-I is not sufficient to fully capture the acceleration due to the channeling of the flow down these fjord systems. This is consistent with high-resolution modeling of piteraqs in the Sermilik Fjord (M. Oltmanns, pers. comm.).

Both reanalyses also capture the two distinct local maxima in the occurrence of katabatic flow, one to the south of the Sermilik Fjord and the other to the north of Scoresby Sund. The latter is easily understandable as being the result of the steepness of the ice sheet in this region that is the result of the high topography of the North Dome. Topographic gradients are not as large in the vicinity of the southern maximum and in addition, the occurrence frequency is diminished to the north. It is probable that the confluence associated with the topographic saddle point (between the North and South Domes) contributes to the southern maximum, but it is also likely that the impact of northwesterly flow behind cyclones, which are more common farther south (Hoskins and Hodges 2002), also plays a role in the location of this maximum. In this regard, the relative

minimum in katabatic flow occurrence in the vicinity of the Kangerdlugssuaq Fjord may also be the result of the infrequent occurrence of cyclones to the north of this fjord.

It is of course important to validate the winds from any reanalysis, especially in topographically complex and data sparse regions such as the southeast coast of Greenland. This is a challenge because, as mentioned previously, the limited observations in the region may exhibit a 'fair weather' bias (Cappelen et al. 2001; Oltmanns et al. 2014). This problem can be illustrated through a comparison of the 10 m wind speed from both the ERA-I and ASR-I at the weather stations near the mouths of the Kangerdlugssuaq Fjord, the Aputiteeq station, and the Sermilik Fjord, the Tasiilaq station. For both stations, the correlation coefficient between the observed wind speeds and those from both reanalysis during the winter are on the order of 0.5. Consideration of the directionality of the observed and reanalysis winds lead to smaller correlation coefficients. Given these results, it is difficult to see how such data can be used to validate the reanalysis winds. There is nevertheless evidence that, at least on the regional scale, that the ASR-I is better

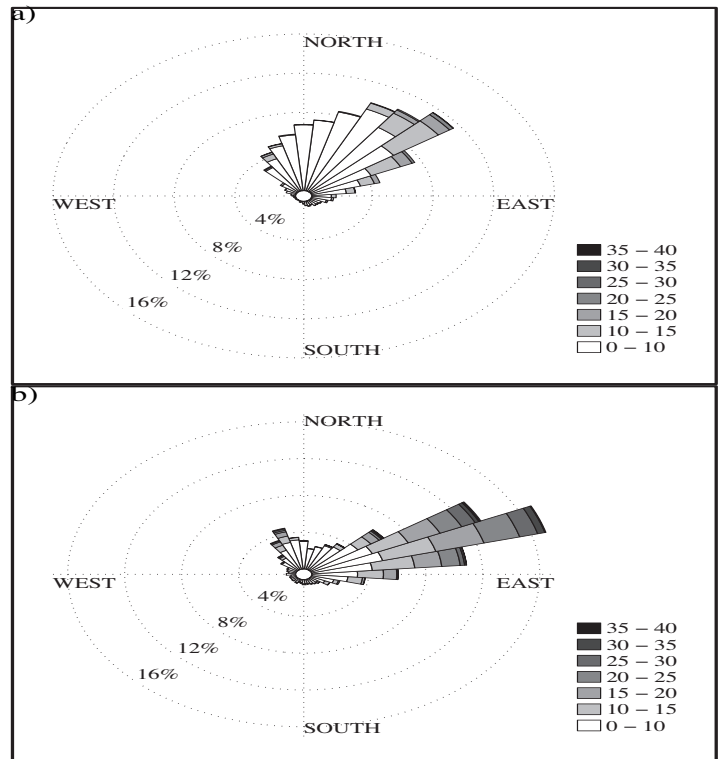


Fig. 3 The wind rose of the surface wind (m/s) during winter at Tasiilaq (near Sermilik Fjord) as represented in the: (a) ERA-I and (b) the ASR-I.

able to capture details of the coastal wind field as compared to the ERA-I. Figure 3 shows the wind roses at Tasiilaq as represented in the ERA-I and ASR-I. The ERA-I (Fig. 3a) clearly captures the prevalent northeasterly flow in the region that is associated with the barrier winds and there exists evidence of a clockwise turning of the winds towards northwesterly. The ASR-I (Fig. 3b) also captures this prevalence of barrier flow, albeit with slightly different directional characteristics. In contrast to the ERA-I, the ASR-I also includes a distinct secondary maximum for northwesterly flow that is representative of katabatic flow in the region.

As has been described in this article, the topographically forced weather systems that occur in southeast Greenland play an important role in the regional weather and climate. The changing nature of the climate in the region, such as the warming of the ocean and the retreat in sea ice, may have resulted in modifications of these weather systems. These systems are all strongly impacted by the nature of the storms that pass through the region and changes to their frequency, intensity or track can also impact these winds and their impact on the climate. The data sparse nature of the region and its complex topography along with the

mesoscale nature of these topographic jets makes it a challenge to study them. As a result, atmospheric reanalyses have played a crucial role in their characterization. Reanalyses with sufficient resolution to capture the mesoscale nature of these weather systems are now becoming available. As described in this article, new and potentially important details on their structure are now becoming clear. For example, higher speed barrier flow tends to occur in regions where there are coastal ridges; while katabatic flow is absent from these regions and is focused into the fjords that typically occur along the sides of these ridges. Caution must however be expressed because many features of these weather systems are strongly influenced by the parameterizations that are part of the underlying data assimilation systems. Without a control for these influences, it is a challenge to assess the improvement in the representation of these weather systems that arises from increased horizontal resolution. As was found to be the case in the vicinity of Sermilik Fjord (Oltmanns et al. 2014), the availability of meteorological data in regions that are more representative of these weather systems, as opposed to the current stations that have a fair weather bias, would be of benefit in reducing the uncertainty as to their structure and impact.

References

- Amundson, J.M., M. Fahnestock, M. Truffer, J. Brown, M.P. Lüthi, and R. J. Motyka, 2010: Ice mélange dynamics and implications for terminus stability, Jakobshavn Isbrae Greenland. *J. Geophys. Res.-Earth Surf.*, **115**, F01005.
- Arrigo, K.R., 2007: Chapter 7 physical control of primary productivity in Arctic and Antarctic polynyas. *Polynyas: windows to the worlds oceans*, W.O. Smith and D.G. Barber, Eds., Elsevier, Amsterdam, 223-238.
- Barstad, I., and S. Gronas, 2005: Southwesterly flows over southern Norway - mesoscale sensitivity to large-scale wind direction and speed. *Tellus Ser. A*, **57**, 136-152.
- Bromwich, D.H., and D.D. Kurtz, 1984: Katabatic wind forcing of the Terra-Nova Bay Polynya. *J. Geophys. Res.: Oceans*, **89**, 3561-3572.
- Bromwich, D.H., et al., 2014: Contrasting the regional Arctic System Reanalysis with the global ERA-Interim Reanalysis. *Q.J.R. Meteor. Soc.*, submitted.
- Cappelen, J., P.V. Jørgensen, E.V. Laursen, L.S. Stanius, and R.S. Thomsen, 2001: *The observed climate of Greenland, 1958-99 - with climatological standard normals. 1961-90*. Technical Report 00-18, Danish Meteorological Institute, 154p.
- Condron, A., and I.A. Renfrew, 2013: The impact of polar mesoscale storms on northeast Atlantic Ocean circulation. *Nat. Geosci.*, **6**, 34-37.
- Daniault, N., P. Lherminier, and H. Mercier, 2011: Circulation and transport at the southeast tip of Greenland. *J. Phys. Oceanogr.* **41**, 437-457.
- Dee, D. P., et al., 2011: The ERA-Interim reanalysis: configuration and performance of the data assimilation system. *Q.J.R. Meteor. Soc.*, **137**, 553-597.
- Doyle, J.D., and M.A. Shapiro, 1999: Flow response to large-scale topography: The Greenland tip jet. *Tellus Ser. A*, **51**, 728-748.
- DuVivier, A.K., and J.J. Cassano, 2013: Evaluation of WRF model resolution on simulated mesoscale winds and surface fluxes near Greenland. *Mon. Wea. Rev.*, **141**, 941-963.
- Haine, T.W.N., S. Zhang, G.W.K. Moore, and I.A. Renfrew, 2009: On the impact of high-resolution, high-frequency meteorological forcing on Denmark Strait ocean circulation. *Q.J.R. Meteor. Soc.*, **135**, 2067-2085.
- Harden, B.E., and I.A. Renfrew, 2012: On the spatial distribution of high winds off southeast Greenland. *Geophys. Res. Lett.*, **39**, L14806.
- Harden, B.E., I.A. Renfrew, and G.N. Petersen, 2011: A climatology of wintertime barrier winds off southeast Greenland. *J. Climate*, **24**, 4701-4717.
- Heinemann, G., 1999: The KABEG'97 field experiment: An aircraft-based study of katabatic wind dynamics over the Greenland ice sheet. *Bound.-Layer Meteor.*, **93**, 75-116.
- Hocking, C., 1969: Dictionary of disasters at sea during the age of steam. Lloyd's Register of Shipping, London, 493 p.
- Hoskins, B.J., and K.I. Hodges, 2002: New perspectives on the Northern Hemisphere winter storm tracks. *J. Atmos. Sci.*, **59**, 1041-1061.
- Howat, I.M., Y. Ahn, I. Joughin, M.R. van den Broeke, J.T.M. Lenaerts, and B. Smith, 2011: Mass balance of Greenland's three largest outlet glaciers, 2000-2010. *Geophys. Res. Lett.*, **38**, L12501.
- Klein, T., and G. Heinemann, 2002: Interaction of katabatic winds and mesocyclones near the eastern coast of Greenland. *Meteor. Applic.*, **9**, 407-422.
- Laffineur, T., C. Claud, J.-P. Chaboureaud, and G. Noer, 2014: Polar lows over the Nordic Seas: improved representation in ERA-Interim compared to ERA-40 and the impact on downscaled simulations. *Mon. Wea. Rev.*, in press.
- Liu, A.Q., G.W.K. Moore, K.Tsuboki, I.A. Renfrew, 2006: The effect of the sea-ice zone on the development of boundary-layer roll clouds during cold air outbreaks, *Bound-Layer Meteor.*, **118**, 557-581.

- Mills, B.J., and M.R. Anderson, 2003: Monitoring a piteraq storm system using DMSP imagery and Quikscat wind data. Preprints, *12th Conf. on Satellite Meteorology and Oceanography, Long Beach, CA, American Met. Soc.*
- Moore, G.W.K., 2003: Gale force winds over the Irminger Sea to the east of Cape Farewell, Greenland. *Geophys. Res. Lett.*, **30**, 1894.
- Moore, G.W.K., 2012: A new look at Greenland flow distortion and its impact on barrier flow, tip jets and coastal oceanography. *Geophys. Res. Lett.*, **39**, L22806.
- Moore, G.W.K., and I.A. Renfrew, 2005: Tip jets and barrier winds: A QuikSCAT climatology of high wind speed events around Greenland. *J. Climate*, **18**, 3713-3725.
- Murray, T., et al., 2010: Ocean regulation hypothesis for glacier dynamics in southeast Greenland and implications for ice sheet mass changes. *J. Geophys. Res.: Earth Surf.*, **115**, F03026.
- Oltmanns, M., F. Straneo, G.W.K. Moore, S.H. Mernild, 2014: Strong downslope wind events in Ammassalik, southeast Greenland. *J. Climate*, **27**, 977-993.
- Petersen, G.N., and I.A. Renfrew, 2009: Aircraft-based observations of air-sea fluxes over Denmark Strait and the Irminger Sea during high wind speed conditions. *Q.J.R. Meteor. Soc.*, **135**, 2030-2045.
- Pickart, R.S., M.A. Spall, M.H. Ribergaard, G.W.K. Moore, and R.F. Milliff, 2003a: Deep convection in the Irminger Sea forced by the Greenland tip jet. *Nature*, **424**, 152-156.
- Pickart, R.S., F. Straneo, and G.W.K. Moore, 2003b: Is Labrador Sea Water formed in the Irminger basin? *Deep-Sea Res. Part I*, **50**, 23-52.
- Rasmussen, L., 1989: Greenland winds and satellite imagery. *Vejret-Danish Meteor. Soc.*, 32-37.
- Renfrew, I.A., et al., 2008: The Greenland flow distortion experiment. *Bull. Am. Meteor. Soc.*, **89**, 1307-1324.
- Renfrew, I.A., S.D. Outten, and G.W.K. Moore, 2009: An easterly tip jet off Cape Farewell, Greenland. I: Aircraft observations, *Q.J.R. Meteor. Soc.*, **135**, 1919-1933.
- Sampe, T., and S.P. Xie, 2007: Mapping high sea winds from space: A global climatology. *Bull. Am. Meteor. Soc.*, **88**, 1965-1978.
- Skamarock, W.C., 2004: Evaluating mesoscale NWP models using kinetic energy spectra. *Mon. Wea. Rev.*, **132**, 3019-3032.
- Straneo, F., G.S. Hamilton, D.A. Sutherland, L.A. Stearns, F. Davidson, M.O. Hammil, G.B. Stenson, and A. Rosing-Asvids, 2010: Rapid circulation of warm subtropical waters in a major glacial fjord in East Greenland. *Nat. Geosci.*, **3**, 182-186.
- Våge, K., T. Spengler, H.C. Davies, and R.S. Pickart, 2009: Multi-event analysis of the westerly Greenland tip jet based upon 45 winters in ERA-40. *Q.J.R. Meteor. Soc.*, **135**, 1999-2011.
- Walter, J.I., J. E. Box, S. Tulaczyk, E. E. Brodsky, I. M. Howat, Y. Ahn, and A. Brown, 2012: Oceanic mechanical forcing of a marine-terminating Greenland glacier, *Ann. of Glaciol.*, **53**, 181-192.



2014 US AMOC Science Team Meeting

September 9 - 11, 2014
Seattle, Washington



The US Atlantic Meridional Overturning Circulation (AMOC) Science Team,

comprised of over 100 project scientists working to increase the understanding of the AMOC, is convening a meeting to share research findings, identify gaps in understanding and measurement of AMOC, foster collaborations, and discuss near-term priorities and long-term goals to guide future research.

The meeting is open to all US and international scientists interested in learning about and/or sharing research on AMOC, including its linkages with climate variability and change.

[Click here to Register!](#)

Deadline for abstract submission is June 16

Registration: \$100

Student/Early Career: \$50

Atlantic water variability on the southeast Greenland shelf

David A. Sutherland¹, Fiamma Straneo², and Benjamin E. Harden²

¹University of Oregon

²Woods Hole Oceanographic Institution

Rapid climate change is often linked to changes in the freshwater budget of the subpolar North Atlantic Ocean, since this region is sensitive to low-salinity anomalies that might affect the formation of North Atlantic Deep Water (e.g., Weijer et al. 2012). Thus, historically, oceanographers have focused on describing and quantifying the major freshwater pathways with an emphasis on salinity as the critical water property (e.g., Dickson et al. 2007). Recently however, focus has shifted shoreward as the Greenland Ice Sheet (GrIS) underwent rapid and large changes over the decade 2000-2010, with increased net mass loss observed via many of its outlet glaciers (Joughin et al. 2012; Straneo and Heimbach 2013). Glaciers in southeast (SE) Greenland, in particular, accelerated in the early 2000s and peaked in 2005, while glaciers in west Greenland showed mixed velocity variability (Moon et al. 2012). Causes for these dynamic changes are still not well understood, but hypotheses usually include a combination of increased surface melting that drives more lubricating meltwater to the glacier bed, with a) increased submarine melting, and/or b) loss of the buttressing ice mélange due to changes in ocean heat transport (Straneo et al. 2013).

One thing that is clear from the emerging Greenland ice-ocean interactions community is the importance of water temperature, and in particular, the heat content of the Atlantic-origin layer of water that is observed in many of Greenland’s glacial fjords. However, we are still in the beginning phases of understanding the variability and transport of this Atlantic-origin water not only in the fjords, but also around the periphery of Greenland’s coast. Despite an emphasis on obtaining ocean measurements around Greenland to quantify the freshwater pathways, the observational record on the continental shelf is still sparse in space and time.

Here, we focus on the sources and variability of Atlantic-origin water (AW) on the SE Greenland shelf (Fig 1a). AW carries the largest amount of heat to Greenland’s glacial fjords and thus represents a source of variability when considering submarine melting of glaciers and icebergs. In addition, understanding the SE Greenland sector is critical as this is where we see the warmest

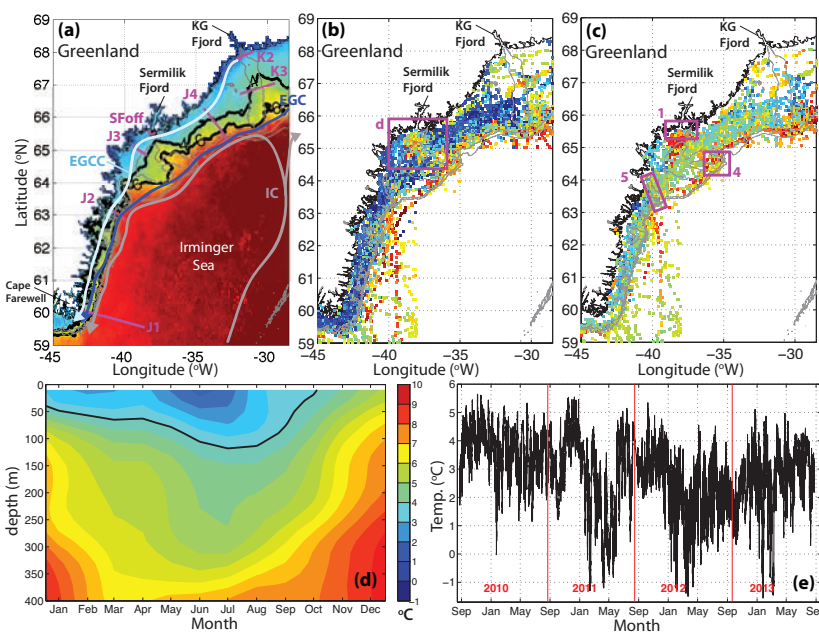


Fig. 1 (a) Annual average 2004 SST data overlaid with regional map of the SE Greenland shelf. Gray lines are from GEBCO bathymetry (400 m and 1000 m), black contours mark the 4°C and 6°C SST isotherms, and arrows show the pathways of major upper layer currents. Magenta lines indicate CTD transects discussed in the text. (b) The seal-derived summertime *T* field averaged over 0-50 m. The magenta box shows where the data analyzed in panel *d* comes from. (c) Same as *b*, but averaged from 200-250 m. Boxed regions show areas where AW vertical structure was analyzed. Panels *a-c* from Sutherland et al. (2013). (d) Seal-derived seasonal cycle of *T* in boxed region shown in panel *b* (Straneo et al. 2010). (e) Complete time series combined from moorings in the channel outside the mouth of SF (Harden et al. 2014). Vertical lines show the deployment years.

AW that circulate around Greenland (Straneo et al. 2012). The observational record on the SE Greenland shelf is arguably the most complete from the subpolar North Atlantic, although, as discussed below, there are many questions and challenges ahead.

Sources of AW

South of Denmark Strait (Fig. 1a), AW comes from two main sources: relatively warm waters direct from the Irminger Sea flow southward in the retroflecting Irminger Current (IC), while a cooled and freshened AW is carried alongside the cold Arctic waters that advect southward in the East Greenland Current (EGC) (e.g., Rudels et al. 2002; Sutherland and Pickart, 2008; Bacon et al. 2014). A sharp temperature and salinity front separates the IC and EGC in the horizontal and is usually located over the shelfbreak and continental slope. The 6°C isotherm from annual averages of SST (Fig. 1a) is a useful indicator of the EGC/IC front at the surface. However, the slope waters from the Irminger Sea also penetrate onto the SE Greenland continental shelf, so a vertical layering of water masses also occurs, with warmer Irminger Sea water overlain by colder EGC waters.

Hydrography from glacial fjords around Greenland all exhibit this cold/warm layering to some extent, with the temperature

of the warm, salty AW dependent on the distance from a source (Straneo et al. 2012). In SE Greenland, one can differentiate AW into several sources. From Sermilik Fjord (SF) south, observations show undiluted Northeast Atlantic Water (NEAW) that comes from the Irminger Sea (e.g., Malmberg et al. 1967; Sutherland and Pickart 2008) with $T > 7^{\circ}\text{C}$ and $S > 35$ (Fig. 2), while waters close to the EGC/IC front show signs of some mixing and have cooled and freshened slightly, with $4.5^{\circ}\text{C} < T < 6.5^{\circ}\text{C}$ and $34.8 < S < 35.1$. We call this water mass Irminger Sea Atlantic Water (ISAW), as it is the main source of AW for most of the SE Greenland shelf. ISAW is the result of mixing between NEAW and Polar Surface Water (PSW), a polar-origin water (PW) contained in the EGC (Fig. 2). Warmed and freshened versions of PSW are grouped into a variable water mass called warm PSW (PSWw). North of the SF region, the continental shelf is wide and cut by the Kangerdlugssuaq Trough that leads to a large outlet glacial fjord, Kangerdlugssuaq Fjord (KG, Fig. 1). In this region, the IC does not affect water properties directly, so the main source of AW has made the circuit into the Nordic Seas, and potentially into the Arctic Ocean, before returning through Denmark Strait. This water mass is called Re-circulating Atlantic Water (RAW), and is cooler, $0^{\circ}\text{C} < T < 2^{\circ}\text{C}$, and fresher, $34.5 < S < 34.8$ (Fig. 2), than the other types of AW (Rudels et al. 2002).

Observations of AW on the SE Greenland shelf

We base the discussion of AW here on hydrographic observations collected on the shelf over the last decade and recent glacial fjord studies. In 2004, the RRS *James Clark Ross* occupied cross-shelf transects (J1-J4, Fig. 1) from Cape Farewell to north of Denmark Strait (Sutherland and Pickart 2008). In 2008, the R/V *Knorr* studied the KG trough region (K2-K3, Fig. 1a), taking sections across the trough to resolve flow of water in the submarine canyon (Sutherland et al. 2014). And since 2008, repeat CTD sections have been collected across a narrow (~15 km), deep (~650 m) channel that cuts across the mouth of SF (SFoff, Fig. 1a).

We supplement these highly spatially resolved CTD transects with several other sources of data to describe the broader spatial variability, as well as the temporal variability. First, we look at temperature profiles obtained from 104 deep-diving seals tagged with satellite relay depth loggers that resulted in 37011 individual dives (Fig. 1b,c) on the SE Greenland coast (Sutherland et al. 2013). Second, we use four years of subsurface mooring data (Harden et al. 2014) from the channel outside SF (Fig. 1a,e). The flow through this channel brings with it the deeper AW originally from the shelfbreak (Sutherland et al. 2014; Harden et al. 2014).

Finally, we rely on numerous other studies that have collected observations on the shelf and inside both SF and KG. In KG, data

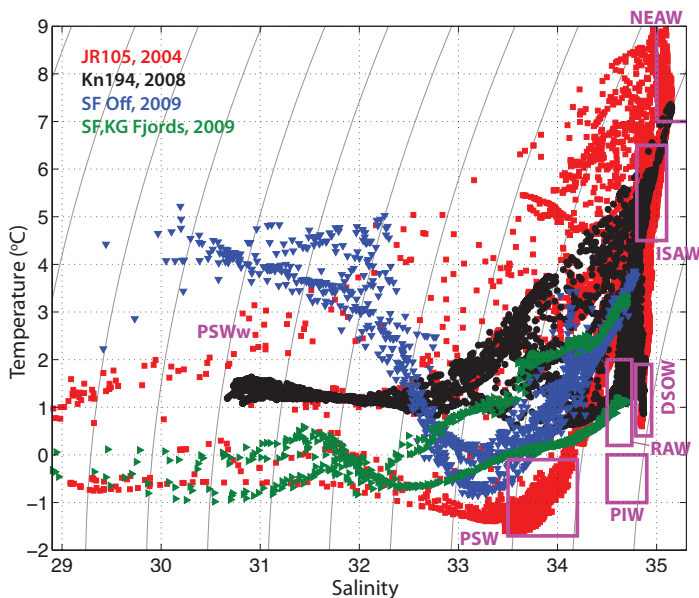


Fig. 2 Potential temperature-salinity diagram for data from various observations on the SE Greenland shelf discussed in text. Boxes delineate water masses defined in text. Gray lines are σ_{θ} isopycnals contoured every 0.5 kg m^{-3} , with the densest contour equal to 28 kg m^{-3} .

have been collected in summertime synoptic surveys sporadically since 1994 (Azetsu-Scott and Tan 1997; Christoffersen et al. 2011; Sutherland et al. 2014; Inall et al. 2014), showing AW at depth. In SF, the record only extends back to 2008 (Straneo et al. 2010), but now is arguably the most well studied fjord system in Greenland (e.g., Murray et al. 2010; Sutherland et al. 2014), with deep layer T ranging from 3-4°C that reflect their Irminger Sea origin.

Spatial variability

Along and across shelf gradients

Two main mechanisms drive AW variability in the along-shelf direction on the shelf. First, the retroflexion of the IC at Denmark Strait causes ISAW to be introduced to the shelf at a latitude of ~65°N. Thus the shelf south of that latitude shows warmer and saltier water properties than the northern shelf in general. Second, submarine canyons that cut across the shelf essentially divert the EGC/IC system shoreward, bringing the warmer and saltier AW (either ISAW or RAW) in closer proximity to the glacial fjord mouths (Fig. 1). This results in warm anomalies over the northward rims of most submarine canyon features on the shelf (Fig. 1).

These canyons also act as conduits for the AW to reach the fjords at deeper levels, as most of the AW in the IC sits below shelfbreak depths. A section across the KG trough near the mouth of KG fjord illustrates this mechanism (Fig. 3e). On the east side of the trough, relatively warm (3-4°C) and salty ($S>34.5$) water is observed flowing towards the fjord mouth. Outside SF, we observe AW at depth as well, with the warmest ($T>3^{\circ}\text{C}$) and saltiest ($S>34.5$) water occupying the layers below 400 m (Fig. 3d). The waters here flow towards the southeast across the mouth of SF (Sutherland et al. 2014; Harden et al. 2014). This differs from the flow up the KG trough that leads directly into the KG fjord.

Across the shelf, AW cools and freshens in general from its value in the Irminger Sea interior (Fig. 1). A 2004 section across the shelf (Fig. 3f) illustrates this gradient, as NEAW is observed at the shelfbreak offshore of the EGC/IC front. Continuing onshore, the warmest water is observed underneath the cooler PW layer. This pattern of across-shelf variability is observed in most cross-shelf transects (e.g., J1-J3, Fig. 1) – it breaks down where submarine canyons are present that allow more direct communication with the interior.

Vertical structure

The vertical structure of water properties on the SE Greenland shelf depends on the mechanism responsible for bringing AW onto the shelf. For example, when the EGC/IC is diverted towards shore by the presence of submarine canyons, the vertical layering of PW over AW is preserved. There is typically a two-layer structure on the shelf with PW overlaying AW. The fact that AW is observed to be cooler and fresher across the shelf suggests that some mixing has

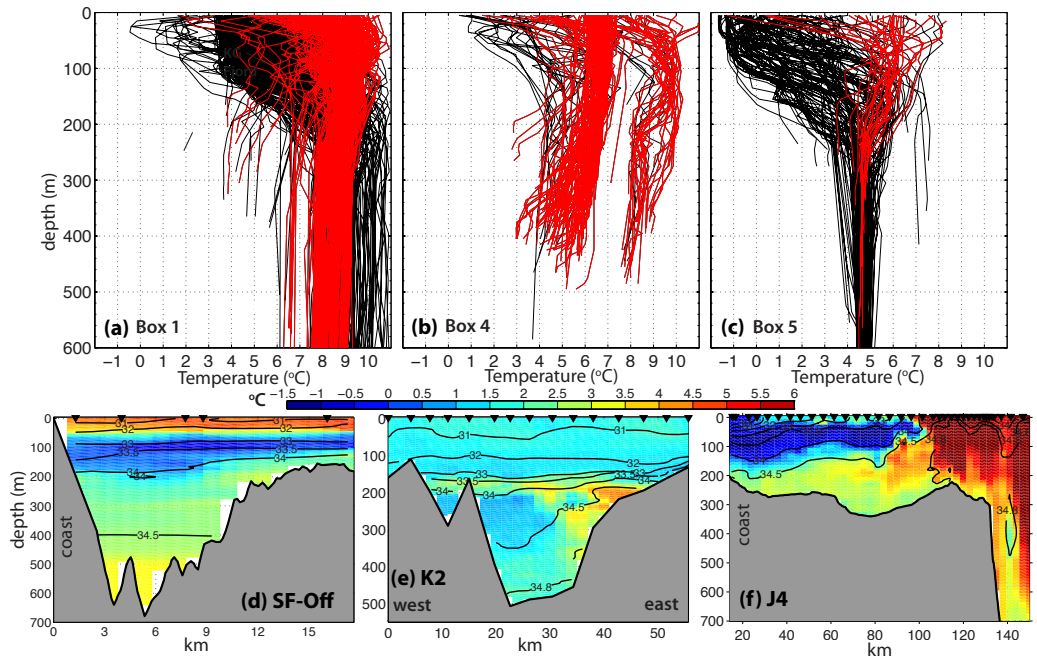


Fig. 3 (a-c) Seal-derived temperature profiles versus depth for each box in Figure 1c (Sutherland et al. 2013). For profiles deeper than 200 m, color highlights “warm” mode (red) and “cold” mode (black). (d) Temperature section from CTD transect across channel outside SF mouth (SFoff) with select salinity contours in black. CTD locations are marked by black triangles. Panels d-e from Sutherland et al. 2014. (e) Same as d, but for the KG trough section K2. Note the color scale stays constant in all panels, but the depth scale and x-axis change. (f) Same as d, but for the JR105 across-shelf transect J4 (Sutherland and Pickart 2008). Note the color scale is saturated at warm temperatures for this section.

occurred between the two water masses – this mixing line is almost linear, connecting the AW type to PW on a T/S diagram (Fig. 2).

However, we also find times when vertical profiles of T and S have little depth variation resulting in full depth warm profiles. (Fig. 3a-c). This vertical structure is present off the shelf in the interior of the Irminger Sea. On the shelf, it is likely indicative of AW eddies that form and propagate shoreward from the EGC/IC front, or an excursion of the IC into the larger submarine canyons. It is well known that the EGC/IC front is baroclinically unstable here (e.g., Magaldi et al. 2011). The link between the mesoscale variability associated with the EGC/IC front and the cyclones produced by the Denmark Strait overflow is uncertain. Regardless, these eddies keep the AW inside their core relatively unmixed in their travel across the shelf.

The seal data provide the best look at the occurrence of these two modes of AW vertical structure. Sutherland et al. (2013) grouped seal profiles by region (Fig. 1c) to examine the timing of what they term “cold” mode (PSW present in the upper layer) and “warm” mode (all AW) temperature profiles (Fig. 3a-c). We hypothesize that the warm mode profiles must derive from the interior of the Irminger Sea, outside the influence of the EGC where temperature values match those found in the warm mode profiles. A large majority (78%) of all profiles in box 4, located offshore of the EGC in the Irminger Sea, are warm mode, as expected.

The majority of all seal dives occurred in box 1, located near the mouth of SF. 29% of the box 1 profiles were warm mode, with some bottom $T > 8^{\circ}\text{C}$, suggesting that NEAW is advected this far inshore, an observation supported by mooring time series outside SF (Harden et al. 2014). There is no evidence that water this warm enters SF, most likely due to bathymetric constraints and the coastal wedge of freshwater acting as a barrier, forcing modification of the AW as it mixes with PSW. In another trough cutting towards the Greenland coast in box 5, the T structure resembles that from box 1, but without the unmodified IC waters present (Fig. 3c). The absence of NEAW is presumably due to the lack of a pure advective pathway into this area, as well as being further alongstream in the EGC/IC system.

In an average sense, however, the cold mode prevails on the shelf, which can be seen by looking at binned seal T data at different depth levels. Fig. 1b-c show two depth levels, 0-50 m, and 200-250 m, of averaged T gridded into 5 km boxes, and support the importance of bathymetry in channeling flows along the coast. NEAW is found seaward of the continental shelf/slope region at both depths. The coldest water, stemming from the polar-origin EGC, is found at the shallower depth on the bank north of the submarine canyon extending towards SF, then in a narrow band sandwiched between

the coast and the warmer IC water. This is consistent with the observed behavior of the East Greenland Coastal Current (EGCC) in this area (Bacon et al. 2014; Sutherland and Pickart, 2008). The warm water intrudes along the 300-400 m isobath in all layers, creating strong horizontal temperature gradients in the upper 150 m. Downstream of SF, colder water is found again in a widened band, suggesting the intrusion of AW is a meander of the IC along with the EGC towards the coast. The KG Trough (Fig. 1) also significantly influences $T(z)$ there (Christoffersen et al. 2011).

Temporal variability

Synoptic scale

Variations in AW properties, and the proportion of the water column they constitute, occur over a wide range of temporal scales, and are linked to the mechanisms responsible for the spatial variability discussed above. On synoptic timescales, wind and instabilities of the EGC/IC front can cause variability in the AW observed on the shelf. Along-shelf winds have been shown to modulate the isopycnal tilt of the EGC/IC front, leading to depth variations in water properties (Sutherland and Pickart 2008; Bacon et al. 2014). Strong downwelling favorable winds dominate the southeast Greenland coast, peaking in winter during the stormy period (e.g., Harden et al. 2014), and this can steepen the EGC/IC front. The influence of these winds on the PW/AW interface is thought to be a main control on the circulation variability observed in SF and KG fjord, termed intermediary circulation (Straneo et al. 2010; Sutherland et al. 2014; Jackson et al. 2014). Presumably, these winds could also excite coastally trapped waves that propagate along the coast, so remote wind events could drive variability, although the irregular bathymetry of the shelf makes these waves hard to predict using traditional methods (Harden et al. 2014).

Synoptic variability is observed at the mooring site outside SF in the AW layer over all four years of the time series (Fig. 1e). The high-frequency variability is superimposed on seasonal and interannual variations. However, the synoptic variability in the isotherm depths (and isopycnal depths) is significant, showing changes at a fixed depth on the order of $1\text{-}2^{\circ}\text{C}$, with maximum swings of 4°C over a timescale of days. Harden et al. (2014) showed that strong downwelling wind events are well correlated with anomalies in SSH and potential density at this location.

Seasonal cycle

The seasonal cycle of water properties on the shelf is not intuitive: the warmest waters show up starting in the fall months and peak in Nov-Dec (Fig. 1d,e). Mooring observations support this cycle (Fig. 1e), though they are somewhat masked by the vigorous synoptic and interannual variability. Here, we use the seal data averaged over a

region near SF (Fig. 1*b*) for the years 2004–2008 to build a seasonal cycle of T on the shelf (Fig. 1*d*). These data show the thickening of a colder, PW layer from mid-winter through spring and into mid-summer down to 100 m. Local sea ice and iceberg melt would lead to peak freshwater signals in July–August. Thus, the observed cooling is presumably due to the seasonal strengthening of the EGC and increased freshwater export out of the Arctic Ocean through Fram Strait that peaks in late summer and takes 4–5 months to advect down to the SE Greenland shelf (Harden et al. 2014). During the fall and winter months, the entire water column T down to 400 m increases. This picture of seasonal variability is supported by a mooring time series (not shown) located at 63°N (Bacon et al. 2014). This suggests that a similar late fall warming is happening over the southern part of the SE Greenland shelf – we lack the data to speculate on whether the same seasonal cycle emerges near KG and northward.

Interannual variations

Perhaps of most interest to glaciologists are variations in heat content on interannual time scales, as these are what are implicated in the warm ocean trigger hypothesis of outlet glacier acceleration (e.g., Holland et al. 2008). Basin-wide studies of the subpolar North Atlantic suggest that the interior waters are warming, and have been doing so since the late 1990s (Straneo and Heimbach 2013). Bottom temperatures on the west Greenland shelf were observed to increase at the same time, implicating the subpolar North Atlantic as the source of increased heat content (Holland et al. 2008). However, we have no coincident time series from inside the glacial fjord systems to make the link between the shelf conditions and the water properties near glacier termini. In addition, an increase in heat content in the fjords can be the result of two different mechanisms: an increase in the abundance of AW on the shelf that is advected into the fjords, or a change in the end-member AW properties themselves with no change in AW volume on the shelf.

The longest time series we have from the SE Greenland shelf come from the subsurface moorings located outside the SF mouth (Fig. 1*a*). Time series from 2009–2013 show large interannual variations,

with mean annual values differing by as much as 3°C (e.g., 2009–2010 compared to 2012–2013). To extend this to other areas on the shelf requires the use of hydrographic cruise data. The most common measurements are collected in individual summertime research cruises – thus the interannual variability inferred from these observations must be handled carefully in light of the large seasonal and synoptic variability discussed above. Nevertheless, these data are often the only observations available. Christoffersen et al. (2011) show a significant warming of waters in KG fjord from 1993 to 2004, based on synoptic CTD sections.

Conclusions and future challenges

Much has been learned about water mass property changes in the interiors of the subpolar and subtropical North Atlantic Ocean from ARGO float deployments and years of hydrographic cruise data. We lack both of these pieces of evidence on the southeast Greenland shelf, where there have been only a handful of successful time-series observations collected and only a few research cruises undertaken mainly in summer. However, we do know that Atlantic Water enters Greenland's glacial fjords in some modified form, so mechanisms do exist for across-shelf transport, either directly via submarine canyons or as mesoscale eddies. The challenge is to relate the observed and predicted changes in AW from the large-scale interior across the shelf and into the fjords. Then, of course, this water must make it to the glacier termini. The southeast Greenland continental shelf is as difficult a place to make long-term oceanographic measurements as any outlet glacier fjord – deep-keeled icebergs, sea ice, and stormy winters all limit the availability of observations in this region. Progress will have to come from clever uses of moorings hidden in troughs, outside the influence of ice, and the combination of existing observations with high-resolution, regional ocean models that have accurate bathymetry. Understanding the variability of Atlantic Water on the southeast Greenland shelf is critical to improving predictions of heat transport to the Greenland Ice Sheet, ultimately informing scientists about future sea level rise rates and the impact of increased freshwater discharge on the subpolar North Atlantic circulation.

References

- Azetsu-Scott, K., and F.C. Tan, 1997: Oxygen isotope studies from Iceland to an East Greenland fjord: behavior of glacial meltwater plume. *Marine Chem.*, **56**, 239–251.
- Bacon, S., A. Marshall, N.P. Holliday, Y. Aksenov, and S.R. Dye, 2014: Seasonal variability of the East Greenland Coastal Current. *J. Geophys. Res.*, in press.
- Christoffersen, P., R.I. Mugford, K.J. Heywood, I. Joughin, J.A. Dowdeswell, J.P.M. Syvitski, A. Luckman, and T.J. Benham, 2011: Warming of waters in an East Greenland fjord prior to glacier retreat: mechanisms and connection to large-scale atmospheric conditions. *Cryosphere*, **5**, 701–714, doi:10.5194/tc-5-701-2011.
- Dickson, R., B. Rudels, S. Dye, M. Karcher, J. Meincke, and I. Yashayaev, 2007: Current estimates of freshwater flux through Arctic and subarctic seas. *Prog. Oceanogr.*, **73**, 210–230.
- Harden, B.E., F. Straneo, and D.A. Sutherland, 2014: Moored observations of synoptic and seasonal variability in the East Greenland Coastal Current, *J. Geophys. Res.*, submitted.
- Holland, D. M., R.H. Thomas, B. De Young, M.H. Ribergaard, and B. Lyberth, 2008: Acceleration of Jakobshavn Isbræ triggered by warm subsurface ocean waters, *Nature Geosci.*, **1**, 659–664.

- Inall, M.E., T. Murray, F.R. Cottier, K. Scharrer, T.J. Boyd, K.J. Heywood, and S.L. Bevan, 2014: Oceanic heat delivery via Kangerdlugssuaq Fjord to the south-east Greenland ice sheet. *J. Geophys. Res.*, **119**, doi:10.1002/2013JC009295.
- Jackson, R.H., F. Straneo, and D.A. Sutherland, 2014: Ocean temperature at Helheim Glacier controlled by shelf-driven flow in non-summer months, *Nature Geosci.*, in review.
- Joughin, I., R. Alley, and D.M. Holland, 2012: Ice-sheet response to ocean forcing. *Science*, **338**, 1172-1176.
- Magaldi, M.G., T.W.N. Haine, and R.S. Pickart, 2011: On the nature and variability of the East Greenland Spill Jet: a case study in summer 2003. *J. Phys. Oceanogr.*, **41**, 2307-2327, doi:10.1175/JPO-D-10-05004.1.
- Malmberg, S-A., H.G. Gade, and H.E. Sweers, 1967: Report on the second joint Icelandic-Norwegian expedition to the area between Iceland and Greenland Aug-Sept 1965. *NATO, Oceanogr. Res.*, Tech. Report 41, 44 pp.
- Moon, T., I. Joughin, B. Smith, and I. Howat, 2012: 21st-Century evolution of Greenland outlet glacier velocities, *Science*, **336**, 576-578, doi:10.1126/science.1219985.
- Murray, T., Scharrer, K., James, T.D., Dye, S.R., Hanna, E., Booth, A.D., Selmes, N., Luckman, A., Hughes, A.L.C, Cook, S., Huybrechts, P., 2010: Ocean-regulation hypothesis for glacier dynamics in south-east Greenland and implications for ice-sheet mass changes. *J. Geophys. Res.*, **115**, F03026, doi:10.1029/2009JF001522.
- Rudels, B., E. Fahrbach, J. Meincke, G. Budeus, and P. Eriksson, 2002: The East Greenland Current and its contribution to Denmark Strait overflow. *ICES J. Mar. Sci.*, **59**, 1133-1154.
- Straneo, F., G.S. Hamilton, D.A. Sutherland, L.A. Stearns, F. Davidson, M.O. Hammill, G.B. Stenson, and A. Rosing-Asvid, 2010: Rapid circulation of warm subtropical waters in a major, East Greenland glacial fjord. *Nature Geosci.*, **3**, 182-186, doi:10.1038/ngeo764.
- Straneo, F., D.A. Sutherland, D. Holland, C. Gladish, G. Hamilton, H. Johnson, E.
- Rignot, Y. Xu, and M. Koppes, 2012: Characteristics of ocean waters reaching Greenland's glaciers. *Ann. Glaciol.*, **53**, 202-210, doi:10.3189/2012AoG60A059.
- Straneo, F. and P. Heimbach, 2013: North Atlantic warming and the retreat of Greenland's outlet glaciers. *Nature*, **504**, doi:10.1038/nature12854.
- Straneo, F. et al., 2013: Challenges to understand the dynamic response of Greenland's marine terminating glaciers to oceanic and atmospheric forcing. *Bull. Amer. Met. Soc.*, **94**, 1131-1144.
- Sutherland, D.A. and R.S. Pickart, 2008: The East Greenland Coastal Current: structure, variability, and forcing, *Progr. Oceanogr.*, **78**, 58-77, doi:10.1016/j.pocean.2007.09.006.
- Sutherland, D.A., F. Straneo, G.B. Stenson, F.J.M. Davidson, M.O. Hammill, and A.
- Rosing-Asvid, 2013: Atlantic water variability on the SE Greenland continental shelf and its relationship to SST and bathymetry. *J. Geophys. Res.*, **118**, 847-855, doi:10.1029/2012JC008354.
- Sutherland, D.A., F. Straneo, and R.S. Pickart, 2014: Characteristics and dynamics of two major Greenland glacial fjords. *J. Geophys. Res.*, in review.
- Weijer, W., M.E. Maltrud, M.W. Hecht, H.A. Dijkstra, and M.A. Klijhuis, 2012: Response of the Atlantic Ocean circulation to Greenland Ice Sheet melting in a strongly-eddy ocean model. *Geophys. Res. Lett.*, **39**, L09606, doi:10.1029/2012GL051611.

Temperature variability in West Greenland's major glacial fjord: A driver of rising sea levels

Carl Gladish¹ and David Holland^{1,2}

¹New York University, Abu Dhabi

²New York University

The flooding of coastal cities by rising oceans is, in the public consciousness, perhaps the most vivid and dreaded effect of global climate change. Yet climate scientists cannot predict how rapidly melting of the Greenland and Antarctic ice sheets will contribute to sea level this century (Joughin et al. 2012a).

Global mean sea level has been increasing since tide gauges in harbors around the world began monitoring the ocean surface over one hundred years ago. These instruments show, in agreement with measurements from satellite altimetry over the last two decades, that mean sea level rose 3 mm/yr since the early 1990s and 2 mm/year over the 20th century

(Church and White 2011). These average rates hide the fact that sea level, even after averaging over tides and storms, does not rise uniformly around the world. Above-average rates of sea level rise, associated with decadal shifts in ocean currents, are already disrupting the lives of inhabitants of the tropical Western Pacific (Becker et al. 2012). On the other hand, continental uplift tends to make sea levels *fall* relative to Canadian or Scandinavian coastlines. More subtly, when water is unlocked from an ice sheet and spreads around the world ocean, the modification to Earth's gravity field pulls the ocean surface unevenly, such that sea levels around the UK will not be much affected by the melting of Greenland's ice sheet (Milne 2007, Milne et al. 2009).

Ocean triggered glacier change

Since the late 1990s several Greenland outlet glaciers¹ have started to discharge more ice into the ocean, mainly as icebergs, than they receive from the interior of the ice sheet, where ice accumulates from snowfall (Rignot & Kanagaratnam 2006). Along with changes in snowfall and surface melting, the net effect of these dynamical changes has been a significant acceleration in Greenland’s contribution to sea level (Rignot et al. 2011).

Thomas et al. (2003) found that Jakobshavn Glacier, the most prolific glacier in West Greenland, began to thin rapidly in 1997 in response to increased melting beneath the ten-kilometer tongue of floating ice that then preceded the final terminus of the glacier in Ilulissat Icefjord. This fjord, about 60 km long and less than 10 km wide, connects the terminus of Jakobshavn Glacier with Disko Bay to the west. Disko Bay is

in turn connected by the Egedesminde sea-floor trough to the continental shelf break along the eastern rim of Baffin Bay (Fig. 1). The West Greenland Current carries relatively warm water along the shelf break from Cape Farewell at the southern tip of Greenland and northwards past the entrance to Egedesminde trough. Thomas et al. (2003) pointed out that the warm core of the West Greenland Current warmed by about 1°C between summers of 1994 and 1999, measured just north of Cape Farewell, and therefore proposed that excessive heat carried by this current made its way into Ilulissat Icefjord and caused the thinning of Jakobshavn Glacier in 1997. This thinning was followed by ice acceleration and terminus retreat that has not yet halted (Joughin et al. 2012b). Holland et al. (2008) presented the spatial pattern of the sudden increase of summer ocean temperatures along the West Greenland coast around 1997 and related the warming to a shift in large-scale winds over

the North Atlantic starting in 1995. Hansen et al. (2012) showed that the warming of Disko Bay took place essentially during April 1997. Motyka et al. (2011) showed that the 1°C warming observed just outside the fjord, if communicated to the glacier through the fjord, was probably enough to cause the 25% increase in basal melting necessary to explain the observed thinning of the floating tongue. The warming of West Greenland waters since the 1990s and the correlation with changes at Jakobshavn Glacier have now been well documented (Myers et al. 2007; 2009).

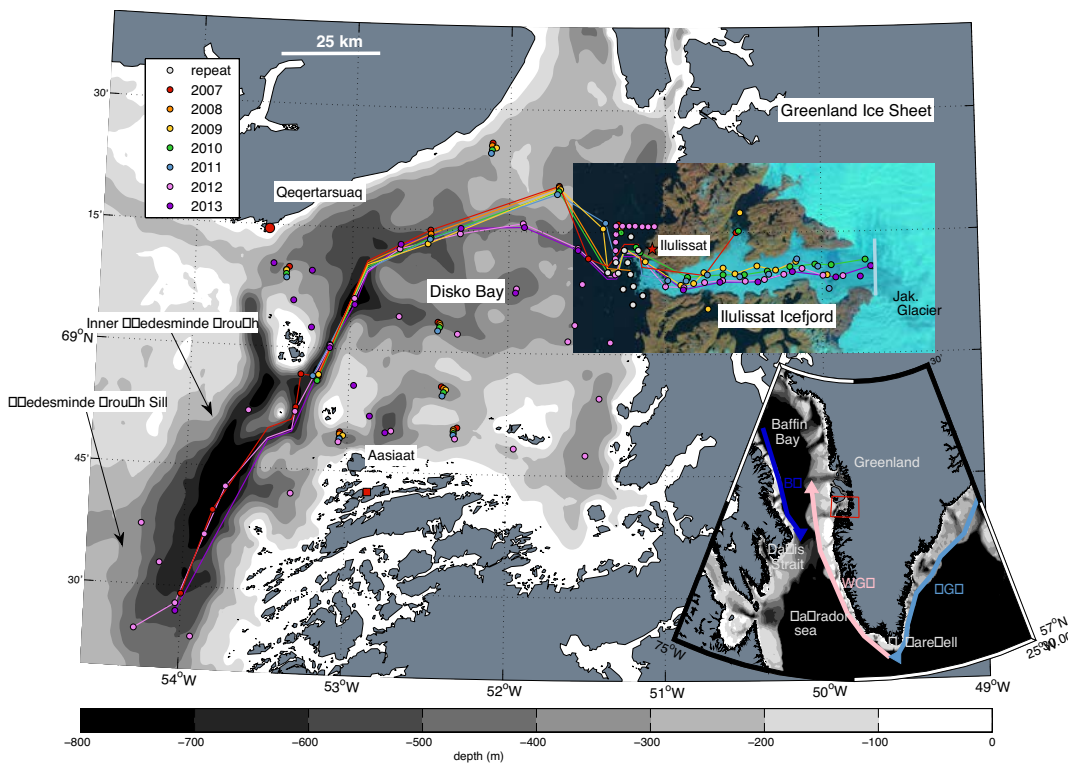


Fig. 1 Regional Map of Disko Bay and Ilulissat Icefjord with contours of sea-floor depth. A LANDSAT image from Sept 1999 shows the terminus of Jakobshavn Glacier when it still had a floating tongue. The light blue line shows a typical longitude of the terminus from 2010. Sites of ocean profiles are shown for 2007-2013 and thin lines join sites used in the Figure 2 sections. The inset overview map shows the Baffin Current (BC), West and East Greenland Currents (WGC & EGC).

¹Outlet glaciers are the fast-flowing streams of ice that drain the interior ice sheet into the ocean, typically flowing into the ocean at the heads of fjords which are 5 km to 20 km wide and tens of kilometers long. Greenland’s five biggest outlet glaciers drain 30% of the ice sheet, by area.

More generally, synchronous dynamic glacier changes around Greenland are unambiguous (Pritchard et al. 2009) and there is observational and model evidence that this is associated with ocean warming around Greenland (Straneo et al. 2012; Rignot et al. 2012). Changes occurring at Greenland outlet glaciers, including Jakobshavn Glacier, are now responsible for about half of Greenland's ongoing mass loss; surface melting over a wide low-elevation band around the ice sheet accounts for the other half (Straneo and Heimbach 2013).

Although the ocean-triggering hypothesis at Jakobshavn Glacier and elsewhere is broadly supported by available evidence, there are still important missing details. First, there is the question of exactly how warming of nearby fjord waters leads to thinning, acceleration and retreat of glaciers, especially when they lack a floating tongue. It has been shown with a numerical model that tripling the longitudinal strain rate of ice at the grounded terminus of Helheim Glacier, an important SE Greenland glacier, induces a glacier response similar to what was observed there in the early 2000s (Nick et al. 2009). That study did not, however, quantitatively explain how such a perturbation might come from ocean warming. On the other side of the ice-ocean interface, a super-linear dependence of melting on the temperature of ambient fjord waters has been determined using idealized plume (Jenkins 2011) and high-resolution ocean simulations (Xu et al. 2013). A guiding hypothesis for current research is that warmer waters enhance melting most near the base of the glacier terminus wall, particularly in summer when fresh water flowing out of the glacial hydrological system drives convection and consequently promotes turbulent heat transfer (e.g., Xu et al. 2013; Sciascia et al. 2013). The uneven melting then induces glacial stresses that promote iceberg calving (O'Leary and Christoffersen 2013) to the point that the terminus retreats, with a consequent force perturbation on upstream ice, as in Nick et al. (2009). Many questions remain regarding the inaccessible environments in the vicinity of Greenland glacial termini.

Fjord temperature variability

We also lack knowledge of how and why oceanic heat is delivered to the vicinity of outlet glaciers. Before the 2000s, there had been no direct measurements of seawater properties (i.e., temperature and salinity) near the terminus of Jakobshavn Glacier. Therefore, even possessing several decades of ocean observations along coastal West Greenland (e.g., Myers et al. 2009), it was not possible to

confidently infer how the ambient ocean conditions for Jakobshavn Glacier have changed in time.

In 2007 we began a program of ocean observations inside Ilulissat Icefjord and in Disko Bay. Locations where we collected ocean profiles appear in Figure 1. In this region the warmest waters, which can be traced back to surface waters of the sub-polar North Atlantic Ocean (McCartney and Talley 1982) are also the saltiest, and they turn out to be denser than colder and fresher waters coming from the Arctic Ocean. The warm Atlantic waters are therefore found below a layer of colder water, generally about 200 m thick, between Cape Farewell and Disko Bay. We found that the *basin waters*² filling the deepest 500 m of Ilulissat Icefjord were typically 2.5-3°C and came from an intermediate depth outside the fjord (Fig. 2). Judging by both the temperature and salinity, this basin water is made up of roughly equal fractions of warm Atlantic water and cooler Arctic water (see Gladish et al. 2014a,b for further details).

The 250 m deep sill guarding the entrance to Ilulissat Icefjord is the reason the 500 m thick basin water layer comes from a much shallower and thinner layer in Disko Bay, at essentially the depth of the interface between the upper Arctic water and warmer Atlantic water. The warmest summer deep waters in Disko Bay, typically 4°C, are in turn slightly cooler than the warmest waters traveling north in summer in the West Greenland Current, which have generally exceeded 4.5°C since the late 1990s (Myers et al. 2007). It appears, therefore, that sea-floor impediments block more and more of the warmest (i.e., deepest) water layers over the 500 km journey from the shelf break, along the Egedesminde trough, across Disko Bay, over the fjord sill, and towards the terminus of Jakobshavn Glacier (Gladish et al. 2014b). The fact that the majority of the water confronting Jakobshavn Glacier is an almost equal mixture of low-salinity Arctic water and high-salinity Atlantic water means that temperature variability in either water type significantly influences the thermal environment of the glacier.

In summer of 2010, the sub-surface waters of both Disko Bay and Ilulissat Icefjord were about one degree cooler than in

²There is a *sill* (a shallow sea-floor ridge) crossing the fjord mouth, close to the red star in Fig. 2. The sill, which reaches 250 m at its deepest point, gives the lower 500 m of the 800 m deep fjord the character of a giant bathtub and *basin waters* here refers to the quite homogeneous waters found in the "bathtub" below the sill depth.

other years from 2009 to 2013 (Fig. 2). This isolated anomaly is rich in implications for fjord dynamics and for sources of inter-annual ocean variability. First, the 2010 anomaly tells us, with high confidence, that fjord waters are fully exchanged with Disko Bay on a timescale of at most one year, despite the sill barrier. Renewal occurring on a shorter timescale can not be resolved with summer-only measurements. Nevertheless, synoptic velocity profiles taken in the fjord in summer 2013 suggest that currents of ~10 cm/s in the deep fjord basin and corresponding shallow outflows were, at that time, on track to renew the fjord in just 1-2 months. Furthermore, model simulations show that such a flow could be driven by realistic rates of subglacial discharge of surface melt waters in summer (Gladish et al. 2014a). If exchange between the fjord and Disko Bay is driven in this way in summer, the admixture of buoyant freshwater into the fjord basin near the glacier terminus must create large amounts of water denser than the fresh surface cap³ but lighter than the salty water pouring over the sill. We therefore ought to observe fast counter-flowing currents over the narrow saddle point of the sill. However, the presence of large and potentially dangerous icebergs in the sill area makes such observations difficult.

To complete the picture above, we would like to rule out the possibility of fjord renewal in the absence of subglacial meltwater discharge (i.e., outside of summer). Indeed, we found from short mooring time-series (weeks to months) in the fjord and from instrumented seals and halibut that temperatures each winter are very stable in the fjord basin (changing by tenths of a degree below sill depth over several winter months). The reason for such quiescence is either: a) there is a lack of exchange with Disko Bay outside of summer, or b) Disko Bay itself has small temperature variability over winter at the depths which feed the fjord. A year-long mooring in Disko Bay at 350 m depth between summer of 2011 and 2012 showed only a gradual trend of warming from about 3.0°C to 3.5°C, with weekly to monthly variability smaller than the overall trend (Gladish et al. 2014a). This mooring was at least 100 m below the layer of Disko Bay water that enters the fjord, however, so neither hypothesis a) or b) can be confidently eliminated. Disko Bay bottom water may be shielded from variability on the outer shelf by the sill-like

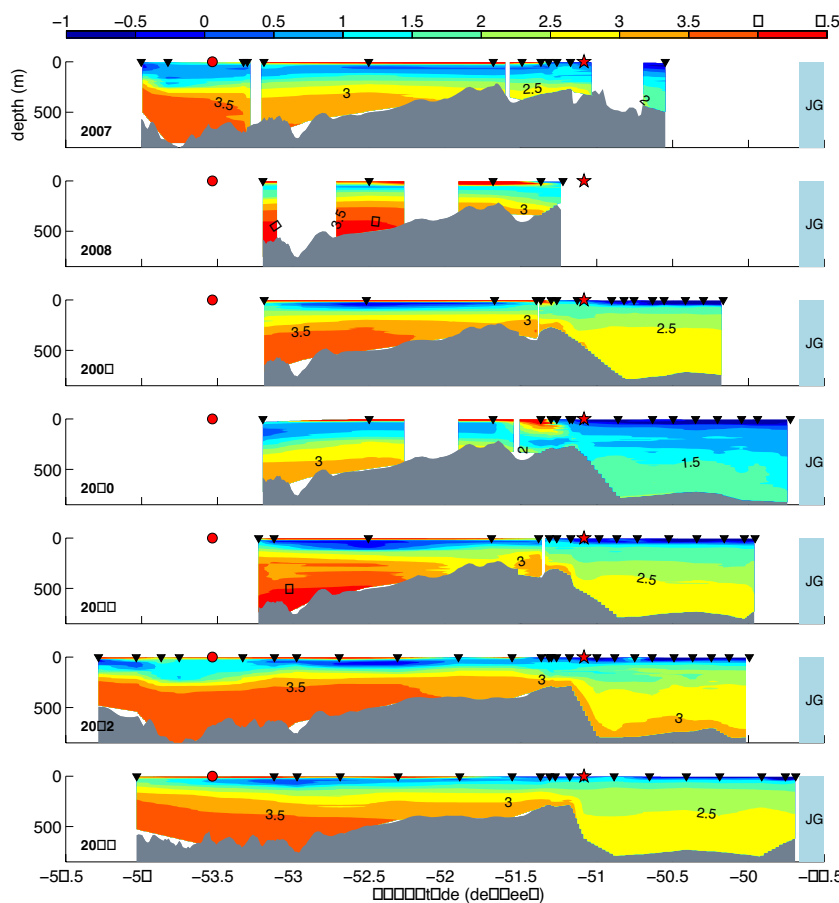


Fig. 2 Cross-sections of potential temperature through Disko Bay and Ilulissat Icefjord from 2007 to 2013. Ocean profiles are marked by inverted black triangles. The glacier terminus (JG) is shown at the location of the blue line in Figure 1. White areas indicate missing data or large time gaps in between adjacent profiles. The red circle and star marks two towns, as shown in Figure 1, to help interpretation. Grey regions outside the fjord indicate bathymetry from IBCAO v3.

barrier that blocks the Egedesminde Trough below 300 m depth just west of Disko Bay (Fig. 1, see Gladish et al. (2014b) for discussion). Straneo et al. (2010) found that Sermilik fjord (associated with Helheim glacier) can be renewed on a timescale of weeks as a result of baroclinic pressure gradients at the fjord mouth produced by along-shore winds.

³The thin freshwater cap disappears outside of summer, so it must be maintained by freshwater runoff and the sub-aerial melting of icebergs in the fjord.

The wind forcing over the west-central coast of Greenland is not necessarily comparable to that along the SE coast of Greenland, but our findings do suggest that its bathymetric idiosyncrasies makes Ilulissat Icefjord less susceptible to high-frequency (i.e., synoptic to sub-seasonal) meteorological forcing than Sermilik Fjord, which has a deeper entrance and a less restricted connection to the shelf break.

We know that from 2009 to 2013 the fjord basin contained water with potential density $\sigma\theta$ in the range of 27.2 to 27.3, despite the one-degree inter-annual changes. Furthermore, the depth of waters in this density range has not changed in a statistically significant way since the 1980s in western Disko Bay. So we can tentatively assume that the temperature of Disko Bay waters in this density range are representative of fjord temperatures going back to the 1980s. In summer 2010 the fjord basin waters were nearly as cool, we therefore infer, as they were prior to the abrupt warming of the late 1990s. The isolated cool anomaly in summer 2010 was remarkable in that it temporarily reversed most of the warming of the late 1990s. It is more remarkable, however, that the glacier exhibited little discernible modulation of its behavior while the basin was filled with cool water, probably from summer of 2010 to summer of 2011, if fjord renewal occurs in summer only. Joughin et al. (2012, 2014) show that, since 2005 there has been an annual speed-up, particularly near the terminus, with peak glacier velocities occurring in summer or early autumn. In 2010, it appears the summer speed-up may have ended sooner and more abruptly than usual and the onset of the 2011 speed-up appears to have been slightly delayed. The lack of a more striking change of behavior suggests that the glacier is far from equilibrium with its marine environment and is now less sensitive to ocean temperature changes than it was in 1997.

Source of temperature variability

Summer and autumn ocean profiles between Cape Farewell and Disko Bay show that independent changes in the temperatures of both the sub-surface Atlantic waters and near-surface Arctic waters have led to temperature variability in Ilulissat Icefjord since 1990. In particular, the step-like warming of 1997 in the $\sigma\theta=27.2$ to 27.3 layer did not persist until the present, despite the sustained presence of 5°C Atlantic water near Cape Farewell. In fact, the mean summer fjord basin temperature in 1998-1999 was 2.7°C, according to our Disko Bay proxy, while the mean summer temperature from 2000-2007 (excluding 2002 and 2003) was just 1.9°C. From summers of 2005 to

2013, for which we have good mooring data in Davis Strait, Disko Bay temperatures were coolest (for $\sigma\theta = 27.2$ to 27.3 and $\sigma\theta > 27.3$) in 2006 and 2010. During those summers Atlantic waters in the West Greenland Current were no cooler than in typical warm fjord summers. We find evidence, rather, that an excessive amount of cold water from the south-flowing Baffin Current crossed over to the Greenland shelf in early spring and cooled the density layer destined for the fjord basin (the evidence is clearer for 2010 than 2006). The change in Baffin Current behavior in 2010 appears to be well correlated with a sharp increase in freshwater flux through the Canadian Arctic Archipelago leading up to that summer (Gladish et al. 2014b and references within).

Conclusions

Our analysis of ocean data from the Ilulissat Icefjord and a wider region along West Greenland brings some new definiteness to our understanding of temperature variability there but certainly not simplicity. Ilulissat Icefjord temperatures appear to change slowly except in the summer when circulation is driven by subglacial meltwater discharge. Bathymetric controls permit only a thin layer of water in Disko Bay to flow over the sill, which then inflates in thickness to fill the entire fjord basin. This thin layer is right at the interface of Atlantic water and overlying Arctic water; Jakobshavn Glacier therefore feels temperature variability in either fraction. Inter-annual changes in the Arctic water temperature could be due to variability of atmospheric forcing on water parcels flowing around southern Greenland in the East Greenland and then West Greenland Current (Fig. 1). Alternatively, as in 2010, the amount of Baffin Current water (usually colder than West Greenland Current Arctic water at the same density) entering Disko Bay may vary. Summer temperature changes in the warm Atlantic water have been subtle, especially compared to the large-amplitude cycles of temperature on isopycnals in the West Greenland Current detected by moorings in Davis Strait (Curry et al. 2014; Gladish et al. 2014b).

Predicting oceanic thermal forcing on Jakobshavn Glacier for the purposes of sea level predictions is a delicate matter involving fluxes from the Arctic Ocean (by two different major pathways) and the North Atlantic Ocean. The timing of inflow into Disko Bay and Ilulissat Icefjord involves the interplay of bathymetry and the annual vertical oscillations of isopycnals in West Greenland Current Waters (Gladish et al. 2014b) as well as seasonal subglacial meltwater production over the catchment basin of Jakobshavn Glacier.

Acknowledgements

NYU observations at Ilulissat were supported by NSF Office of Polar Program grants ARC-0806393 and ARC-1304137, NASA Polar Programs grant NNX08AN52G, and the NYU Abu Dhabi Center for Global Sea Level Change grant G1204.

References

- Becker, M., B. Meyssignac, C. Letetrel, W. Llovel, A. Cazenave, and T. Delcroix, 2012: Sea level variations at tropical Pacific islands since 1950. *Global Planet. Change*, **80-81**, 85-98 doi:10.1016/j.gloplacha.2011.09.004.
- Church, J.A., and N.J. White, 2011: Sea-level rise from the late 19th to the early 21st Century. *Surv. Geophys.*, **32**, 585-602, doi:10.1007/s10712-011-9119-1.
- Curry, B., C. Lee, B. Petrie, R. Moritz, and R. Kwok, 2014: Multi-year volume, liquid freshwater, and sea ice transports through Davis Strait, 2004-2010. *J. Phys. Oceanogr.* **44**, 1244-1266, doi:10.1175/JPO-D-13-0177.1.
- Gladish, C.V., D.M. Holland, A. Rosing-Asvid, J.W. Behrens, J. Boje, 2014a: Oceanic boundary conditions for Jakobshavn Glacier: Part I. Variability and renewal of Ilulissat Icefjord waters, 2001-2013. *J. Phys. Ocean.*, in review.
- Gladish, C.V., D.M. Holland, and C. Lee, 2014b: Oceanic boundary conditions for Jakobshavn Glacier: Part II. Provenance and sources of variability of Disko Bay and Ilulissat Icefjord waters, 1990-2011. *J. Phys. Ocean.*, in review.
- Hansen, M., T. Nielsen, C. Stedmon, and P. Munk, 2012: Oceanographic regime shift during 1997 in Disko Bay, Western Greenland. *Limnol. Oceanogr.*, **57**, 634-644.
- Holland, D.M., R.H. Thomas, B. De Young, M.H. Ribergaard, and B. Lyberth, 2008: Acceleration of Jakobshavn Isbræ triggered by warm subsurface ocean waters. *Nat. Geosci.*, **1**, 659-664, doi:10.1038/ngeo316.
- Jenkins, A., 2011: Convection-driven melting near the grounding lines of ice shelves and tidewater glaciers. *J. Phys. Ocean.*, **41**, 2279-2294, doi:10.1175/JPO-D-11-03.1.
- Joughin, I., R.B. Alley, and D.M. Holland, 2012a: Ice-sheet response to oceanic forcing. *Science*, **338** 1172, doi:10.1126/science.1226481.
- Joughin, I., B.E. Smith, I.M. Howat, D. Floricioiu, R.B. Alley, M. Truffer, and M. Fahnestock, 2012b: Seasonal to decadal scale variations in the surface velocity of Jakobshavn Isbræ, Greenland: Observation and model-based analysis. *J. Geophys. Res.*, **117**, F02030, doi:10.1029/2011JF002110.
- Joughin, I., B.E. Smith, D.E. Shean, and D. Floricioiu, 2014: Brief communication: Further summer speedup of Jakobshavn Isbræ, *The Cryosphere*, **8**, 209-214, doi:10.5194/tc-8-209-2014.
- McCartney, M.S., and L.D. Talley, 1982: The subpolar mode water of the North Atlantic Ocean. *J. Phys. Ocean.*, **12**, 1169-1188.
- Milne, G. A., 2007: How the climate drives sea-level changes. *Astron. Geophys.*, **49**, 2.24-2.28, doi:10.1111/j.1468-4004.2008.49224.x.
- Milne, G.A., W.R. Gehrels, C.W. Hughes, and M.E. Tamisiea, 2009: Identifying the causes of sea-level change. *Nat. Geosci.*, **2**, 471-478, doi:10.1038/ngeo544.
- Motyka, R.J., M. Truffer, M. Fahnestock, J. Mortensen, S. Rysgaard, and I. Howat, 2011: Submarine melting of the 1985 Jakobshavn Isbræ floating tongue and the triggering of the current retreat. *J. Geophys. Res.*, **116**, F01007, doi:10.1029/2009JF001632.
- Myers, P., N. Kulan, and M. Ribergaard, 2007: Irminger Water variability in the West Greenland Current. *Geoph. Res. Lett.*, **34**, L17601, doi:10.1029/2007GL030419.
- Myers, P., C. Donnelly, and M. Ribergaard, 2009: Structure and variability of the West Greenland current in summer derived from 6 repeat standard sections. *Prog. in Ocean.*, **80**, 93-112.
- Nick, F.M., A. Vieli, I.M. Howat, and I. Joughin, 2009: Large-scale changes in Greenland outlet glacier dynamics triggered at the terminus. *Nat. Geosci.*, **2**, 110-114, doi:10.1038/NNGEO394.
- O'Leary, M. and P. Christoffersen, 2013: Calving on tidewater glaciers amplified by submarine frontal melting. *The Cryosphere*, **7**, 119-128. doi:10.5194/tc-7-119-2013.
- Pritchard, H.D., R.J. Arthern, D.G. Vaughan, and L.A. Edwards, 2009: Extensive dynamic thinning on the margins of the Greenland and Antarctic ice sheets. *Nature*, **461**, 971-975, doi:10.1038/nature08471.
- Rignot, E., and P. Kanagaratnam, 2006: Changes in the velocity structure of the Greenland Ice Sheet. *Science*, **311**, 986, doi:10.1126/science.1121381.
- Rignot, E., I. Velicogna, M.R. van den Broeke, A. Monaghan, and J.T.M. Lenaerts, 2011: Acceleration of the contribution of the Greenland and Antarctic ice sheets to sea level rise. *Geophys. Res. Lett.*, **38**, L05503, doi:10.1029/2011GL046583.
- Rignot, E., I. Fenty, D. Menemenlis, and Y. Xu, 2012: Spreading of warm ocean waters around Greenland as a possible cause for glacier acceleration. *Ann. Glaciol.*, **53**, 60.
- Sciascia, R., F. Straneo, C. Cenedese, and P. Heimbach, 2013: Seasonal variability of submarine melt rate and circulation in an East Greenland fjord. *J. Geophys. Res. Oceans*, **118**, 2492-2506, doi:10.1002/jgrc.20142.
- Straneo, F., and P. Heimbach, 2013: North Atlantic warming and the retreat of Greenland's outlet glaciers. *Nature*, **504**, 36-43, doi:10.1038/nature12854.
- Straneo, F., G.S. Hamilton, D.A. Sutherland, L.A. Stearns, F. Davidson, M.O. Hamill, G.B. Stenson, A. Rosing-Asvid, 2010: Rapid circulation of warm subtropical waters in a major glacial fjord in East Greenland. *Nature Geosci.*, **3**, 182-186, doi:10.1038/NNGEO764.
- Straneo, F., D. Sutherland, D. Holland, C. Gladish, G.S. Hamilton, H.L. Johnson, E. Rignot, Y. Xu, and M. Koppes, 2012: Characteristics of ocean waters reaching Greenland's glaciers. *Ann. Glaciol.*, **53**, 60.
- Thomas, R.H., W. Abdalati, E. Frederick, W.B. Krabill, S. Manizade, and K. Steffen, 2003: Investigation of surface melting and dynamic thinning on Jakobshavn Isbræ, Greenland. *J. Glac.*, **49**(165), 231-239.
- Xu, Y., E. Rignot, I. Fenty, D. Menemenlis, and M.M. Flexas, 2013: Subaqueous melting of Store Glacier, west Greenland from three-dimensional, high-resolution numerical modeling and ocean observations. *Geophys. Res. Lett.*, **40**, 1-6, doi:10.1002/grl.50825.

Modeling of Greenland Ice Sheet and ocean interactions: Progress and challenges

Stephen Price¹ and Helen Seroussi²

¹Los Alamos National Laboratory

²NASA Jet Propulsion Laboratory

Over the last decade there have been significant improvements in the modeling of ice sheets, in the collection of observations needed for initialization and validation of these models, and in the coupling of these models to Earth System Models (ESMs). Here, we review these recent advances, along with ongoing work and future challenges, with an eye towards using modeling to better understand Greenland's future evolution in response to current and future warming in the North Atlantic.

As summarized in previous review papers (Straneo et al. 2013; Straneo and Heimbach 2013), recent observations and modeling studies argue that the following key processes and interactions need to be accounted for by coupled ice and climate models of Greenland: (1) the flux of heat and salt from the open ocean into fjords, where regional and local circulation transfers heat and salt to the marine termini of outlet glaciers; (2) interactions between relatively warm and/or salty fjord waters, glacier ice, and fresh, subglacial melt water, which transfer heat to the ice (resulting in melting) and fresh water to the fjord (contributing to fjord circulation and further entrainment of warm far field waters); (3) resistive stresses provided by marine glacier termini, which impede the flow of inland ice, and the reduction or loss of that resistance following i) submarine and atmospheric melting, ii) calving, iii) weakening of the seasonal ice melange, or iv) a combination of these factors; (4) the transfer of stress change at marine termini of outlet glaciers to the ice sheet interior, ultimately resulting in dynamic thinning and changes in the discharge of ice flux to the ocean (see also Figure 4 from Straneo et al. 2013).

Here, we mainly focus on progress and challenges associated with processes (3) and (4), i.e., those processes contained within or proximal to the ice sheet, but where appropriate, and particularly in the context of coupling with Earth system models (ESMs), we also briefly discuss processes (1) and (2). We emphasize that numerous important feedbacks between the ice sheet

and other components of the climate system (atmosphere, ocean, and sea ice) impact directly on these processes, and we discuss how these feedbacks are (or can be) captured within prognostic models. We begin by reviewing progress and challenges concerning relevant observations, followed by a comparable review for large- and process-scale models. We conclude with a discussion on progress and challenges related to model coupling.

Observations

Numerical ice sheet models are highly dependent on observations, which are needed for providing model initial and boundary conditions and external forcings (or for calibration and validation of external forcing provided by ESMs). They are also heavily used by data assimilation approaches (to infer model parameters that cannot be directly observed), for validation of model output and for improved understanding of important physical processes from which process-scale models and parameterizations are constructed. While the past decade has seen the acquisition of large amounts of very high quality data, both from remotely sensed and in-situ measurements, significant gaps remain.

Observations of ice surface velocity over Greenland are almost complete, in the sense that a single composite snapshot (representing the 2000's) of the surface velocity field at spatial resolution of 500 meters with near full spatial coverage is now available (see review by Moon, this issue). Interferometric Synthetic Aperture Radar (InSAR) data acquired by RADARSAT, Envisat, and ALOS PALSAR show the contrast between the few large glaciers of the North and the numerous narrow, fast-flowing glaciers in the South (Joughin et al. 2010; Rignot and Mouginot 2012). Errors in velocity observations are estimated to be ~1-17 m/yr and ~0.5-20 degrees (along the coast and in slow moving areas, respectively). High accumulation rates in southeastern Greenland lead to image decorrelation, and spatial coverage there is relatively less complete, especially along the coast. A general concern

with these velocity data is that existing maps are composites of all existing datasets, including data acquired during different years (and different times of year), which is limiting in highly dynamic areas where large changes in velocities have been observed during the past decade.

Airborne and satellite-based radar and laser altimetry data have been used to confirm an oceanic influence on the dynamic thinning of Greenland's margins during the past decade (e.g., Pritchard et al. 2009). A concern is that altimetry data suffer from some of the same shortcomings mentioned above for velocity data. Additional concerns include the penetration of radar signals into the snow and firn and the seasonal variations of the ice sheet surface due to firn compaction, which affects the surface elevation as seen by laser altimetry. Both effects introduce biases into maps and time series of ice-equivalent elevation change. These biases are not accounted for by large-scale models, which generally deal only in units of ice-equivalent thickness.

Ice thickness is a critical observation for modeling, since the ice sheet geometry is a first-order control on velocity (through the driving stress) and ice flux. While the ice surface elevation is well mapped from airborne and satellite altimetry, at high spatial resolution and with small errors (order ~100 and 5 m, respectively), accurate mapping of the bedrock elevation is limited to locations where ice thickness has been measured

using ground penetrating radar (ground-based or airborne). Distance between flight lines varies, for example, between 500 m on Russell glacier (the glacier with the highest coverage) in West Greenland and several tens or hundreds of kilometers in the interior of the continent, with a relatively higher density of measurements along the coasts. While recent observations, such as those made by CReSIS and NASA's Operation IceBridge, have led to greatly improved continental scale bed maps (Bamber et al. 2013), data interpolated between flight lines have been shown to be highly erroneous. In many locations, observed velocities and rates of elevation change allow for a consistency check on interpolated ice thickness and are found to be inconsistent with the principle of mass conservation (e.g., Rasmussen 1988; Seroussi et al. 2011). When ignored, these errors lead to large and unphysical oscillations in the modeled flux divergence field that affect ice sheet model initialization and coupling. This problem has led to the development of mass conserving interpolation techniques, which combine velocity and ice thickness measurements along flight lines to greatly improve interpolated ice thickness between flight lines (e.g., Morlighem et al. 2011; 2013). While the resulting maps of ice thickness are much more suitable for ice sheet modeling, the technique is limited to regions with good observations of ice velocity, and cannot be applied over regions with data gaps (discussed above). A related problem is that measured and interpolated bed elevations within glaciated fjords generally do not agree well with those obtained from bathymetry in ad-

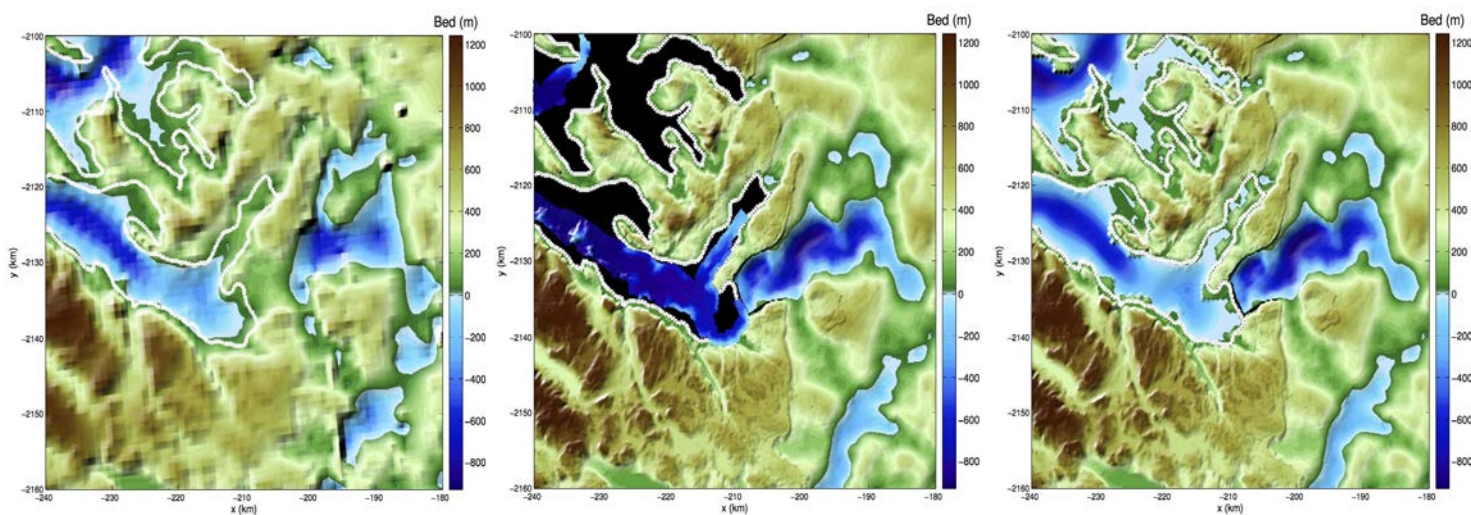


Fig. 1 Subglacial bed topography and its connection with bathymetry of Store Glacier, West Greenland. Left: Topography from Bamber et al. (2013). Right: Basal topography derived from mass conserving ice-thickness interpolation and bathymetry from IBCAO v3 (Jakobsson et al. 2012). Center: Basal topography derived from mass conserving ice-thickness interpolation and swath bathymetry measurements (Morlighem et al. 2014, reproduced with permission of the authors).

adjacent oceanic fjords (Fig. 1). Bathymetry in fjords is poorly known except in a few places where it has been accurately measured (e.g., Jakobsson et al. 2012). This lack of continuity in basal topography data near the calving front of outlet glaciers will become increasingly problematic for studies using coupled ice sheet and ocean/fjord circulation models.

Observational studies during the past decade have contributed immensely to our understanding of how Greenland's outlet glaciers respond to forcing from meltwater that is generated at the surface and routed to the ice sheet base through moulins and/or hydrofracture (Chu 2014; Rennermalm et al. 2013). These observations have increased our understanding about the seasonal evolution of the subglacial drainage system beneath ice sheets – from a low capacity, low-effective pressure system (sliding highly sensitive to water input) early in the season to a high capacity, high-effective pressure system (sliding rate less sensitive to water input) later in the season. They also show that subglacial hydrology probably does not play a large role in regulating the seasonal speed of outlet glaciers (e.g., Joughin et al., 2008c). Subglacial hydrology still plays a role in affecting outlet glacier dynamics indirectly, through its impacts on estuarine circulation in fjords and the entrainment of warm, far-field ocean waters to marine glacier termini (e.g., Motyka et al. 2011; Xu et al. 2012; Sciascia et al. 2013). In general, observations on the quantity and timing of subglacial freshwater flux into fjords, and its impact on estuarine circulation, are sparse. Surface melting, and thus surface mass balance (SMB; net accumulation less ablation and sublimation), is the dominant control on subglacial hydrology evolution in Greenland. We discuss SMB further below.

Additional and highly relevant observations on Greenland outlet glacier behavior that have become available include recent (past decade) time series of terminus positions (e.g., Howat et al. 2007; Moon and Joughin 2008; Joughin et al. 2008a,b; McFadden et al. 2011), outlet glacier flux (Enderlin et al. 2014), and longer-term (past century and older) records of past outlet glacier termini locations (Csatho et al. 2008; Howat and Eddy 2011; Bjork et al. 2012). Lack of knowledge about ice sheet geometry and climate forcing prior to the last several decades may limit the utility of these data for ice sheet model validation to the more recent decades. Furthermore, the extreme sensitivity of outlet glacier termini to geometry, climate forcing, and other unknown factors (Moon and Joughin 2008; McFadden et al. 2011) make it unlikely that even a perfect model could be expected to reproduce observed behaviors for any but the largest, most well stud-

ied outlet glaciers. A more practical goal for models might be to capture the statistics of observed retreat and advance behaviors within a given region of the ice sheet.

Ice sheet modeling

In its fourth assessment report (AR4), the IPCC declined to include estimates of future sea-level rise from ice sheet dynamics (changes in the momentum balance that directly affects ice flow and ice discharge into the ocean). This was largely due to a perceived immaturity of ice sheet models at the time, including their inability to reproduce or explain observed dynamic behaviors like the acceleration of several of Greenland's largest outlet glaciers. Ice sheet modeling was indeed historically used to reproduce paleoclimate variations and the focus to providing decadal to centennial estimates of ice sheet evolution only emerged in the past decades. Support from funding agencies has enabled concerted efforts between AR4 and AR5 towards improvements, including the representations of ice dynamics, the representation of important physical processes within ice sheet models, and the coupling between ice sheet models and ESMs (Little et al. 2007; Lipscomb et al. 2009). Below, we discuss progress in these areas as well as ongoing and future challenges related to ice sheet modeling.

Large-scale modeling of ice flow

Thanks in large part to sustained support by US, UK, and EU scientific funding agencies, the past decade has seen tremendous progress in the development of a new generation of community supported ice sheet models (Bueler and Brown 2009; Rutt et al. 2009; Larour et al. 2012; Gagliardini et al. 2013; Brinkerhoff and Johnson 2013) able to perform continental scale simulations. These models run on high performance, massively parallel computer architectures using 10^2 - 10^3 CPU cores and take advantage of modern, well supported solver libraries (e.g., PETSc (Balay et al. 2008), Trilinos (Heroux et al. 2005)). A primary initial focus for most models was an improved representation of the momentum balance equations¹ through the development of so-called higher-order (e.g., Patryn 2003) and full-Stokes models, rather than traditional lower-order approximations (e.g., shallow ice (SIA; Hutter 1983) and shallow-shelf (SSA) or shelfy-stream (MacAyeal 1989)), a combination of SIA and SSA to produce hybrid models (Bueler and Brown 2009; Pollard and Deconto 2009; Goldberg 2011), or combinations of the full range of approximations up to and including Stokes (Seroussi et al. 2012). These new models account for both vertical and horizontal stress gradients, allowing for more realistic and accurate simulations of fast flowing regions, such as outlet glaciers, ice streams, and ice shelves,

and more realistic and accurate transfer of perturbations from marginal to inland regions (Fig. 2). Additional improvements to the overall modeling framework included the integration of unstructured (Larour et al. 2012; Gagliardini et al. 2014; Brinkerhoff and Johnson 2013) or adaptive meshes (Cornford et al. 2013) for focusing resolution and computational power where needed, such as at ice sheet grounding lines, where ice detaches from the underlying bedrock and goes afloat due to buoyancy. Along with the development and regular use of higher-order and Stokes flow models, formal optimization and data assimilation techniques are now standard for model initialization. Surface observations are used to infer poorly known ice properties or parameters, such as the friction coefficient at the ice-bedrock interface (Morlighem et al. 2010; Larour et al. 2012; Gillet-Chaulet et al. 2012; Brinkerhoff and Johnson 2013) or the rheology of floating ice shelves (Khazendar et al. 2009), allowing for an optimal match between modeled and observed velocities.

Despite these improvements, models remain limited in their ability to reproduce observed trends in Greenland mass loss, as highlighted by the large spread in model response to similar forcings, in particular with respect to ocean forcing (Bindschadler et al. 2013). Primary sources of the variability in model response are errors introduced during model initialization. Models relying on a standard spin-up, driven by long-term reconstructions of climate forcing from proxy records, may capture internal fields like temperature, but fail to accurately reproduce current observations of ice sheet geometry and velocity. Conversely, models using formal optimization and data assimilation methods generally assume present-day equilibrium conditions, in which case they reproduce current observations of ice sheet geometry and velocity but fail to capture accurate transients in internal state variables and therefore lead to unrealistic future volume evolution. Further, formal optimization methods generally do not account for climate forcing (e.g., SMB) or uncertainties in ice thickness, which results in large, sudden and unphysical transient evolutions when integrating forward in time under realistic climate forcing. To limit the impact of these unphysical behaviors, models have to be relaxed with long forward runs under steady forcing or by applying flux corrections on top of the true climate forcing. Improved initialization approaches will combine both spin-up and data-assim-

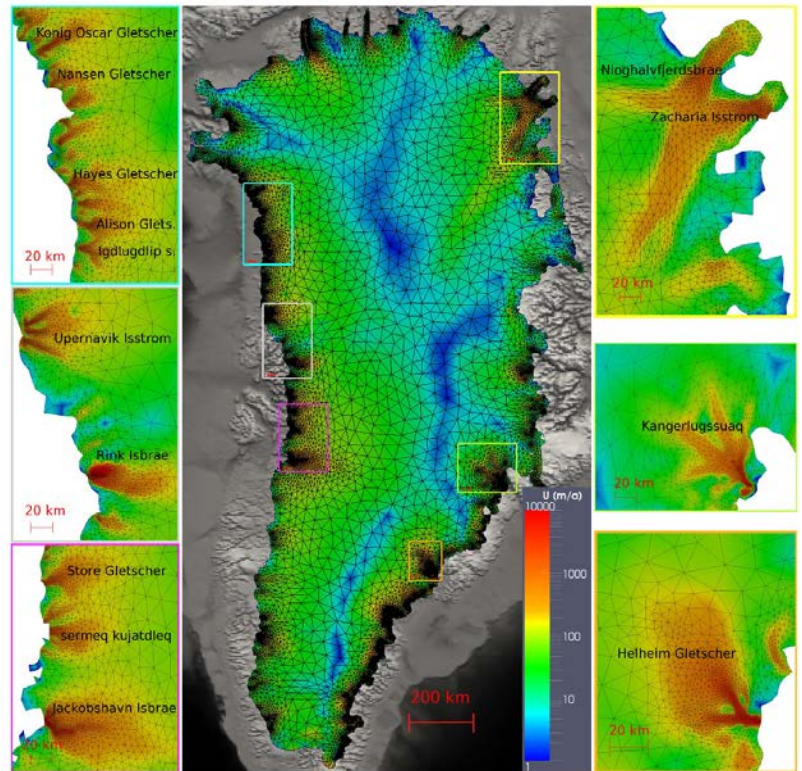


Fig. 2 Unstructured, finite element mesh and optimized model surface velocities for Greenland using the ELMER/Ice model (Gillet-Chaulet et al. 2012, reproduced with permission of the authors).

ilation-based techniques (Goldberg and Heimbach 2013). These approaches should not only include constraints from observed surface velocities and elevation, but also from internal temperature, ice age observations, and observations or modeled SMB forcing.

While efforts towards the verification and validation of new ice flow models have begun, considerable work remains. A number of community accepted benchmarks are now available for verification of output from higher-order models (Pattyn et al. 2008; Pattyn et al. 2013). Though not verification in the formal sense (i.e., confirming that a computational model correctly solves the equations it purports to), these benchmark test cases have proven critical for conducting code-to-code comparisons during model development. Formal verification tests (e.g., using manufactured

¹See Schoof and Hewitt (2013) for a review of the momentum balance equations for ice sheets.

solution methods) are starting to become available (Leng et al. 2013), but more are needed, particularly to verify lower-order approximations of full-Stokes models. Model validation (i.e., confirming that a computational model represents the physical system it aims to mimic) is a much more difficult process. This is particularly the case for ice sheet models due to the relative lack and short timeframe of observational data, much of which may have already been used for model initialization, and the long time scales inherent in ice sheet dynamics (order 10^2 - 10^5 years). Time series of surface elevation rate of change and rate of mass change are good candidates for use in model validation. However, there is currently a lack of standardized datasets for use in the process. Vetting and packaging of the relevant datasets into model-friendly frameworks is something only recently being discussed between modelers and observationalists. In addition to standardized datasets for use in model validation, validation experiments (e.g., initial and boundary condition specification, forcing datasets) and model-to-data comparison protocols need to be agreed upon. The *SeaRISE* and *Ice2Sea* projects took essential initial steps towards these goals and planned follow-ons, possibly as part of CMIP6, will motivate further progress.

Process-scale modeling

A number of important physical processes, previously identified as both lacking in current models and as a top priority for improvement in next-generation models (Little et al. 2007; Lipscomb et al. 2009), are also of critical importance for modeling of ice sheet and ocean interactions in Greenland. These include supra-, en-, and sub-glacial hydrology, evolution of ice sheet rheology, and iceberg calving. While none of these processes are currently standard or included at an appropriately complex level in next-generation models, significant progress has been made and good process scale models are becoming available.

For glacial hydrology, a number of process scale models have been developed to simulate the flow of water over the surface of ice sheets (Banwell et al. 2012; Clason et al. 2012) and the transfer of that water (and in some cases latent heat) to an englacial system (Phillips et al. 2010; Clason et al. 2012). At the base of the ice sheet, substantial progress has been made in the modeling of subglacial hydrology, in particular the modeling of inefficient, distributed drainage versus efficient, channelized drainage, and its impact on the evolution of basal effective pressure (overburden ice pressure minus water pressure), which is the physical link between hydrology and basal sliding. These process scale models allow for physically motivated, “automatic” switching between distributed, channelized, and mixed drainage systems. They have been linked to realistic, theoretically, and experimentally motivated sliding

laws, which are capable of capturing feedbacks between subglacial effective-pressure and changes in ice sheet geometry (Pfeffer 2007), and have been shown to mimic observed subglacial drainage system behaviors (Flowers 2008; Pimental et al. 2010; Schoof 2010; Werder et al. 2013; Hewitt 2013). Few of these models, however, include connections to the supra- and en-glacial systems mentioned above, and those that do (Werder et al. 2013; Hewitt 2013) include broad simplifications to one or more parts of the full system. While coupling of subglacial hydrology models with higher-order ice flow models has been demonstrated for some idealized domains and test cases (Hewitt 2013; Hoffman and Price 2014) they have yet to be demonstrated working robustly at the continental scale. In addition to complications in coupling these models with ice sheet models, inclusion of active subglacial hydrology models will require new thinking about optimization. Rather than “tuning” a scalar map for the basal friction coefficient, the hydrology sub-model will control basal sliding, requiring that output from the sub-model, or parameters within it, will need to be initialized correctly to match observed velocities.

Ice sheet models have generally assumed an isotropic, power-law rheology with dependence primarily on ice temperature and possibly as a function of a tuneable scalar enhancement factor, with the latter generally used to capture the effects of softer ice-age ice. More sophisticated treatments are likely necessary to accurately model the observed flow field and to capture important feedbacks. For example, recent studies suggest that the continued acceleration of Jakobshavn Isbrae in West Greenland is in part the result of shear-induced softening and weakening at its margins (van der Veen et al. 2011; Joughin et al. 2012). Modeling such changes in ice rheology, for example using damage mechanics (Pralong and Funk 2005; Albrecht and Levermann 2012, Borstad et al. 2013), and including the effects in large-scale models, is an area of active research.

Closely related to damage mechanics is the process of calving, whereby icebergs detach from marine outlet glacier termini, generally along pre-existing failure planes. Calving can be modeled as taking place when ice exceeding some prescribed damage threshold falls within some prescribed distance of the terminus. While promising progress has been made on physically-based, process-scale models of calving (see review by Bartholomaeus and Bassis, this issue) these models have yet to be incorporated, tested, or validated in large-scale ice sheet models. In the meantime, some physically motivated, semi-heuristic models have demonstrated reasonable calving behavior in large-scale models (Albrecht and Levermann 2012; Nick et al. 2010). Moving ice fronts can involve topological changes (separation of a retreating glacier

into two branches, merging of two advancing fronts), which require complex numerical treatments. A continuum approach based on the level set method (Sethian 1999) that tracks the boundary of the ice domain implicitly within a larger domain would aid in overcoming this difficulty (Pralong and Funk 2004).

Coupling between ice sheet models and ESMs

Along with post-AR4 efforts at improving ice sheet models came more focused efforts at improving the coupling between ice sheet models and components of ESMs. Ice sheets not only evolve in response to forcing from the climate system (e.g., melting at upper and lower surfaces due to interactions with the atmosphere and oceans) but their evolution also forces changes in other components through changes in surface albedo, elevation, and freshwater and heat fluxes. Further, the processes (1)-(4) discussed in the introduction involve feedbacks between one or more components of the climate system and, as such, the coupling of these components is critical for capturing these feedbacks. While progress in coupling of ice sheet models has occurred between most standard components of ESMs, as reviewed in Vizcaino (2014), we only review coupling to the atmosphere and ocean components here.

The coarse resolution (order 1°) of most ESM atmosphere models requires that temperature and precipitation are down-scaled, ideally conservatively, from the coarse resolution atmosphere grid to the much higher resolution ice sheet model grid (order ≤ 5 km) on which SMB is calculated. Downscaling of SMB (Lipscomb et al. 2013) has proven very successful for Greenland (Vizcaino et al. 2013; Fig. 3), where SMB calculations using a global scale ESM show excellent agreement with those calculated from a high-resolution (~ 10 km) regional climate model (Ettema et al. 2009) and also with available *in situ* observations of surface mass balance (e.g., Vernon et al., 2013). Currently, runoff from surface melting is routed

(conceptually) overland to the ocean. Thus remaining to be done is the coupling of freshwater runoff from the ice sheet surface to supra- and en-glacial hydrology models.

Despite recent progress in modeling both regional (Hellmer et al. 2012) and continental (Kushara et al. 2013) submarine circulation and melting in Antarctica, these models have generally used relatively coarse spatial resolution (>10 km) and have not included a dynamic ice sheet component. Very recent work improves on both, by using higher spatial resolution for the ocean model (order 5 km for most ice shelves; Asay Davis et al. 2014) and coupling to a dynamic, higher-order ice sheet model (Martin et al. 2014). Yet it remains unclear if this progress will translate to progress on ice sheet and ocean coupled simulations for Greenland. The small scale of Greenland fjords (km's wide and 10's of km long) will remain challenging or prohibitive for most global scale ocean circulation models, even those using variable resolution meshes (e.g., Ringler et al. 2013). Further, hydrostatic models (the standard for global-scale

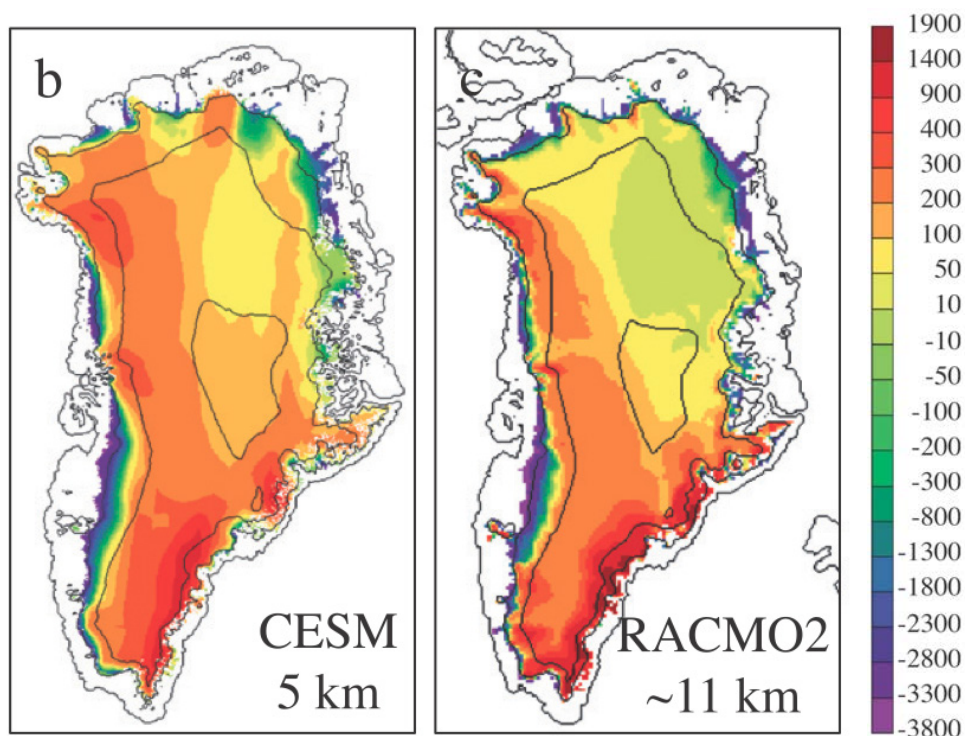


Fig. 3 Comparison of 1960-2005 mean SMB ($\text{kg m}^{-2} \text{yr}^{-1}$) calculated using the Community Earth System Model (CESM; left) and the Regional Atmospheric Climate Model (RACMO; right). CESM SMB is calculated from atmospheric fluxes at 1° resolution downscaled onto the 5 km resolution ice sheet grid. RACMO SMB is calculated at the ~ 11 km resolution of the model (figure after Vizcaino et al. 2013).

ocean models) are not appropriate for accurately capturing plume dynamics that lead to enhanced submarine melting at the ice/ocean interface (in the first hundred meters from the ice front). Some work on modeling of fjord and near ice-front circulation has been done using regional-scale, non-hydrostatic models (Xu et al. 2012, 2013; Sciascia et al. 2013) but is still lacking a comprehensive, validated boundary layer theory for meteoric (glacier) ice, which accurately quantifies the transfer of heat and freshwater between the ocean and ice sheet. These results will help parameterize ocean-induced melting at outlet glacier termini in climate models. Unlike Antarctica, where most progress on ice sheet and ocean model coupling has been made, Greenland has only a few floating ice tongues. Recent studies emphasize the role of channels at the base of these floating tongues (Rignot and Steffen 2008), which may control the overall sub-ice shelf melting rate and serve as conduits for meltwater flow in the sub-ice-shelf cavity. These channels may be initiated by irregularities in ice thickness at the grounding line and grow in response to the relatively high sub-ice shelf melting rates (Gladish et al. 2012; Sergienko 2013). For the majority of Greenland's marine outlets, however, interaction with the ocean occurs near vertical calving fronts, where parameterizations will likely be needed to quantify how fjord waters erode the terminus. Finally, the injection of freshwater into fjords from the subglacial hydrological system is a key factor in controlling submarine melting and fjord circulation, and thus the delivery of relatively warm, far field ocean waters to outlet glacier termini. Thus, glacial hydrological sub-models will also need to be coupled to fjord and ocean circulation models.

Little if any work has been done to couple sea ice models to land ice models. However, the seasonal ice melange (a mixture of calved icebergs welded together by sea ice) that fills many fjords is known to suppress calving by acting like a weak, seasonal ice shelf, thereby affecting outlet glacier dynamics (Amundson et al. 2010). Arctic sea ice extent and thickness has changed dramatically during the last few decades in response to high latitude warming and it is reasonable to expect further changes in the future. In turn, these changes will have downstream effects on ice melange strength and outlet glacier calving rates. This potential need for coupling between ice sheet and sea ice models, in addition to the atmosphere and ocean model coupling requirements discussed above, argues that ice sheet models should be included as fully coupled components of ESMs for exploring the future evolution of Greenland and the North Atlantic climate.

Summary and outlook

During the past decade, there has been a tremendous increase in the amount and type of data needed to initialize, constrain, and validate ice sheet models. The most important observations will continue to be those improving our knowledge of the bed

topography beneath the ice and the bathymetry of ice-marginal fjords. To make best use of new ice thickness data, they need to be combined with models and velocity observations to ensure consistency with principles of mass conservation. Process scale observations will continue to be important for formulating and validating process-scale models and parameterizations for use in large-scale, prognostic models of ice flow. Time series of elevation, mass, and velocity change will become increasingly important for use in model validation.

There have been very significant improvements to ice sheet models since IPCC AR4, particularly with respect to the complexity and fidelity of the equations they solve and the numerical and computational tools they employ. In this respect, new ice sheet models are on par with, or even exceed the sophistication of other ESM components. Significant challenges remain in terms of model initialization methods, which not only allow for reproducing "snapshots" of the current ice sheet state, but also accurately capture observed transients, a requirement for demonstrating predictive skill. The modeling of key physical processes has also progressed significantly, leading to improved understanding, but in general these sub-models have not yet been incorporated and tested within large-scale models. Progress towards improved model verification needs to continue and should focus on the development of standard test cases and the formalization of observational datasets for use in model validation.

Progress towards the coupling of ice sheet models to other components of ESMs has also been substantial. Many of the remaining challenges for Greenland revolve around the unprecedented high-spatial resolution that would be required of global-scale ocean models, even for the case of models using variable resolution grids. Hydrostatic ocean models, the current standard for global-scale models, are appropriate for modeling circulation within fjords and within the adjacent open ocean but fail at capturing plume dynamics at the ice/ocean interface. The coupling of freshwater fluxes, originating as surface melt, modified by flow through the glacial hydrological system, and injected into fjords at depth, while challenging, will likely be a critical link in the coupling of fjord circulation to atmospheric forcing and ice sheet evolution. Similarly, the future evolution of sea ice, which may strongly modulate iceberg calving (via ice melange) and thus ice dynamics, is currently not accounted for in large-scale ice sheet models. The importance of feedbacks and interactions between ice sheets and all other standard ESM components (atmosphere, ocean, and sea ice) argue that Greenland's future evolution is likely best explored within the framework of fully coupled ESM simulations.

References

- Albrecht, T., and A. Levermann, 2012: Fracture field for large-scale ice dynamics, *J. Glaciol.*, **58**, 165–176, doi:10.3189/2012JoG11J191.
- Amundson, J.M., M. Fahnestock, M. Truffer, J. Brown, M.P. Lüthi, and R.J. Motyka, 2010: Ice mélange dynamics and implications for terminus stability, Jaobshavn Isbrae, Greenland, *J. Geophys. Res.*, **115**, F01005, doi:10.1029/2009JF001405.
- Asay Davis, X., D. Martin, S. Price, and M. Maltrud, 2014: Simulations of Antarctic ice shelves and the Southern Ocean in the POP2x ocean model coupled to the BISICLES ice-sheet model, *Geophys. Res. Abs.*, **16**, EGU2014-10000.
- Balay, S., K. Buschelman, K. V. Eijkhout, W.D. Gropp, D. Kaushik, M.G. Knepley, L.C. McInnes, B.F. Smith and H. Shang, 2008: PETSc Users Manual, Argonne National Laboratory.
- Bamber, J. L. and Coauthors, 2013: A new bed elevation dataset for Greenland, *Cryosphere*, **7**, 499–510, doi:10.5194/tc-7-499-2013.
- Banwell, A. F., N. S. Arnold, I. C. Willis, M. Tedesco, and A. P. Ahlström, 2012: Modeling supraglacial water routing and lake filling on the Greenland Ice Sheet. *J. Geophys. Res.*, **117**, F04012, doi:10.1029/2012JF002393.
- Bindschadler, R. A. and Coauthors, 2013: Ice-sheet model sensitivities to environmental forcing and their use in projecting future sea level (the SeaRISE project). *J. Glaciol.*, **59**, 195–224, doi:10.3189/2013JoG12J125.
- Björk, A.A. and Coauthors, 2012: An aerial view of 80 years of climate-related glacier fluctuations in southeast Greenland. *Nat. Geosci.*, **5**, 427–432, doi:10.1038/ngeo1481.
- Borstad, C.P., E. Rignot, J. Mouginot and M.P. Schodlok, 2013: Creep deformation and buttressing capacity of damaged ice shelves: theory and application to Larsen C ice shelf. *Cryosphere*, **7**, 1931–1947, doi:10.5194/tc-7-1931-2013.
- Brinkerhoff, D.J., and J.V. Johnson, 2013: Data assimilation and prognostic whole ice sheet modelling with the variationally derived, higher order, open source, and fully parallel ice sheet model VarGlaS. *Cryosphere*, **7**, 1161–1184, doi:10.5194/tc-7-1161-2013.
- Bueler, E., and J. Brown, 2009: Shallow shelf approximation as a “sliding law” in a thermomechanically coupled ice sheet model. *J. Geophys. Res.*, **114**, 1–21, doi:10.1029/2008JF001179.
- Chu, V.W., 2014: Greenland ice sheet hydrology: A review. *Prog. Phys. Geog.*, **38**, 19–54, doi:10.1177/0309133313507075.
- Clason, C., D.W.F. Mair, D.O. Burgess, and P.W. Nienow, 2012: Modelling the delivery of supraglacial meltwater to the ice/bed interface: application to southwest Devon Ice Cap, Nunavut, Canada. *J. Glaciol.*, **58**, 361–374, doi:10.3189/2012JoG11J129.
- Cornford, S.L. and Coauthors, 2013: Adaptive mesh, finite volume modeling of marine ice sheets. *J. Comput. Phys.*, **232**, 529–549, doi:10.1016/j.jcp.2012.08.037.
- Csatho, B., T. Schenk, C. van der Veen, and W. Krabill, 2008: Intermittent thinning of Jakobshavn Isbræ, West Greenland, since the Little Ice Age. *J. Glaciol.*, **54**, 131–144.
- Enderlin, E.M., I.M. Howat, S. Jeong, M.J. Noh, J.H. Angelen, and M.R. Broeke, 2014: An improved mass budget for the Greenland Ice Sheet. *Geophys. Res. Lett.*, **41**, 1–7, doi:10.1002/(ISSN)1944-8007.
- Ettema, J., M.R. Van Den Broeke, E. Van Meijgaard, W.J. Van De Berg, J.L. Bamber, J.E. Box, and R.C. Bales, 2009: Higher surface mass balance of the Greenland ice sheet revealed by high-resolution climate modeling. *Geophys. Res. Lett.*, **36**, L12501, doi:10.1029/2009GL038110.
- Flowers, G., 2008: Subglacial modulation of the hydrograph from glacierized basins. *Hydrol. Process.*, **22**, 3903–3918.
- Gagliardini, O., and Coauthors, 2013: Capabilities and performance of Elmer/Ice, a new-generation ice sheet model. *Geosci. Model Dev.*, **6**, 1299–1318, doi:10.5194/gmd-6-1299-2013.
- Gillet-Chaulet, F., and Coauthors, 2012: Greenland ice sheet contribution to sea-level rise from a new-generation ice-sheet model. *Cryosphere*, **6**, 1561–1576, doi:10.5194/tc-6-1561-2012.
- Gladish, C.V., D.M. Holland, P.R. Holland, and S.F. Price, 2012: Ice-shelf basal channels in a coupled ice/ocean model. *J. Glaciol.*, **58**, 1527–1544, doi:10.3189/2012JoG12J003.
- Goldberg, D.N., 2011: A variationally derived, depth-integrated approximation to a higher-order glaciological flow model. *J. Glaciol.*, **57**, 157–170.
- Goldberg, D.N., and P. Heimbach, 2013: Parameter and state estimation with a time-dependent adjoint marine ice sheet model. *Cryosphere*, **7**, 1659–1678, doi:10.5194/tc-7-1659-2013.
- Hellmer, H.H., F. Kauker, R. Timmermann, J. Determann, and J. Rae, 2012: Twenty-first-century warming of a large Antarctic ice-shelf cavity by a redirected coastal current. *Nature*, **485**, 225–228, doi:10.1038/nature11064.
- Heroux, M.A., R.A. Bartlett, V.E. Howle, R.J. Hoekstra, J.J. Hu, T.G. Kolda, R.B. Lehoucq, K.R. Long, R.P. Pawlowski, E.T. Phipps, A.G. Salinger, H.K. Thornquist, R.S. Tuminaro, J.M. Willenbring, A. Williams, and K.S. Stanley, 2005: An overview of the Trilinos project, *ACM Trans. Math. Softw.*, **31**, 397–423.
- Hewitt, I.J., 2013: Seasonal changes in ice sheet motion due to melt water lubrication. *Earth Planet. Sc. Lett.*, **371–372**, 16–25, doi:10.1016/j.epsl.2013.04.022.
- Hoffman, M., and S. Price, 2014: Feedbacks between coupled subglacial hydrology and glacier dynamics. *J. Geophys. Res.-Earth Surf.*, **119**, 414–436 doi:10.1002/(ISSN)2169-9011.
- Howat, I.M., and A. Eddy, 2011: Multi-decadal retreat of Greenland’s marine-terminating glaciers. *J. Glaciol.*, **57**, 389–396.
- Howat, I., I. Joughin, and T. Scambos, 2007: Rapid changes in ice discharge from Greenland outlet glaciers. *Science*, **315**, 1559–1561, doi:10.1126/science.1138478.
- Hutter, K., 1983: *Theoretical Glaciology: Material Science of Ice and the Mechanics of Glaciers and Ice Sheets*, D. Reidel, Dordrecht, The Netherlands, 548 pp.
- Jakobsson, M. and Coauthors, 2012: The International Bathymetric Chart of the Arctic Ocean (IBCAO) Version 3.0. *Geophys. Res. Lett.*, **39**, L12609, doi:10.1029/2012GL052219.
- Joughin, I., I. Howat, R. Alley, and G. Ekstrom, M. Fahnestock, T. Moon, M. Nettles, M. Truffer, and V. Tsai, 2008a: Ice-front variation and tidewater behavior on Helheim and Kangerdlugssuaq Glaciers, *J. Geophys. Res.*, **13**, F1.
- Joughin, I., I.M. Howat, M. Fahnestock, B. Smith, W. Krabill, R.B. Alley, H. Stern, and M. Truffer, 2008b: Continued evolution of Jakobshavn Isbrae following its rapid speedup. *J. Geophys. Res.*, **113**, 1–14, doi:10.1029/2008JF001023.
- Joughin, I., S. Das, M. King, B. Smith, I. Howat, and T. Moon, 2008c: Seasonal speedup along the western flank of the Greenland Ice Sheet. *Science*, **320**, 5877.
- Joughin, I., B.E. Smith, I.M. Howat, T. Scambos, and T. Moon, 2010: Greenland flow variability from ice-sheet-wide velocity mapping. *J. Glaciol.*, **56**, 415–430.
- Joughin, I., B.E. Smith, I.M. Howat, D. Floricioiu, R.B. Alley, M. Truffer, and M. Fahnestock, 2012: Seasonal to decadal scale variations in the surface velocity of Jakobshavn Isbrae, Greenland: Observation and model-based analysis. *J. Geophys. Res.*, **117**, F02030, doi:10.1029/2011JF002110.

- Khazendar, A., E. Rignot, and E. Larour, 2009: Roles of marine ice, rheology, and fracture in the flow and stability of the Brunt/Stancomb-Wills Ice Shelf, *J. Geophys. Res.*, **114**, doi:10.1029/2008JF001124.
- Larour, E., H. Seroussi, M. Morlighem, and E. Rignot, 2012: Continental scale, high order, high spatial resolution, ice sheet modeling using the Ice Sheet System Model (ISSM). *J. Geophys. Res.*, **117**, doi:10.1029/2011JF002140.
- Leng, W., L. Ju, M. Gunzburger, and S. Price, 2013: Manufactured solutions and the verification of three-dimensional Stokes ice-sheet models. *Cryosphere*, **7**, 19–29, doi:10.5194/tc-7-19-2013.
- Lipscomb, W., R. Bindschadler, S. Price, E. Bueler, D. Holland, J. Johnson, and S. Price, 2009: A community ice sheet model for sea level prediction. *Eos Trans. AGU*, **90**, 23.
- Lipscomb, W.H. and Coauthors, 2013: Implementation and initial evaluation of the Glimmer Community Ice Sheet Model in the Community Earth System Model. *J. Climate*, **26**, 7352–7371, doi:10.1175/JCLI-D-12-00557.1.
- Little, C., and Coauthors, 2007: Toward a new generation of ice sheet models. *Eos Trans. AGU*, **88**, 578–579, doi:10.1029/2007EO520002.
- MacAyeal, D. R., 1989: Large-scale ice flow over a viscous basal sediment - Theory and application to Ice Stream-B, Antarctica. *J. Geophys. Res.*, **94**, 4071–4087.
- Martin, D., S. Cornford, X. Asay Davis, S. Price, E. Ng, and A. Payne, 2014: Fully resolved whole-continent Antarctica simulations using the BISICLES AMR ice sheet model coupled with the POP2x ocean model. *Geophys. Res. Abs.*, **16**, EGU2014-9851-1.
- McFadden, E.M., I.M. Howat, I. Joughin, B.E. Smith, and Y. Ahn, 2011: Changes in the dynamics of marine terminating outlet glaciers in west Greenland (2000–2009). *J. Geophys. Res.*, **116**, doi:10.1029/2010JF001757.
- Moon, T., and I. Joughin, 2008: Changes in ice front position on Greenland's outlet glaciers from 1992 to 2007. *J. Geophys. Res.-Earth*, **113**, F02022.
- Morlighem, M., E. Rignot, H. Seroussi, E. Larour, H. Ben Dhia, and D. Aubry, 2010: Spatial patterns of basal drag inferred using control methods from a full-Stokes and simpler models for Pine Island Glacier, West Antarctica. *Geophys. Res. Lett.*, **37**, L14502, doi:10.1029/2010GL043853.
- Morlighem, M., E. Rignot, H. Seroussi, E. Larour, H. Ben Dhia, and D. Aubry, 2011: A mass conservation approach for mapping glacier ice thickness. *Geophys. Res. Lett.*, **38**, doi:10.1029/2011GL048659.
- Morlighem, M., E. Rignot, J. Mouginit, X. Wu, H. Seroussi, E. Larour, and J. Paden, 2013: High-resolution bed topography mapping of Russell Glacier, Greenland, inferred from Operation IceBridge data. *J. Glaciol.*, **59**, 1015–1023, doi:10.3189/2013JoG12J235.
- Morlighem, M., E. Rignot, J. Mouginit, H. Seroussi, and E. Larour, 2014: Deeply incised submarine glacial valleys beneath the Greenland Ice Sheet. *Nat. Geosci.*, doi:10.1038/ngeo2167.
- Motyka, R.J., M. Fahnestock, M. Truffer, J. Mortensen, and S. Rysgaard, 2011: Submarine melting of the 1985 Jakobshavn Isbræ floating tongue and the triggering of the current retreat. *J. Geophys. Res.*, **116**, F01007.
- Nick, F.M., C.J. van der Veen, A. Vieli, and D.I. Benn, 2010: A physically based calving model applied to marine outlet glaciers and implications for the glacier dynamics. *J. Glaciol.*, **56**, 781–794.
- Pattyn, F., 2003: A new three-dimensional higher-order thermomechanical ice sheet model: Basic sensitivity, ice stream development, and ice flow across subglacial lakes. *J. Geophys. Res.*, **108**, 2382, doi:10.1029/2002JB002329.
- Pattyn, F. and Coauthors, 2008: Benchmark experiments for higher-order and full Stokes ice sheet models (ISMIP-HOM). *Cryosphere Discuss.*, **2**, 111–151.
- Pattyn, F. and Coauthors, 2013: Grounding-line migration in plan-view marine ice-sheet models: results of the ice2sea MISMIP3d intercomparison. *J. Glaciol.*, **59**, 410–422, doi:10.3189/2013JoG12J129.
- Pfeffer, W., 2007: A simple mechanism for irreversible tidewater glacier retreat. *J. Geophys. Res.*, **112**, F03S25, doi:10.1029/2006JF000590.
- Phillips, T., H. Rajaram, and K. Steffen, 2010: Cryo-hydrologic warming: A potential mechanism for rapid thermal response of ice sheets. *Geophys. Res. Lett.*, **37**, L20503, doi:10.1029/2010GL044397.
- Pimentel, S., G.E. Flowers, and C.G. Schoof, 2010: A hydrologically coupled higher-order flow-band model of ice dynamics with a Coulomb friction sliding law. *J. Geophys. Res.*, **115**, F04023, doi:10.1029/2009JF001621.
- Pollard, D., and R.M. Deconto, 2009: Modelling West Antarctic ice sheet growth and collapse through the past five million years. *Nature*, **458**, 329–332, doi:10.1038/nature07809.
- Pralong, A. and M. Funk, 2004: A level-set method for modeling the evolution of glacier geometry. *J. Glaciol.*, **50**, 171, 485–492, doi:10.3189/172756504781829774.
- Pralong, A., and M. Funk, 2005: Dynamic damage model of crevasse opening and application to glacier calving. *J. Geophys. Res.*, **110**, doi:10.1029/2004JB003104.
- Pritchard, H., R. Arthern, D. Vaughan, and L. Edwards, 2009: Extensive dynamic thinning on the margins of the Greenland and Antarctic ice sheets. *Nature*, **461**, 971–975.
- Rasmussen, L., 1988: Bed topography and mass-balance distribution of Columbia Glacier, Alaska, USA, determined from sequential aerial photography. *J. Glaciol.*, **34**, 208–216.
- Rennermalm, A. K. and Coauthors, 2013: Understanding Greenland ice sheet hydrology using an integrated multi-scale approach. *Environ. Res. Lett.*, **8**, 015017, doi:10.1088/1748-9326/8/1/015017.
- Rignot, E., and J. Mouginit, 2012: Ice flow in Greenland for the International Polar Year 2008–2009. *Geophys. Res. Lett.*, **39**, doi:10.1029/2012GL051634.
- Rignot, E. and K. Steffen, 2008: Channelized bottom melting and stability of floating ice shelves. *Geophys. Res. Lett.*, **35**, L02503, doi:10.1029/2007GL031765.
- Ringler, T., M. Petersen, R.L. Higdon, D. Jacobsen, P. W. Jones, and M. Maltrud, 2013: A multi-resolution approach to global ocean modeling. *Ocean Model.*, **69**, 211–232, doi:10.1016/j.ocemod.2013.04.010.
- Rutt, I., M. Hagdorn, N. Hulton, and A. Payne, 2009: The Glimmer community ice sheet model. *J. Geophys. Res.*, **114**, F02004.
- Schoof, C., 2010: Ice-sheet acceleration driven by melt supply variability. *Nature*, **468**, 803–806, doi:10.1038/nature09618.
- Schoof, C., and I. Hewitt, 2013: Ice-sheet dynamics. *Ann. Rev. Fluid Mech.*, **45**, 217–239, doi:10.1146/annurev-fluid-011212-140632.
- Sciascia, R., F. Straneo, C. Cenedese, and P. Heimbach, 2013: Seasonal variability of submarine melt rate and circulation in an East Greenland fjord. *J. Geophys. Res. Oceans*, **118**, 2492–2506, doi:10.1002/jgrc.20142.
- Sergienko, O.V., 2013: Basal channels on ice shelves. *J. Geophys. Res.*, **118**, 1342–1355. doi:10.1002/jgrf.20105.
- Seroussi, H., H. Ben Dhia, M. Morlighem, E. Larour, E. Rignot, and D. Aubry, 2012: Coupling ice flow models of varying orders of complexity with the Tiling method. *J. Glaciol.*, **58**, 776–786, doi:10.3189/2012JoG11J195.
- Seroussi, H., M. Morlighem, E. Rignot, E. Larour, D. Aubry, H. Ben Dhia, and S.S. Kristensen, 2011: Ice flux divergence anomalies on 79north Glacier, Greenland. *Geophys. Res. Lett.*, **38**, L19503, doi:10.1029/2011GL047338.
- Sethian, J.A., 1999: *Level Set Methods and Fast Marching Methods*. Cambridge University Press, 378 pp.

- Straneo, F., and P. Heimbach, 2013: North Atlantic warming and the retreat of Greenland's outlet glaciers. *Nature*, **504**, 36–43, doi:10.1038/nature12854.
- Straneo, F. and Coauthors, 2013: Challenges to understanding the dynamic response of Greenland's marine terminating glaciers to oceanic and atmospheric forcing. *Bull. Amer. Meteor. Soc.*, **94**, 1131–1144, doi:10.1175/BAMS-D-12-00100.1.
- van der Veen, C.J., J.C. Plummer, and L. A. Stearns, 2011: Controls on the recent speed-up of Jakobshavn Isbrae, West Greenland. *J. Glaciol.*, **57**, 770–782.
- Vernon, C.L., J.L. Bamber, J.E. Box, M.R. Van Den Broeke, X. Fettweis, E. Hanna, and P. Huybrechts, 2013: Surface mass balance model intercomparison for the Greenland ice sheet. *Cryosphere*, **7**, 599–614, doi:10.5194/tc-7-599-2013.
- Vizcaíno, M., W.H. Lipscomb, W.J. Sacks, J.H. van Angelen, B. Wouters, and M.R. Van Den Broeke, 2013: Greenland surface mass balance as simulated by the Community Earth System Model. Part I: model evaluation and 1850–2005 results. *J. Climate*, **26**, 7793–7812, doi:10.1175/JCLI-D-12-00615.1.
- Vizcaíno, M., 2014: Ice sheets as interactive components of Earth System Models: progress and challenges. *Wiley Interdiscip. Rev.: Clim. Change*, in press.
- Xu, Y., E. Rignot, D. Menemenlis and M. Koppes, 2012: Numerical experiments on subaqueous melting of Greenland tidewater glaciers in response to ocean warming and enhanced subglacial discharge. *Ann. Glaciol.*, **53**, 229–234.
- Xu, Y., E. Rignot, I. Fenty, D. Menemenlis, and M. Flexas, 2013: Subaqueous melting of Store Glacier, West Greenland from three-dimensional, high-resolution numerical modeling and ocean observations. *Geophys. Res. Lett.*, **40**, 2013, doi:10.1002/grl.50825.
- Werder, M.A., I.J. Hewitt, C.G. Schoof, and G.E. Flowers, 2013: Modeling channelized and distributed subglacial drainage in two dimensions. *J. Geophys. Res. Earth Surf.*, **118**, 2140–2158 doi:10.1002/jgrf.20146.

Progress and challenges to understanding iceberg calving around the Greenland Ice Sheet

Timothy C. Bartholomaus¹ and Jeremy N. Bassis²

¹University of Texas at Austin

²University of Michigan

Mass loss from the Greenland Ice Sheet is a key component of sea level rise and contributes significantly to the freshwater flux entering the ocean, thereby affecting global climate change. The Greenland Ice Sheet is surrounded by glaciers that terminate in near-vertical ice cliffs partially submerged in the ocean (called tidewater glaciers) and glaciers where the terminus separates from the bed and floats freely in the ocean (called ice tongues). Observations show that it is these marine margins that are most susceptible to rapid change and radically increased mass loss (Schenk and Csathó 2012). Moreover, mass loss from the fronts of Greenland's glaciers is presently responsible for as much as half of the ice sheet mass loss and is driving the spatial patterns of ice sheet thinning (Harig and Simons 2012; Enderlin et al. 2014).

Mass loss in marine terminating regions of the Greenland Ice Sheet is dominated by (1) warm seawater's gradual erosion of ice by frontal melting and (2) the sudden, sporadic detachment of blocks of ice in a process called iceberg calving. Mass loss associated with abrupt increases in iceberg calving rate can be extremely rapid. For example, between 1998 and 2002, the floating ice tongue that protruded from Jakobshavn Isbrae, one of Greenland's largest outlet glaciers, com-

pletely disintegrated, and the increased ice discharge that followed continues to this day (Joughin et al. 2012). Interannual and spatial variability in calving rate and terminus retreat is often complicated. For example, glaciers throughout southeast Greenland retreated during the mid-2000s, but these rates subsequently decreased. In some locations, adjacent glaciers exhibit opposite trends, with one glacier advancing and another retreating in a neighboring fjord (Moon and Joughin 2008). This observation is inconsistent with a view in which mass loss at glacier termini is tied purely to some broader environmental forcing, such as regional climate or regional ocean temperatures, and suggests some degree of local control associated with individual glaciers. In Alaska, historical observations, combined with glacial and marine geology, have shown that these glaciers have a complex cycle of slow advance and rapid retreat that is also only weakly related to climate (Post et al. 2011). This cycle is often attributed to instabilities driven by feedbacks between near-terminus sediment transport, calving behavior, and ice flow dynamics (Motyka et al. 2006; Pfeffer 2007). Because data on the centennial-scale positions of Greenland's tidewater outlets or from the bottoms of Greenland's fjords is sparse, it is unknown whether these theories are appropriate for Greenland's glaciers.

At present, the broad causes of terminus retreat and the processes responsible for iceberg calving remain poorly understood, much less accurately represented in ice sheet models. This lack of understanding casts doubt on the predictive skill of ice sheet models and potentially introduces large uncertainties into sea level rise projections in the coming decades and centuries. We outline below some of the challenges associated with a better understanding of iceberg calving and the frontiers on which progress in its quantification and predictions are being made.

The calving menagerie

Iceberg calving is ultimately related to the mechanical failure of ice. However, predicting mass loss from calving events remains challenging because calving takes on different forms under different conditions. For example, large tabular icebergs sporadically detach from freely floating ice tongues with many years of quiescence between major calving events. This type of calving regime is exemplified by the 2010 and 2012 Petermann Glacier calving events during which the glacier shed icebergs larger than the size of Manhattan (Falkner et al. 2011). In the presence of ample surface melt, hydro-fracturing can fragment ice shelves so completely that they disintegrate into plumes of needle shaped icebergs, as occurred in the spectacular collapse of the Larsen B ice shelf over 6 weeks in 2002 (Scambos et al. 2003). This type of catastrophic failure event has yet to be observed in Greenland, but remains a possibility for floating ice tongues in regions with sustained increases in surface melt. Grounded glaciers, in contrast, calve more frequent, smaller icebergs than floating glaciers. The simplest of these events may be termed a serac failure, when an ice block (10 – 100 m scale) breaks free either above or below the water line. These types of events occur at all tidewater glaciers. Where thicker glaciers (>~800 m) flow into the ocean, larger, more intact icebergs can separate from the terminus 100s of meters back from the glacier front. These large slabs (1000 m scale) are buoyantly unstable and frequently capsize after detachment. Slab rotations, which in Greenland occur only at the largest 15 or so tidewater glaciers (Veitch and Nettles 2012), are accompanied by innumerable smaller serac failures (Walter et al. 2012). In some fjords, accumulated iceberg debris bound together by sea ice is found seasonally near the termini of Greenland's calving glaciers. The presence of this material, termed *ice mélange*, potentially limits the occurrence of slab rotation calving (Amundson et al. 2010). This diversity in calving regimes has prompted some to question whether fundamentally different processes control calving in disparate environments, or if the same processes operate in all regimes with changes in the style and vigor of calving resulting from a smooth change in controlling parameters (Bassis and Jacobs 2013).

Quantifying iceberg calving

A glacier terminus will advance when the rate of ice flow at the glacier terminus exceeds the combined rates of calving and frontal melting (Fig. 1):

$$(1) \quad \frac{dL}{dt} = u_t - u_c - u_m,$$

where each term is averaged over the cross-sectional area of the glacier terminus and over a time interval that is long compared to the recurrence interval between calving events. Here dL/dt is the rate of advance (or retreat) of the calving front, u_t is the terminus velocity, u_c is the calving rate (length of glacier lost due to iceberg calving per unit time), and u_m is the length lost due to frontal melting at the terminus per unit time. The calving rate represents an average of discrete iceberg calving events, the timing and size of which have a stochastic component that makes individual events impossible to forecast. The calving rate thus provides a description of glacier dynamics akin to a “climatology” of calving whereas individual calving events represent the “weather” of the glacier system.

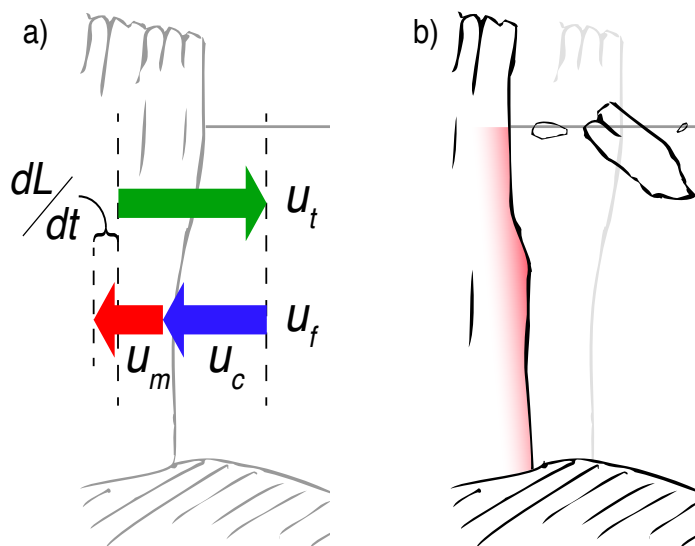


Fig. 1 Processes acting at the terminus of a marine-terminating glacier. Cross-sectional view. (a) The components of Equation 1, the terminus velocity u_t and frontal ablation rate u_f , made up of calving u_c and melt u_m . The relative magnitudes of these components dictate how quickly a terminus will advance or retreat dL/dt . (b) Cartoon showing each of the terminus processes at work during a given time period. Ice flow at the terminus has the potential to move the terminus forward (light gray). However, iceberg calving and submarine melt of the glacier terminus lead to a net retreat.

Of the four terms encompassed by Equation (1), it is straightforward to measure the rate of change in glacier terminus position (dL/dt) and geodetic and remote sensing techniques can provide the surface velocity at the terminus. Hence, dL/dt and u_t can be used to infer the combination of iceberg calving and submarine melt. Glaciological studies historically conflated iceberg calving and frontal melting by either ignoring submarine melt altogether or lumping the two mass loss processes into a single term loosely referred to as the *effective calving rate*. This can introduce significant confusion as recent measurements show that melting can be comparable to or even exceed calving when fjord seawater is warm (Bartholomaus et al. 2013; Motyka et al. 2013). Recently, a more precise term has come into use; the *frontal ablation rate* is the sum of the calving and frontal melting rates $u_f = u_c + u_m$. While frontal ablation, $u_f = u_t - dL/dt$, is comparatively easy to measure, it is the independent components u_c and u_m that must be identified if we seek process-based models of calving and melt.

The relative contributions of submarine melt and iceberg calving likely vary from location to location (Enderlin and Howat 2013). On one end of the spectrum, the Alaska Coastal Current transports water with summer temperatures in excess of 10°C into Alaska’s glacierized fjords. There, melt rates are sufficient to pace the rate of iceberg calving by melting the foundations of subaerial seracs (Bartholomaus et al. 2013). In contrast, in northern Greenland fjords, where water temperatures are colder and runoff is less, calving is often the dominant

frontal ablation process. However, frontal melting and iceberg calving are not necessarily independent and it remains unclear if it is possible – or even desirable – to fully separate our understanding of these two processes. In the sections that follow, we examine different approaches used to include calving in ice flow models.

Empirical calving laws

The earliest attempts to understand glacier retreat focused on seeking empirical relationships between frontal ablation rate and a suite of external and internal variables. This type of relationship is often called a ‘calving law’, although calving parameterization may be a more accurate description. These studies revealed various correlations between frontal ablation and water depth (Brown et al. 1982) or terminus position and some terminus height above the threshold at which the terminus would begin to float (Meier and Post 1987; C.J. van der Veen 2002). These empirical relationships are consistent with the general observation that glaciers terminating in deep water or that rest on beds sloping down into the interior are unstable. However, subsequent observations have cast doubt on the validity of these empirically based calving laws, suggesting that many of the correlations are spurious and do not reflect causal relationships (C. J. van der Veen 2002; Bassis and Walker 2012; Bassis and Jacobs 2013). Moreover, empirical calving laws proposed to date do not allow glaciers to form floating termini, a severe setback in Greenland where many glaciers form seasonal floating ice tongues.

This experience hints that we need to be cautious in seeking statistical correlations to establish causative relationships. Fortunately, if empirical relationships are sought going forward, larger datasets that span a wide variety of calving regimes and environmental conditions are becoming available to develop and test improved calving laws.

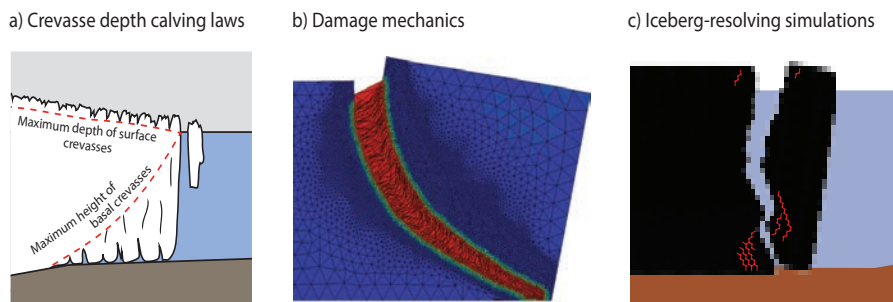


Fig. 2 Cross-sectional illustrations of three leading models for understanding and predicting iceberg calving. (a) The crevasse depth model assumes that surface and basal crevasses are formed in response to longitudinal stresses (Nick et al. 2010). Calving occurs where surface and basal crevasses intersect to penetrate the entire thickness of the glacier terminus (illustration by Sophie Gilbert). (b) Damage mechanics treats microfractures within the glacier as a bulk material property, described by a continuously defined state variable. Calving occurs when this “damage variable” exceeds some threshold (figure from Duddu and Waisman 2013). (c) Iceberg-resolving simulations model the forces between discrete elements of ice elastically, with some finite strength (figure from Bassis and Jacobs 2013). Calving occurs when the bonds connecting a mass of ice “boulders” to the glacier are broken.

Crevasse-depth calving laws

A second type of calving law relies on the understanding of iceberg calving as a fracturing process, and frames calving as an extension of the crevassing that is ubiquitous near the fronts of nearly every calving glacier. This calving law predicts that the terminus is located where the combination of surface and basal crevasses at the glacier front exceed a threshold penetration, ostensibly intersecting to form separate icebergs (Fig. 2a; Benn et al. 2007; Nick et al. 2010). Crevasses form when the stress within a glacier exceeds the strength of ice. This model is, in principle

at least, appropriate for floating and grounded ice and has been successful in reproducing trends of advance and retreat of several major Greenland outlet glaciers, including those with floating ice tongues (Nick et al. 2012; 2013). A number of complications, however, remain. For example, instead of allowing crevasses to initiate and advect from up-glacier of the terminus, researchers tend to assume that crevasses only form in response to the local stress field. Furthermore, researchers typically use a heuristic formulation in which the lateral extent of crevasses along with any time history is ignored. These simplifications likely contribute to the most severe deficiency of this approach: the prediction that crevasses only penetrate the entire ice thickness when surface crevasses are filled with melt water. Melt water is used as a poorly constrained tuning knob to force models to agree with observations, limiting confidence in predictions. Further work is needed to refine our understanding of the fracture process within ice and reconcile it with observed glacier behavior, but it is encouraging that first-order agreement between models and observations is, to some extent, now possible.

Damage mechanics based calving laws

An alternative approach seeks to model the bulk failure of ice, without explicitly resolving individual fractures, an approach that is frequently called damage mechanics (Fig. 2b; Pralong and Funk 2005). Continuum versions of this phenomenological approach have been applied to study the failure of hanging glaciers, accumulation of damage in floating ice shelves, and surface crevasse penetration (Pralong and Funk 2005; Albrecht and Levermann 2012; Borstad et al. 2012; Duddu et al. 2013). These flavors of damage mechanics can easily be incorporated into continuum ice sheet models. However, evolution of damage is controlled by an (as of yet) heuristic law, and this law is tuned to match limited laboratory observations or sparse field measurements. The lack of observations that span relevant fracture regimes of glacier ice makes it difficult to deconvolve damage (i.e., fracture) from other processes, like recrystallization. Damage has yet to be fully integrated into ice sheet models, but it provides a promising avenue of future research.

Iceberg resolving models

A third productive direction for iceberg calving literature has been the simulation of individual calving events using discontinuous damage mechanics or discrete element models (Fig. 2c). These models idealize glacier ice as a granular material, with adjacent ice “boulders” bound together by cohesive and frictional forces, acting under the influence of gravity and buoyancy. These models are able to qualitatively reproduce the observed styles of iceberg calving events (Åström et al. 2013; Bassis and Jacobs 2013). The computational expense of these

seconds-to-minutes-scale simulations of “iceberg weather” is too great for inclusion in century to millennial-scale ice flow simulations. However, the success of these conceptual process models thus far indicates that scientists are beginning to understand some of the essential physics of iceberg calving.

Outlook and opportunities for further progress

Further progress in understanding iceberg calving is likely to be substantially interdisciplinary. Studies simultaneously drawing on glaciological and oceanographic methods have the potential to disentangle calving and submarine melt contributions to frontal ablation. Remote sensing data can inform modeling results, while field data temporally “fill the gaps” between satellite scenes. Field data also allow for the observation of individual calving events as they occur, coincident with other environmental data such as the passage of ocean waves and air temperatures. Crucially, neither satellite nor field observations are currently able to constrain key parameters needed for models. For example, we have very limited ability to measure the extent to which crevasses are water filled and have little knowledge of the location and geometry of fractures within the ice that are ultimately responsible for calving events.

We expect that significant improvements in our understanding of ice loss from glacier termini in Greenland and elsewhere will come from disentangling the two components of frontal ablation: iceberg calving and frontal melting. At present it is unclear how or even if this can be done in general settings; modeling studies have come to conflicting conclusions as to whether submarine melt may sufficiently alter the stress field within an unfractured glacier front to modulate calving rates (O’Leary and Christoffersen 2013; Cook et al. 2013). In extremely warm fjord environments with massive front melting, observations demonstrate that summer iceberg calving rates can be paced by rates of submarine melt – thus calving and melt components are practically inseparable (Bartholomaus et al. 2013). However, examining glaciers in cold ocean settings where frontal melting is negligible provides a window into calving that may be uncontaminated by melting. Although, remote sensing offers a coarse, if easily attainable picture of frontal ablation rates, studies of the individual submarine melt and calving components often require expensive, labor-intensive fieldwork. Heat and salt budget methods, combined with subglacial discharge estimates or fjord current speeds, allow for the quantification of submarine melt within seawater (Straneo et al. 2011; Motyka et al. 2013), but methods that allow for the direct measurement of iceberg calving fluxes are in their infancy. Focused, high-rate, ground-based observations of glacier

termini using either seismic methods or ground-based interferometric radar are likely to yield new insights (Fig. 3). Innovative field experiments are essential as scientists disentangle the calving and submarine melt components of frontal ablation.

Iceberg calving is an emerging, unsettled field and the broad spectrum of temporal and spatial scales has thwarted attempts to develop convenient parameterizations. Nonetheless, observational work has shown that frontal ablation (and calving) varies at a number of timescales, including seasonally and tidally (Schild and Hamilton 2013; Bartholomaus 2013). Additional field observations combined with improved process-based models may allow us to better understand the processes and conditions that occur during individual iceberg calving events, but history suggests we should be cautious generalizing results to other glaciers, even those nearby. Alternatively, bulk parameterizations of the climatology of calving are easier to observe and more directly ingestible into numerical models. However, models based on bulk parameterizations are necessarily more heuristic, less tightly constrained by fundamental physics, and risk breaking down when extrapolated to future conditions. A consequence is that creation and validation of process physics based models and even empirical parameterization requires detailed – daily or better – resolution of local meteorological, oceanographic, and glaciological variables for a large suite of glaciers that surround the Greenland Ice Sheet. We anticipate this will require new observational platforms that complement existing methods to propel understanding forward.

References

- Albrecht, T., and A. Levermann, 2012: Fracture field for large-scale ice dynamics. *Journal of Glaciology*, **58**, 165–176.
- Amundson, J.M., M. Fahnestock, M. Truffer, J. Brown, M.P. Lüthi, and R.J. Motya, 2010: Ice mélange dynamics and implications for terminus stability, Jakobshavn Isbræ, Greenland. *J. Geophys. Res.*, **115**, 1–12.
- Åström, J.A., T.I. Riikilä, T. Tallinen, T. Zwinger, D. Benn, J.C. Moore, and J. Timonen, 2013: A particle based simulation model for glacier dynamics. *The Cryosphere*, **7**, 1591–1602.
- Bartholomaus, T.C., 2013: *Seismicity, seawater and seasonality: new insights into iceberg calving from Yaktse Glacier, Alaska*. Ph.D. Dissertation. University of Alaska Fairbanks.
- Bartholomaus, T.C., C.F. Larsen, and S. O’Neel, 2013: Does calving matter? Evidence for significant submarine melt. *Earth Planet. Sci. Lett.*, **380**, 21–30.
- Bassis, J.N., and S. Jacobs, 2013: Diverse calving patterns linked to glacier geometry. *Nat. Geosci.*, **7**, 1–4.
- Bassis, J.N., and C.C. Walker, 2012: Upper and lower limits on the stability of calving glaciers from the yield strength envelope of ice. *Proc. R. Soc. A*, **468**, 913–931.
- Benn, D.I., N.R.J. Hulton, and R.H. Mottram, 2007: “Calving laws”, “sliding laws” and the stability of tidewater glaciers. *Ann. Glaciol.*, **46**, 123–130.

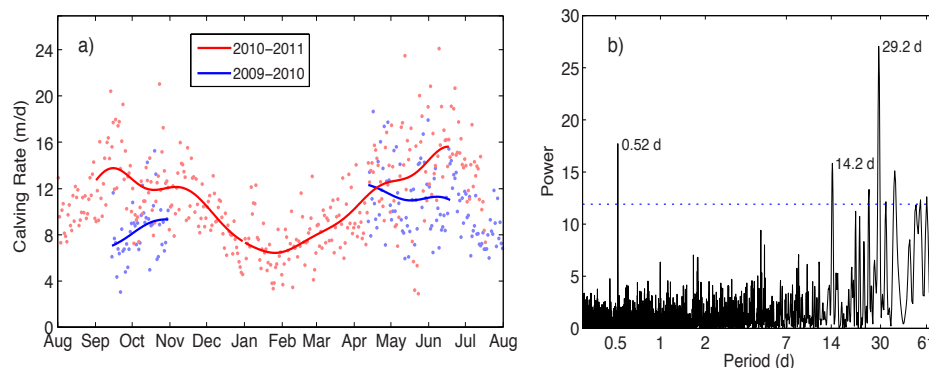


Fig. 3 Views of interannual, seasonal, daily, and tidal calving variability at tidewater Yaktse Glacier, Alaska (Bartholomaus 2013). The calving rate is estimated seismically, using the properties of “icequakes” produced when icebergs impact the sea surface. (a) The daily calving rate is lowest during the winter, and varies amongst years and from day to day. (b) Periodogram showing the strength of variations in calving rate at a range of different timescales. Strong peaks in power are present at semi-diurnal, fortnightly, and monthly periods – all important tidal timescales at Yaktse Glacier. Units are arbitrary; dotted line shows the 95% confidence interval on the peaks.

Conclusions

Despite challenges, understanding of calving and frontal ablation has developed significantly over recent decades. Observational work reveals that iceberg calving is not steady, and, in addition to interannual and decadal variability, calving varies seasonally and tidally. Numerical models are beginning to reproduce this behavior while providing insight into the essential character of calving. We anticipate that progress will continue as new observations and models add to our understanding. However, rapid progress requires a concerted effort to use observations to discriminate between models so that we can begin to whittle down the complex ecology inherent within proposed calving laws. Finally, we must be sure to look beyond traditional disciplinary boundaries, as breaching these barriers is the most direct route to significant progress and understanding.

- Borstad, C.P., A. Khazendar, E.Y. Larour, M. Morlighem, E. Rignot, M.P. Schodlok, and H. Seroussi, 2012: A damage mechanics assessment of the Larsen B ice shelf prior to collapse: Toward a physically-based calving law. *Geophys. Res. Lett.*, **39**, L18502.
- Brown, C.S., M.F. Meier, and A. Post, 1982: Calving speed of Alaska tidewater glaciers, with application to Columbia Glacier. *USGS Prof. Pap.*, **1258-C**, C1–C13.
- Cook, S., I.C. Rutt, T. Murray, A. Luckman, N. Selmes, A. Goldsack, and T. Zwinger, 2013: Modelling environmental influences on calving at Helheim Glacier, East Greenland. *The Cryosphere Discuss.*, **7**, 4407–4442.
- Duddu, R., and H. Waisman, 2013: A nonlocal continuum damage mechanics approach to simulation of creep fracture in ice sheets. *Comput. Mech.*, **51**, 961–974.
- Duddu, R., J.N. Bassis, and H. Waisman, 2013: A numerical investigation of surface crevasse propagation in glaciers using nonlocal continuum damage mechanics. *Geophys. Res. Lett.*, **40**, 3064–3068.
- Enderlin, E.M., and I.M. Howat, 2013: Submarine melt rate estimates for floating termini of Greenland outlet glaciers (2000 – 2010). *J. Glaciol.*, **59**, 67–75.
- Enderlin, E.M. I.M. Howat, S. Jeong, M.-J. Noh, J.J. van Angelen, and M.R. van den Broeke, 2014: An improved mass budget for the Greenland ice sheet. *Geophys. Res. Lett.*, **41**, 1–7.
- Falkner, K.K., H. Melling, A.M. Münchow, J.E. Box, T. Wohlleben, H.L. Johnson, P. Gudmandsen, R. Samelson, L. Copland, K. Steffen, E. Rignot, and A.K. Higgins, 2011: Context for the recent massive Petermann Glacier calving event. *Eos Trans. AGU*, **92**, 117–118.
- Harig, C. and F.J. Simons, 2012: Mapping Greenland's mass loss in space and time. *Proc. Nat. Acad. Sci.*, **109**, 19934–19937.
- Joughin, I., B.E. Smith, I.M. Howat, D. Floricioiu, R.B. Alley, M. Truffer, and M. Fahnestock, 2012: Seasonal to decadal scale variations in the surface velocity of Jakobshavn Isbræ, Greenland: Observation and model-based analysis. *J. Geophys. Res.*, **117**, 1–20.
- Meier, M.F., and A. Post, 1987: Fast tidewater glaciers. *J. Geophys. Res.*, **92**, 9051–9058.
- Moon, T. and I. Joughin, 2008: Changes in ice front position on Greenland's outlet glaciers from 1992 to 2007. *J. Geophys. Res.*, **113**, 1–10.
- Motyka, R.J., M. Truffer, E.M. Kuriger, and A.K. Bucki, 2006: Rapid erosion of soft sediments by tidewater glacier advance: Taku Glacier, Alaska, USA. *Geophys. Res. Lett.*, **33**, L24504.
- Motyka, R.J., W.P. Dryer, J. Amundson, M. Truffer, and M. Fahnestock, 2013: Rapid submarine melting driven by subglacial discharge, LeConte Glacier, Alaska. *Geophys. Res. Lett.*, **40**, 1–6.
- Nick, F.M., C.J. Van der Veen, A. Vieli, and D. Benn, 2010: A physically based calving model applied to marine outlet glaciers and implications for the glacier dynamics. *J. Glaciol.*, **56**, 781–794.
- Nick, F.M., A. Luckman, A. Vieli, C.J. Van der Veen, D. van As, R.S.W. van de Wal, F. Pattyn, A.L. Hubbard, and D. Floricioiu, 2012: The response of Petermann Glacier, Greenland, to large calving events, and its future stability in the context of atmospheric and oceanic warming. *J. Glaciol.*, **58**, 229–239.
- Nick, F.M., A. Vieli, M.L. Andersen, I. Joughin, A. Payne, T.L. Edwards, F. Pattyn, and R.S.W. van de Wal, 2013: Future sea-level rise from Greenland's main outlet glaciers in a warming climate. *Nature*, **497**, 235–238.
- O'Leary, M., and P. Christoffersen, 2013: Calving on tidewater glaciers amplified by submarine frontal melting. *The Cryosphere*, **7**, 119–128.
- Pfeffer, W.T., 2007: A simple mechanism for irreversible tidewater glacier retreat. *J. Geophys. Res.*, **112**, 1–12.
- Post, A., S. O'Neel, R.J. Motyka, and G. Streveler, 2011: A complex relationship between calving glaciers and climate. *Eos Trans. AGU*, **92**, 305.
- Pralong, A., and M. Funk, 2005: Dynamic damage model of crevasse opening and application to glacier calving. *J. Geophys. Res.*, **110**, 1–12.
- Scambos, T.A., C. Hulbe, and M. Fahnestock, 2003: Climate-induced ice shelf disintegration in the Antarctic Peninsula. *Antarctic Peninsula Climate Variability: Historical and Paleoenvironmental Perspectives*, *Artarct. Res. Ser.*, Vol. 79, E. Domack, Ed., AGU, 79–92.
- Schenk, T. and B. Csathó, 2012: A new methodology for detecting ice sheet surface elevation changes from laser altimetry data. *IEEE Trans. Geosci. Remote Sens.*, **50**, 3302–3316.
- Schild, K.M., and G.S. Hamilton, 2013: Seasonal variations of outlet glacier terminus position in Greenland. *J. Glaciol.*, **59**, 759–770.
- Straneo, F., R.G. Curry, D.A. Sutherland, G.S. Hamilton, C. Cenedese, K. Våge, and L.A. Stearns, 2011: Impact of fjord dynamics and glacial runoff on the circulation near Helheim Glacier. *Nat. Geosci.*, **4**, 322–327.
- Van der Veen, C.J., 2002: Calving glaciers. *Prog. Phys. Geog.*, **26**, 96–122.
- Veitch, S.A. and M. Nettles, 2012: Spatial and temporal variations in Greenland glacial-earthquake activity, 1993 – 2010. *J. Geophys. Res.*, **117**, 1–20.
- Walter, F., J.M. Amundson, S. O'Neel, M. Truffer, M. Fahnestock, and H. A. Fricker, 2012: Analysis of low-frequency seismic signals generated during a multiple-iceberg calving event at Jakobshavn Isbræ, Greenland. *J. Geophys. Res.*, **117**, 1–11.



Greenland Ice Sheet Workshop Report

Download the report from the [International Workshop on Understanding the Response of Greenland's Marine-Terminating Glaciers to Oceanic and](#)

[Atmospheric Forcing](#). The report provides a prioritized set of recommendations for interdisciplinary and internationally coordinated observations, data access, and process studies to improve understanding of physical

process and their representation in climate models. Investment in these priorities over the next decade will provide more reliable, physically based projections of freshwater flux from the Greenland Ice Sheet and its contributions to changes to sea level, the North Atlantic circulation, and related climate changes. The workshop was sponsored by US CLIVAR agency contributions from NASA, NOAA, NSF, and DoE, and the NSF Office of Polar Programs.

ANNOUNCEMENTS

New 2014 US CLIVAR Panel Members

US CLIVAR welcomes nine new panel members, who have joined to lend their expertise and ensure progress toward US CLIVAR goals. The new members are serving through 2017.

Phenomena, Observations, and Synthesis (POS) Panel

Carol Anne Clayson

Woods Hole Oceanographic Institution

Emanuele Di Lorenzo

Georgia Institute of Technology

Renellys Perez

University of Miami/NOAA Atlantic Oceanographic and Meteorological Laboratory

Process Study and Model Improvement (PSMI) Panel

Gidon Eshel

Bard College

Maria Flatau

Naval Research Laboratory

Caroline Ummenhofer

Woods Hole Oceanographic Institution

Predictability, Prediction, and Applications Interface (PPAI) Panel

Enrique Curchitser

Rutgers University

Xin-Zhong Liang

University of Maryland

Scott Weaver

NOAA Climate Prediction Center

Kristan Uhlenbrock joins the Project Office

The US CLIVAR Project Office welcomes our newest team member, Kristan Uhlenbrock. As Program Specialist for the office, Kristan manages the program's communication and outreach activities and provides organizational support to facilitate science planning, program implementation, and interagency coordination.

Kristan brings to the position solid experience in driving communication and outreach to advance ocean science and policy. Prior to joining US CLIVAR, she served as the Associate Director for Ocean Communication at the Center for American Progress, as a Public Affairs Coordinator with the lead on ocean issues for the American Geophysical Union, as a National Ocean Policy Fellow in the oceans and coastal protection division of the Environmental Protection Agency, and as an intern at the White House Council on Environmental Quality, where she assisted the interagency Ocean Policy Task Force to develop and advance the National Ocean Policy. Kristan received her M.S. in marine science from the University of South Florida College of Marine Science, studying nutrient distributions and their impacts on coastal and estuarine systems, as well as their role in sustaining harmful algal blooms in the Gulf of Mexico. She also holds a B.S. in chemistry.



www.usclivar.org
uscpo@usclivar.org
twitter.com/usclivar

US Climate Variability and Predictability (CLIVAR) Program

1201 New York Ave. NW, Suite 400
Washington, DC 20005
(202) 787-1682

US CLIVAR acknowledges support from these US agencies:



This material was developed with federal support of NASA (AGS-0963735), NOAA (NA11OAR4310213), NSF (AGS-0961146), and DOE (AGS-1357212). Any opinions, findings, conclusions or recommendations expressed in this material are those of the authors and do not necessarily reflect the views of the sponsoring agencies.